

**“STUDIES ON POTENTIAL GREEN CORROSION
INHIBITORS FOR MILD STEEL IN DIFFERENT
MEDIA”**

A

Thesis

Submitted to

University of Kota, Kota

For the Award of Degree of

DOCTOR OF PHILOSOPHY

In the Faculty of Science (Chemistry)

By

PRIYA BHARDWAJ



Under the supervision of

Dr. (Ms.) Seema Agarwal

(Co-supervisor)

Lecturer in Chemistry

P.G. Department of Chemistry

Govt. College Kota

Kota (Rajasthan)

Dr. (Mrs.) Kalpana

(Supervisor)

Lecturer in Chemistry

P.G. Department of Chemistry

Govt. College Kota

Kota (Rajasthan)

2017

DEDICATED TO MY FAMILY

Candidate's Declaration

I hereby certify that the work, which is being presented in this thesis, entitled **“STUDIES ON POTENTIAL GREEN CORROSION INHIBITORS FOR MILD STEEL IN DIFFERENT MEDIA”** in partial fulfilment of the requirement for the award of the Degree of Doctor of Philosophy, carried under the supervision of Dr. (Mrs.) Kalpana and co-supervision of Dr. (Ms.) Seema Agarwal and submitted to the (University Department of Chemistry/ University Research Center), University of Kota, Kota represents my ideas in my own words and where other ideas or words have been included I have adequately cited and referenced the original sources. The work presented in this thesis has not been submitted elsewhere for the award of any other degree or diploma from any Institution. I also declared that I have adhered to all principles of academic honesty and integrity and have not misrepresented or fabricated or falsified any idea/data/fact/source in my submission. I understand that any violation of the above will be cause for disciplinary action by the University and can also evoke action from the sources which have thus not been properly cited or from whom proper permission has not been taken when needed.

Date:

Ms. Priya Bhardwaj

This is to certify that above statement made by Priya Bhardwaj (Enrolment No. RS/1756/13) is correct to the best of our knowledge.

Date:

Dr. (Mrs.) Kalpana

Supervisor

P.G. Department of Chemistry

Govt. College Kota, Kota

University of Kota, Kota

Dr. (Ms.) Seema Agarwal

Co-supervisor

P. G. Department of Chemistry

Govt. College Kota, Kota

University of Kota, Kota

CERTIFICATE

I feel great pleasure in certifying that the thesis entitled “**STUDIES ON POTENTIAL GREEN CORROSION INHIBITORS FOR MILD STEEL IN DIFFERENT MEDIA**” submitted by **Ms. Priya Bhardwaj** is an original piece of research work carried out under our guidance and supervision. She has completed the following requirements as per Ph.D regulations of the university.

- (1) Course work as per the university rules.
- (2) Residential requirements of the university (200 days).
- (3) Regularly submitted annual progress report.
- (4) Presented her work in the departmental committee.
- (5) Published/accepted minimum of one research paper in a referred research journal.

We recommend the submission of thesis.

Date

Dr. (Mrs.) Kalpana

(Supervisor)

Lecturer in Chemistry

P.G. Department of Chemistry

Govt. College Kota

Kota (Rajasthan)

Dr. (Ms.) Seema Agarwal

(Co-supervisor)

Lecturer in Chemistry

P.G. Department of Chemistry

Govt. College Kota

Kota (Rajasthan)

ACKNOWLEDGEMENT

“सरस्वती नमस्तुभ्यं, वरदे कामरूपिणी।

विद्यारम्भं करिष्यामि, सिद्धिर्भवतु मे सदा”

“Saraswati Namastubhyam, Varde Kaamroopini

Vidyaarambham Karishyaami, Siddhir Bhavatu Me Sada”

First of all I thank to The Almighty for showering me his blessings, perserverance, internal strength, mental strength, wisdom for completion of my Ph.D thesis.

*The present text in above Sanskrit shloka draws deep sense of profound gratitude and inestimated indebtedness toward my learned supervisor **Dr. (Mrs.) Kalpana** Senior lecturer and co-supervisor **Dr. (Ms.) Seema Agrawal** Lecturer, Department of Chemistry, Govt. College Kota (Rjasthan) for their noble guidance, erudite inspiration, kind and affectionate advise and perpetual encouragement throughout the period of this piece of research work. She has always been an open person to me and I consider myself very fortunate to receive her able supervision and guidance. She always encouraged me in every stage of this research work and her constructive criticism during the course of investigations made this endeavour a success. She always encouraged me to frame new ideas and thoughts by acting on it leads to this thesis salvation as: “**Man’s actions are the best interpreters of his thoughts.**”*

I owe to my heartfelt gratitude to her for being my mentor and the torchbearer for my doctoral degree research endeavour.

*I feel extremely grateful to **Principal**, Govt. College Kota and **Head**, P.G. Department of Chemistry, Govt. College Kota for providing me all the necessary facilities and support for carrying out this research work.*

*My special thanks to all **staff members** of Chemistry Department, Govt. College Kota for their kindness, encouragement, assistance and invaluable suggestions during this critical period.*

*I am highly indebted to **Dr. Suman Sharma**, **Dr. Krishna Rani Kapoor**, **Dr. Sadhana Chittora**, **Dr.S.M. Nafees**, **Dr. Nitin Gupta** for their help and boosting my morale time to time.*

*Words can hardly express the deep sense of gratitude: I express my appreciation to all my research colleagues especially **Mr. Anillesh Yadav** and **Ms. Preeti Singhal** for helping me in innumerable ways and positive attitude at the time of critical need.*

*I would also like to thank **Lab incharges, Lab staff members and Library staff** members for their help and support.*

*I owe the highest debt of gratitude to my loving mother **Smt. Shakuntala Bhardwaj** and my father **Shri Birdhi Lal Bhardwaj** for their blessings, moral support and best wishes which maketh me to have courage and perserverance to complete this work however difficult it may be and one day it will award me with flamboyant colours.*

*I am also highly indebted to my brother **Mr. Akash Bhardwaj**, who has spent his valuable time in typing of this thesis and solving the technical problems related. I am at a loss of words to acknowledge his indispensable help received. Without his contribution this thesis would not have been in this form.*

*I owe a lot of thanks to my Didi **Mrs. Prachi Pareek** and Jijaji **Mr. Krishna Kant Pareek** for their encouragement and best wishes.*

Lastly I thank to one and the all who helped me directly or indirectly in smooth conduction of my research programme and who have been inadvertently forgotten at this moment and end my words with these truly, beautiful and golden lines:

“Laboratories are temple of the future, of wealth and of walfare; in them humanity grows greater, stronger and better”

Ms. Priya Bhardwaj

LIST OF TABLES

S.No	Title	PageNo.
Table1	Mild steel corrosion rates in 1M HCl solution in absence and presence of different concentrations of AECPL at different temperatures	33
Table 2	Inhibition efficiencies of AECPL at different concentrations and temperatures in 1M HCl solution	34
Table 3	Kinetic parameters for mild steel corrosion in 1M HCl solution with AECPL	35
Table 4	Activation and thermodynamic parameters for mild steel corrosion in 1M HCl solution with AECPL	36
Table 5	Adsorption parameters for mild steel corrosion in 1M HCl solution with AECPL	37
Table 6	Mild steel corrosion rates in 1M H ₂ SO ₄ solution in absence and presence of different concentrations of AECPL at different temperatures	38
Table7	Inhibition efficiencies of AECPL at different concentrations and temperatures in 1M H ₂ SO ₄ solution	39
Table8	Kinetic parameters for mild steel corrosion in 1M H ₂ SO ₄ solution with AECPL	40
Table9	Activation and thermodynamic parameters for mild steel corrosion in 1M H ₂ SO ₄ solution with AECPL	41
Table10	Adsorption parameters for mild steel corrosion in 1M H ₂ SO ₄ solution with AECPL	42
Table11	Mild steel corrosion rates in 1M HCl solution in absence and presence of different concentrations of AELCL at different temperatures	43
Table12	Inhibition efficiencies of AELCL at different concentrations and temperatures in 1M HCl solution	44
Table13	Kinetic parameters for mild steel corrosion in 1M HCl solution with AELCL	45
Table14	Activation and thermodynamic parameters for mild steel corrosion in 1M HCl solution with AELCL	46
Table15	Adsorption parameters for mild steel corrosion in 1M HCl solution with AELCL	47
Table16	Mild steel corrosion rates in 1M H ₂ SO ₄ solution in absence and presence of different concentrations of AELCL at different temperatures	48
Table17	Inhibition efficiencies of AELCL at different concentrations and temperatures in 1M H ₂ SO ₄ solution	49
Table18	Kinetic parameters for mild steel corrosion in 1M H ₂ SO ₄ solution with AELCL	50
Table19	Activation and thermodynamic parameters for mild steel corrosion in 1M H ₂ SO ₄ solution with AELCL	51
Table20	Adsorption parameters for mild steel corrosion in 1M H ₂ SO ₄ solution with AELCL	52

Table21	Mild steel corrosion rates in 1M HCl solution in absence and presence of different concentrations of AENOL at different temperatures	53
Table22	Inhibition efficiencies of AENOL at different concentrations and temperatures in 1M HCl solution	54
Table23	Kinetic parameters for mild steel corrosion in 1M HCl solution with AENOL	55
Table24	Activation and thermodynamic parameters for mild steel corrosion in 1M HCl solution with AENOL	56
Table25	Adsorption parameters for mild steel corrosion in 1M HCl solution with AENOL	57
Table26	Mild steel corrosion rates in 1M H ₂ SO ₄ solution in absence and presence of different concentrations of AENOL at different temperatures	58
Table27	Inhibition efficiencies of AENOL at different concentrations and temperatures in 1M H ₂ SO ₄ solution	59
Table28	Kinetic parameters for mild steel corrosion in 1M H ₂ SO ₄ solution with AENOL	60
Table29	Activation and thermodynamic parameters for mild steel corrosion in 1M H ₂ SO ₄ solution with AENOL	61
Table30	Adsorption parameters for mild steel corrosion in 1M H ₂ SO ₄ solution with AENOL	62
Table31	Mild steel corrosion rates in 1M HCl solution in absence and presence of different concentrations of AEWHL at different temperatures	63
Table32	Inhibition efficiencies of AEWHL at different concentrations and temperatures in 1M HCl solution	64
Table33	Kinetic parameters for mild steel corrosion in 1M HCl solution with AEWHL	65
Table34	Activation and thermodynamic parameters for mild steel corrosion in 1M HCl solution with AEWHL	66
Table35	Adsorption parameters for mild steel corrosion in 1M HCl solution with AEWHL	67
Table36	Mild steel corrosion rates in 1M H ₂ SO ₄ solution in absence and presence of different concentrations of AEWHL at different temperatures	68
Table37	Inhibition efficiencies of AEWHL at different concentrations and temperatures in 1M H ₂ SO ₄ solution	69
Table38	Kinetic parameters for mild steel corrosion in 1M H ₂ SO ₄ solution with AEWHL	70
Table39	Activation and thermodynamic parameters for mild steel corrosion in 1M H ₂ SO ₄ solution with AEWHL	71
Table40	Adsorption parameters for mild steel corrosion in 1M H ₂ SO ₄ solution with AEWHL	72

LIST OF FIGURES

S.No	Title	PageNo.
Figure1	Variation in IE% for mild steel corrosion in 1M HCl at different concentrations of AECPL at different studied temperatures	73
Figure2	Variation of log CR with log C_{inh} for mild steel corrosion in 1M HCl in presence of different concentrations of AECPL at various studied temperatures	73
Figure3	Arrhenius plots for mild steel corrosion in 1M HCl in absence and presence of various concentrations of AECPL	74
Figure4	Transition-state plots for mild steel corrosion in 1M HCl in absence and presence of various concentrations of AECPL.	74
Figure5	Langmuir adsorption isotherms of AECPL on mild steel surface in 1M HCl at different studied temperatures	75
Figure6	Freundlich adsorption isotherms of AECPL on mild steel surface in 1M HCl at different studied temperatures	75
Figure7	The variation of ΔG_{ads} (kJ/mol) with T(K) for mild steel corrosion in 1M HCl solution with AECPL	76
Figure8	Variation in IE% for mild steel corrosion in 1M H ₂ SO ₄ at different concentrations of AECPL at different studied temperatures	76
Figure9	Variation of log CR with log C_{inh} for mild steel corrosion in 1M H ₂ SO ₄ in presence of different concentrations of AECPL at various studied temperatures	77
Figure10	Arrhenius plots for mild steel corrosion in 1M H ₂ SO ₄ in absence and presence of various concentrations of AECPL	77
Figure11	Transition-state plots for mild steel corrosion in 1M H ₂ SO ₄ in absence and presence of various concentrations of AECPL	78
Figure12	Langmuir adsorption isotherms of AECPL on mild steel surface in 1M H ₂ SO ₄ at different studied temperatures	78
Figure13	Freundlich adsorption isotherms of AECPL on mild steel surface in 1M H ₂ SO ₄ at different studied temperature	79
Figure14	Temkin adsorption isotherms of AECPL on mild steel surface in 1M H ₂ SO ₄ at different studied temperatures	79
Figure15	The variation of ΔG_{ads} (kJ/mol) with T (K) for mild steel corrosion in 1M H ₂ SO ₄ solution with AECPL	80
Figure16	Variation in IE% for mild steel corrosion in 1M HCl at different concentrations of AELCL at different studied temperatures	80
Figure17	Variation of log CR with log C_{inh} for mild steel corrosion in 1M HCl in presence of different concentrations of AELCL at various studied temperatures	81

Figure18	Arrhenius plots for mild steel corrosion in 1M HCl in absence and presence of various concentrations of AELCL	81
Figure19	Transition-state plots for mild steel corrosion in 1M HCl in absence and presence of various concentrations of AELCL	82
Figure20	Langmuir adsorption isotherms of AELCL on mild steel surface in 1M HCl at different studied temperatures	82
Figure21	Freundlich adsorption isotherms of AELCL on mild steel surface in 1M HCl at different studied temperatures	83
Figure22	Temkin adsorption isotherms of AELCL on mild steel surface in 1M HCl at different studied temperatures	83
Figure23	The variation of ΔG_{ads} (kJ/mol) with T (K) for mild steel corrosion in 1M HCl solution with AELCL	84
Figure24	Variation in IE% for mild steel corrosion in 1M H ₂ SO ₄ at different concentrations of AELCL at different studied temperatures	84
Figure25	Variation of log CR with log C _{inh} for mild steel corrosion in 1M H ₂ SO ₄ in presence of different concentrations of AELCL at various studied temperatures	85
Figure26	Arrhenius plots for mild steel corrosion in 1M H ₂ SO ₄ in absence and presence of various concentrations of AELCL	85
Figure27	Transition- state plots for mild steel corrosion in 1M H ₂ SO ₄ in absence and presence of various concentrations of AELCL	86
Figure28	Langmuir adsorption isotherms of AELCL on mild steel surface in 1M H ₂ SO ₄ at different studied temperatures	86
Figure29	Freundlich adsorption isotherms of AELCL on mild steel surface in 1M H ₂ SO ₄ at different studied temperatures	87
Figure30	Temkin adsorption isotherms of AELCL on mild steel surface in 1M H ₂ SO ₄ at different studied temperature	87
Figure31	The variation of ΔG_{ads} (kJ/mol) with T (K) for mild steel corrosion in 1M H ₂ SO ₄ solution with AELCL	88
Figure32	Variation in IE% for mild steel corrosion in 1M HCl at different concentrations of AENOL at different studied temperatures	88
Figure33	Variation of log CR with log C _{inh} for mild steel corrosion in 1M HCl in presence of different concentrations of AENOL at various studied temperatures	89
Figure34	Arrhenius plots for mild steel corrosion in 1M HCl in absence and presence of various concentrations of AENOL	89
Figure35	Transition-state plots for mild steel corrosion in 1M HCl in absence and presence of various concentrations of AENOL	90
Figure36	Langmuir adsorption isotherms of AENOL on mild steel surface in 1M HCl at different studied temperatures	90

Figure37	Freundlich adsorption isotherms of AENOL on mild steel surface in 1M HCl at different studied temperatures	91
Figure38	The variation of ΔG_{ads} (kJ/mol) with T(K) for mild steel corrosion in 1M HCl solution with AENOL	91
Figure39	Variation in IE% for mild steel corrosion in 1M H ₂ SO ₄ at different concentrations of AENOL at different studied temperature	92
Figure40	Variation of log CR with logC _{inh} for mild steel corrosion in 1M H ₂ SO ₄ in presence of different concentrations of AENOL at various studied temperatures	92
Figure41	Arrhenius plots for mild steel corrosion in 1M H ₂ SO ₄ in absence and presence of various concentrations of AENOL	93
Figure42	Transition-state plots for mild steel corrosion in 1M H ₂ SO ₄ in absence and presence of various concentrations of AENOL	93
Figure43	Langmuir adsorption isotherms of AENOL on mild steel surface in 1M H ₂ SO ₄ at different studied temperatures	94
Figure44	Freundlich adsorption isotherms of AENOL on mild steel surface in 1M H ₂ SO ₄ at different studied temperatures	94
Figure45	Temkin adsorption isotherms of AENOL on mild steel surface in 1M H ₂ SO ₄ at different studied temperatures	95
Figure46	The variation of ΔG_{ads} (kJ/mol) with T (K) for mild steel corrosion in 1M H ₂ SO ₄ solution with AENOL	95
Figure47	Variation in IE% for mild steel corrosion in 1M HCl at different concentrations of AEWHL at different studied temperatures	96
Figure48	Variation of log CR with logC _{inh} for mild steel corrosion in 1M HCl in presence of different concentrations of AEWHL at various studied temperatures	96
Figure49	Arrhenius plots for mild steel corrosion in 1M HCl in absence and presence of various concentrations of AEWHL	97
Figure50	Transition-state plots for mild steel corrosion in 1M HCl in absence and presence of various concentrations of AEWHL.	97
Figure51	Langmuir adsorption isotherms of AEWHL on mild steel surface in 1M HCl at different studied temperatures	98
Figure52	Freundlich adsorption isotherms of AEWHL on mild steel surface in 1M HCl at different studied temperatures	98
Figure53	Temkin adsorption isotherms of AEWHL on mild steel surface in 1M HCl at different studied temperatures	99
Figure54	The variation of ΔG_{ads} (kJ/mol) with T (K) for mild steel corrosion in 1M HCl solution with AEWHL	99

Figure55	Variation in IE% for mild steel corrosion in 1M H ₂ SO ₄ at different concentrations of AEWHL at different studied temperatures	100
Figure56	Variation of log CR with logC _{inh} for mild steel corrosion in 1M H ₂ SO ₄ in presence of different concentrations of AEWHL at different studied temperatures	100
Figure57	Arrhenius plots for mild steel corrosion in 1M H ₂ SO ₄ in absence and presence of various concentrations of AEWHL	101
Figure58	Transition-state plots for mild steel corrosion in 1M H ₂ SO ₄ in absence and presence of various concentrations of AEWHL.	101
Figure59	Langmuir adsorption isotherms of AEWHL on mild steel surface in 1M H ₂ SO ₄ at different studied temperatures	102
Figure60	Freundlich adsorption isotherms of AEWHL on mild steel surface in 1M H ₂ SO ₄ at different studied temperatures	102
Figure61	Temkin adsorption isotherms of AEWHL on mild steel surface in 1M H ₂ SO ₄ at different studied temperatures	103
Figure62	The variation of ΔG _{ads} (kJ/mol)with T (K) for mild steel corrosion in 1M H ₂ SO ₄ solution with AEWHL	103

CONTENTS

<u>CHAPTERS</u>	<u>PAGE NO.</u>
CHAPTER 1	
INTRODUCTION AND REVIEW OF LITERATURE	1-18
CHAPTER 2	
MATERIALS, METHODS AND METHODOLOGY	19-31
CHAPTER 3	
OBSERVATIONS AND RESULTS	32-103
CHAPTER 4	
DISCUSSION ON FINDINGS AND CONCLUSIONS	104-145
BIBLIOGRAPHY	146-173
ANNEXURES	174-177
SUMMARY	178-183

CHAPTER - 1

INTRODUCTION AND REVIEW OF LITERATURE

Mild steel is the commonly used alloy in the industries due to its remarkable features such as low cost, easy availability, high strength, durability etc. It is largely used in designing of various reaction vessels, tanks, for handling of various corrosive liquids, various aggressive solutions like acidic solutions, basic solutions, salt solutions etc. Acid solutions are generally used for descaling, acid cleaning, acid pickling, and in various petrochemical processes. Hydrochloric acid, acetic acid and sulphuric acids are widely used in the pickling process [53]. These acids are also largely used for drilling fracturing and acid simulations at various stages in oil exploration, production and descaling operations and with many industrial applications [100]

Acidic environment corrode mild steel easily. Corrosion is a natural and electrochemical phenomenon caused by potential difference between metal and acid [12]. H^+ ions and dissolved oxygen are named natural motors of corrosion [26] Corrosion results large economic loss of any country across a year. Corrosion is a continuous process and cannot be stopped completely. Therefore application of corrosion inhibitors in industries and in different other fields, is the most effective method to protect the metal from corrosion [17]. Corrosion inhibitors are compounds those cause lowering in the corrosion rates of a metal, when added in suitable amounts without significantly changing the concentration of other agents [245].

A great number of corrosion inhibitors have been studied for mild steel in acidic media. Most of the well known corrosion inhibitors are those organic compounds which containing N, O, S, P and multiple bonds or aromatic rings in their structure [104, 211, 212, 219]. The loosely bonded π electrons and lone pairs in these functional groups are key feature which determine the corrosion inhibition efficiency [46, 112, 231]. The organic compounds present in the inhibitor adsorb on the metal surface and block the active sites and thus reduce the corrosion rate considerably [194]. Besides having good corrosion inhibition property they are costly, non biodegradable and harmful for human beings and environment. The above drawbacks of synthetic corrosion inhibitors provoked the researchers to search for the new

cheap non-toxic, eco-friendly, green, naturally occurring plant products as corrosion inhibitors. Natural products have been reported as corrosion inhibitor for different metals [52, 75, 190, 257]. Extracts of plant roots, seeds, leaves, bark, fruits etc. have been reported in acidic media as corrosion inhibitors [3, 169, 170, 173]. The inhibitive action of natural plant products is due to the presence of organic compounds such as tannins, alkaloids, steroids, amino acids, flavanoids etc. [55, 73, 148]. Researchers have studied that inhibitive effect of some plant extracts is due to the adsorption of some phytochemicals present in the extract and formation of protective film on the metal [74, 167, 250].

Metallic corrosion has been studied in different acidic, basic and neutral medium using different gravimetric and electrochemical methods and different techniques. Hesham T.M. Abdel-Fatah et al. reported Miswak (*Salvadora persica*) aqueous root extract in 1.0 N sulfamic acid solution using mass loss and EIS techniques at 303-313 K temperature [2]. Pandian Bothi Raja et al. studied *Neolamarckia cadamba* extract in 1M HCl medium using PDP, EIS & SEM technique [191]. Aqueous extract of LD (*Lavandula dentata*) was investigated in 1M HCl solution by weight loss, EIS and Potentiodynamic polarization measurements and obtained 95% efficiency at 2wt% extract concentration. Polarisation studies indicate the phytochemical compounds present in LD extract acts as mixed type inhibitor [47].

Raphia hookeri (RH) gum exudates was studied in H₂SO₄ solution by weight loss and hydrogen evolution technique and 71.9% efficiency was obtained at 0.5g/L at 30⁰C [231]. Ehteram A Noor investigated fenugreek leaves extract in 2M HCl & 2M H₂SO₄ solution and found Langmuir adsorption in HCl and Temkin adsorption isotherms in H₂SO₄ solution [159]. *Hibiscus cannabinus* extract inhibitor for mild steel corrosion is reported by M.Ramananda Singh et al. in 0.5 M H₂SO₄ [218]. Ecofriendly Quinazoline derivative was studied by A.S. Fouda et al. in 2M HCl solution using EIS, PDP, electrochemical frequency modulation weight loss technique and 93.8% efficiency was obtained at 30⁰C [81].

Sesbania sesban extract (SSE) for carbon steel was reported as inhibitor in 1M HCl. 91.08% efficiency was obtained at 2.00 g/L at 25⁰C [22]. *Mentha rotundifolia* leaves extract for steel in 1M HCl in the range 298K-338 K was studied as corrosion inhibitor [113]. Inhibitive effect of gramine was studied in 1M HCl by PDP, EIS & gravimetric measurements [185]. *Calotropis gigantea* leaves extract was studied by using weight loss and electrochemical techniques in 1M HCl solution [62]. P.S. Desai investigated *Hibiscus rosa sinensis* leaves extract for mild steel in 1M HCl using gravimetric & electrochemical techniques [61]. Eddy and Mamza studied ethanolic extract of seeds and leaves of *Azadirachta indica* in H₂SO₄ solution using gravimetric, gasometric and IR methods [68]

90% inhibition efficiency was obtained in mild steel corrosion inhibition in 1N H₂SO₄ solution using *Nyctanthes arbortristis* leaves extract [197]. Aqueous extract of *Ammodaucus leucotrichus* fruit was reported as inhibitor for C38 steel in 1M HCl solution using EIS, EDP & weight loss method [145]. Maria V. Fiori Bimbi et al. studied pectin as eco friendly corrosion inhibitor [80]. Bei Ojan studied inhibitive effect of tannic acid on mild steel corrosion in sea water wet/dry cyclic conditions using weight loss & electrochemical methods [184]. Banana peel extract gave 98% inhibition efficiency at Zn⁺² (15ppm) by weight loss method [196].

Alka Singh and Kalpana S. have reported corrosion inhibition of iron surfaces by fenugreek leaves in CH₃COOH & citric acid solution by weight loss method [215,216]. Leaves extract of *Gossipum hirsutum L.* was studied by Olusegun K. Abiola et al. as green corrosion inhibitor for Al in HCl solution. They employed weight loss method for corrosion inhibition studies and 92% inhibition efficiency was obtained at 30⁰C [8].

Corrosion inhibitor for mild steel in 0.5M H₂SO₄ and 1M HCl solution was investigated by P.R. Vijayalakshmi, R. Rajakshmi and S. Subhashini using weight loss and electrochemical measurement techniques. The plant material taken was *Borassus flabellifer Linn.* (palmyra palm) shell

extract. 97.65% and 98.11% inhibition efficiency was obtained in 0.5 M H₂SO₄ and 1M HCl solutions at 3% (v/v) concentration of extract [240].

The inhibitive effect of *Aloe vera barbadensis* gel was studied on copper metal in hydrochloric acid solution using weight loss technique [92]. The inhibitive effect of leaves extract of African bread fruit in 1M H₂SO₄ solution was investigated by P.M. Ejikeme et al. for mild steel and aluminum metal [70]. They obtained 70.55% inhibition efficiency for mild steel and 78.56% inhibition efficiency for Al at 30⁰C in 5g/L concentration of BLE.

Extract of areal parts *Daucus carota* plant was investigated as green corrosion inhibitor for mild steel in hydrochloric acid medium using weight loss method and on theoretical analysis [111]. Maximum 95.72% inhibition efficiency was achieved at 2% (v/v) DCA extract at 5h of immersion at 30⁰C. Cantaloupe (*Cucumis melo*) juice and seed extracts has been investigated for cast iron corrosion inhibition in 1M hydrochloric acid solution [77] using hydrogen evolution measurements (HEM) and mass loss measurements. Adsorption process followed Langmuir adsorption isotherm.

It has been found that *Polyalthia longifolia* leaves extract is a good corrosion inhibitor for mild steel. 92% inhibition efficiency was obtained at 1.5% (v/v) concentration of extract in sulphuric acid medium and 87% inhibition efficiency was obtained at 1.5% (v/v) concentration of extract in hydrochloric acid medium [236,237]. I.J. Alinnor and P.M. Ejikeme investigated aqueous, ethanolic and acidic leaves extract of *Ocimum gratissimum* for corrosion inhibition of aluminum in hydrochloric acid medium using gravimetric method [20]. Narayana Hebbar et al. revealed the anticorrosion behavior of anti inflammatory ketosulfone drug for Zn in acidic medium by polarization and AC-impedance technique at 303-333K. Tafel plots were drawn in experiments which indicated that the drug is a mixed type inhibitor [93].

S. Aejitha, P.K. Kasthuri and P.Geethamani studied the corrosion inhibition efficiency of acidic leaves extract of *Commiphora caudata* (CC) in

1M HCl and 1M H₂SO₄ solutions separately using weight loss and electrochemical techniques [11]. Results showed that inhibitive property of CC is greater in hydrochloric acid solution.

D.G. Ladha et al. evaluated corrosion inhibition properties of aqueous extract of fenugreek seeds (FSE) (*Trigonella foenum graecum*) for aluminum in hydrochloric acid medium using gravimetric, galvanostatic polarization and EIS techniques. Results showed that inhibitive properties are due to the presence of phytochemical constituents such as trigonelline and sites present in extract. Adsorption process follows Langmuir adsorption isotherm [128].

Anticorrosive behavior of *Glycine max* (L.) oil is investigated in 2M H₂SO₄ solution by Bhawsar Jeetendra et al. using weight loss method for mild steel. 47.98% inhibition efficiency was obtained for 20 g/L at 298 K [44]. Abdulrasoul Salih Mahdi and Shymma Kadhem Rahem studied inhibitive properties of aqueous leaves extract of herb *Thymus vulgarize* (thyme) for reinforced steel in simulated chloride contaminated concrete pore solution (SCP) using open circuit potential and potentiodynamic polarization technique [140].

R. Karthik et al. studied the anticorrosion activity of *Cassia senna* for mild steel in 1M hydrochloric acid using weight loss, potential dynamic polarization, electrochemical impedance spectroscopy (EIS), scanning electron microscopy (SEM), UV-visible spectroscopy and x-ray diffraction (XRD) studies [108].

Nutan Kumpawat et al. reported the anticorrosive behavior of *Holy Basil* (Tulsi) for tin metal in HNO₃ solution by using leaves and stem extracts of different varieties by weight loss technique [127]. It has been reported by Kanchan Agarwal that *Fenugreek* leaves and Lemon peel extracts are good corrosion inhibitor for mild steel in 1M HCl solution using weight loss and electrochemical methods [13]. Inhibitive effect of seed extract of Kuchla

(*Strychnos nuxvomica*) has been reported for mild steel in hydrochloric acid solution by Ambrish Singh et al. [25].

Extract of rice husk ash was studied as a good corrosion inhibitor for mild steel in 1M H₂SO₄ and HCl solutions. The study was carried out using mass loss and atomic absorption spectroscopy (AAS) [18]. Iroha et al. revealed anticorrosive behavior of acetone extract of red onion skin for aluminum in 2 M hydrochloric acid solution using weight loss method. [101].

Yaro and Ibraheem revealed the inhibitive effect of Peach juice on low carbon steel corrosion in hydrochloric acid at different temperatures using weight loss and polarization techniques. 91% inhibition efficiency was obtained at 50⁰C in 50cm³/L inhibitor concentration [248]. E.E.Oguzie studied corrosion inhibitor effect of leaves extract of *Sansevieria trifasciata* on aluminum metal by gasometric technique [168].

It has been reported by L.Y.S. Helen et al. that *Aquilaria crassna* leaves extract is a good corrosion inhibitor for mild steel in 1M HCl medium using gravimetric method (weight loss method) [95]. Potato peel extract was investigated as an effective naturally available corrosion inhibitor for mild steel in 2M HCl by Taleb H. Ibrahim et al. [100].

Gopal Ji et al. studied corrosion inhibition effect of root extract of *Chlorophytum borivilianum* on mild steel in HCl and H₂SO₄ solution using various techniques viz. weight loss, electrochemical impedance spectroscopy, Tafel polarization and scanning electron microscopy [88].

Inhibition effect of biomass extract of *Petersianthus macrocarpus* plant was revealed by gravimetric electrochemical impedance and potentiodynamic methods on mild steel corrosion in HCl and H₂SO₄ solutions [17]. Saedah R. Al-Mhyawi found anticorrosive behavior of *Juniperus* plant extract for mild steel in H₂SO₄ solution using chemical (HE and WL) and electrochemical (PDP and EIS) methods [21].

M. Dekmouche et al. investigated corrosion inhibition effect of ethyl acetate extract of *Pistacia atlantica* galls in hydrochloric acid solution for mild steel using weight loss, polarization and AC impedance methods [60]. O. Benali et al. revealed the corrosion inhibition effect of tannin extract of *Chamaerops humilis* plant and potassium iodide on the corrosion of mild steel in 0.5 M H₂SO₄ solution using electrochemical methods [40]. S.A. Umoren et al. investigated synergistic inhibition effect between naturally occurring exudate gum and halide ions on mild steel corrosion in H₂SO₄ medium by hydrogen evolution techniques [234].

L. Afia et al. studied anticorrosive property of Argan Oil (AO) on corrosion of C38 steel by weight loss, electrochemical polarization and EIS methods [12]. Taleb Ibrahim et al. revealed that Thyme leaves extract showed 84% corrosion inhibition efficiency in 2M HCl solution for mild steel by using weight loss measurements and various electrochemical techniques [99].

Osmanthus fragran leaves extract was studied as corrosion inhibitor for carbon steel in hydrochloric acid medium using potentiodynamic polarization, electrochemical impedance spectroscopy (EIS), atomic force microscopy (AFM), Fourier transform infrared spectroscopy (FTIR) and quantum chemical calculations [135]. Bamboo leaf extract was studied by Xianghong Li et al. as corrosion inhibitor for steel in HCl and H₂SO₄ solutions [133]. Xianghong Li et al. also studied bamboo leaves extract as corrosion inhibitor in citric acid solution for steel and zinc using weight loss, potentiodynamic polarization curves and electrochemical impedance spectroscopy (EIS) methods. [134].

M. Faustin et al. investigated corrosion inhibition of C38 steel by *Geissospermum* leave alkaloids extract in hydrochloric acid solution using electrochemical studies [79]. Long chain alkyl carboxylates like stearate, palmitate and myristate were investigated as green corrosion inhibitor for magnesium alloy ZE41 corrosion in aqueous salt solution using potentiodynamic polarization, EIS, SEM and EDX analyses [64]. Black pepper extract was studied by M.A. Quraishi, Dileep Kumar Yadav and

Ishtiaque Ahamad as corrosion inhibitor for mild steel in hydrochloric acid solution using mass loss measurements, PDP, Linear polarization resistance and EIS [187]. Corrosion inhibition of aluminum by *Salvia judica* extract was investigated in 1M NaOH solution by E.M. Nawafleh et al. using weight loss method at different temperatures [154].

Deepa prabhu and Padmalatha Rao found *Garcinia Indica* extract (GIE) as novel green inhibitor for aluminium and 6063 aluminium alloy in 1.0 M H₃PO₄ solution using potentiodynamic polarization, Tafel extrapolation technique and EIS technique [182].

Olasehinde E.F. et al. studied corrosion inhibition effect of *Musa Sapientum* peels extract in HCl solution for mild steel using weight loss method [174]. I.E. Uwah, P.C. Okafor, V.E. Ebiekpe investigated corrosion inhibition effect of leaves bark and roots extract of *Nauclea latifolia* on mild steel in H₂SO₄ solution using weight loss and gasometric techniques [243].

L. Bammou et al. reported *Chenopodium ambrosioides* extract as good corrosion inhibitor for steel in sulphuric acid solution using weight loss method, potentiodynamic polarization and electrochemical impedance spectroscopy (EIS) measurements 94% inhibition efficiency was obtained at 4g/L [33].

M.Dhamani et al. investigated black pepper extract and its piperine as a corrosion inhibitor for C38 steel in 1M HCl by weight loss method [57]. J. Halambek et al. reported natural oil extract from *Lavandula angustifolia* L. as corrosion inhibitor for Al-3Mg alloy by weight loss, polarization measurements and SEM [91].

Corrosion inhibition effect of *Phyllanthus amarus* extracts from leaves and seeds for mild steel corrosion in acidic media has been studied by P.C. Okafor et al. [172]. M. Lebrini et al. reported *Oxandra asbeckii* alkaloids extract as an good corrosion inhibitor for C38 steel in 1M hydrochloric acid

medium using potentiodynamic polarization and electrochemical impedance spectroscopy (EIS) [130].

A.K. Satapathy et al. have been investigated the corrosion inhibition of mild steel by extract of *Justicia gendarussa* plant in hydrochloric acid solution by weight loss and electrochemical techniques. 93% inhibition efficiency was achieved with 150 ppm extract at 25⁰C [199]. Shivakumar and Mohana reported *Centella asiatica* extracts as green corrosion inhibitor for mild steel in 0.5 M sulphuric acid medium using gravimetric, polarization and EIS measurements. 95.08% inhibition efficiency was obtained at 303K [210]. *Spirulina platensis* was reported as green corrosion inhibitor for mild steel by C. Kamal and M.G. Sethuraman using weight loss, PDP method, EIS and SEM analysis [106].

3-[(4-amino-2-methyl-5-pyrimidinyl) methyl]-5-(2-hydroxyethyl)-4-methylthiazoliumchloride hydrochloride was reported as green corrosion inhibitor for copper in HNO₃ solution by Olusegun K. Abiola et al. using weight loss method [7]. M. Behpour et al. investigated two aleo-gum resin exudates from *Ferula assa-foetida* and *Dorema ammoniacum* as corrosion inhibitor for mild steel corrosion in acidic medium using weight loss, PDP and EIS methods [37]. Mahendra Yadav et al. reported synthesized thiourea derivatives for mild steel corrosion inhibition in 15% HCl solution using weight loss, PDP, EIS techniques [246]. Punita Mourya, Sitashree Banerjee and M.M. Singh reported *Tagetes erecta* (marigold flower) extract as green corrosion inhibitor for mild steel in 0.5 M H₂SO₄ solution using gravimetric, PDP and EIS measurements [151]. N.O. Obi-egbedi et al. investigated extracts of *Spondias mombin L.* as green corrosion inhibitor for aluminium in sulphuric acid medium using standard gravimetric technique [162].

L. Bammou et al. studied the corrosion inhibition effect of eco friendly cheap natural substance *Harmal* extract on C-steel in hydrochloric acid solution [32]. They used weight loss and electrochemical methods. Ambrish Singh et al. reported extract of *Zanthoxylum schinifolium* as an

effective corrosion inhibitor for N80 steel in CO₂ saturated 3.5% NaCl solution by using EIS, PDP, XRD, SEM techniques [24].

Mohammad Ismail et al. have been investigated the ethanolic leaves extract of solid waste of Genus *Musa* (Banana), Genus *Saccharum* (Sugarcane) and *Citrullus lanatus* (water melon) as a corrosion inhibitor for mild steel in HCl medium, using weight loss technique [102]. M. Lebrini et al. have been studied effect of alkaloids of plant *Isertia coccinea* on corrosion inhibition of C38 steel in 1M HCl solution using EIS and potentiodynamic polarization techniques [129].

Ambrish Singh et al. studied the corrosion inhibitive influence of *Ginkgo biloba* leaves extract on J55, N80, P110SS and C110 steels in 3.5 wt% NaCl solution with CO₂ using static high pressure high temperature (HPHT) autoclave. The steel surface was studied by XRD, SEM and contact angle measurement technique [23].

N. Soltani and M. Khayatkashani revealed corrosion inhibition property of leaf extract of *Gundelia tournefortii* plant on mild steel in 2M HCl and 1.0 M H₂SO₄ solutions using weight loss method, PDP, EIS techniques [222]. Inhibition effect of *Cnidioscolus chayamansa* leaves extract was investigated for Zn metal in 1N HCl by weight loss measurements by Bright et al. The Protective film on metal surface was studied by UV, FTIR, XRD and SEM-EDX techniques. [51]. Corrosion inhibition effect of leaves extract of *Artemisia holodendron* on mild steel was revealed by electrochemical potentiodynamic polarization measurements and EIS techniques [96].

A. Chetouani et al. revealed the corrosion inhibition property of jojoba oil on corrosion of iron in HCl solution using weight loss measurement and electrochemical polarization methods. [54]. A.A. Rahim et al. studied inhibitive action of mangrove tannins and phosphoric acid of pre-rusted steel in 3.5% NaCl solution [188]. Essential oils obtained from *Thymus satureioides* was tested as green corrosion inhibitor for template in 0.5M HCl solution by L. Bammou et al. [31]. Inhibitive effect of fruit peel extract of *Eugenia*

jambolana on zinc were reported by P.D.Rani et al. in 1N HCl medium using mass loss measurements [194]. Olusegun K. Abiola and A.O. James studied corrosion inhibiting effect of *Aloe vera* leaves extract by weight loss techniques, on the corrosion of zinc in 2M HCl solution [6].

F. Silvio de Souza et al. evaluated caffeine as green corrosion inhibitor for copper using PDP and EIS techniques in aerated 0.1M H₂SO₄ solution [214]. A.S. Yaro et al. showed the inhibitive properties of Apricot juice in 1M phosphoric acid to protect mild steel from corrosion using weight loss technique at different temperatures [249]. S. Sathiya, K. Bharathi and S. Geetha revealed corrosion inhibition of Al metal by *Datura metel* leaves extract in 1M HCl using chemical and electrochemical techniques [201].

S. Ananth Kumar et al. studied aqueous extract of *Magnolia champaca* flower [123] as corrosion inhibitor for mild steel in 0.5 M H₂SO₄ solution and *Magnolia champaca* stem extract [124] using weight loss, PDP, EIS methods for metal steel in 1M HCl. *Tectona grandis* acid seed extract has showed a green corrosion inhibitor for mild steel in HCl solution by G.R. Thusnavis et al. [229]. Gopal ji et al. studied corrosion inhibitive effect of *Argemone mexicana* plant leaves extract [89], *Capsicum annum* fruit extract [87], *Parthenium hysterophorus* plant leaves extract [86] for mild steel in HCl solution.

S. Ananth Kumar et al. also studied the leaves extract of *Oxystelma esculentum* plant as corrosion inhibitor for mild steel in 0.5 M H₂SO₄ solution using weight loss, EIS and polarization techniques [125]. It has been shown that ethanolic extract of *Ricinus communis* leaves is good corrosion inhibitor for mild steel in 100 ppm NaCl solution [202]. Vitamin B-12 solution was tested by S. Ananth Kumar et al. as corrosion inhibitor in 0.5 M H₂SO₄ for mild steel using weight loss, PDP and EIS measurements [27]. A.M. Al-Fakih, M.Aziz and H.M.Sirat were reported the acidic extract of turmeric and ginger rhizomes separately as corrosion inhibitor for mild steel in 1M HCl solution using weight loss and PDP measurements. [19]. Aqueous extract of ginger has also been reported as inhibitor for mild steel in 1M HCl

by weight loss, open circuit potential (OCP), linear and Tafel polarization techniques [76].

Methanolic extract of *Alpina galinga* was tested against mild steel in 0.5 N H₂SO₄ for corrosion inhibition by S.Ananth Kumar et al. using weight loss, PDP and electrochemical impedance measurements [126].

Bryophyllum pinnatum Leaves extract has been proved as a corrosion inhibitor for mild steel in 0.5 M HCl solution by Dakeshwar Kumar Verma and Fahmida Khan using gravimetric and scanning electron microscope technique [238]. Leaves extract of *Millingtonia hortensis* for mild steel corrosion in 1N HCl and 1N H₂SO₄ solutions using mass loss measurements was studied by S. Kulandai Therese and V.G. Vasudha [119].

E.I. Ating et al. also studied leaves extract of *Ananas Sativum* as green inhibitor for aluminum in HCl solutions using weight loss and hydrogen evaluation method [28]. *Cocos nucifera* petiole extract was investigated as inhibitor of corrosion for mild steel in 0.5M H₂SO₄ and 1M HCl solution using mass loss, polarization and electrochemical impedance techniques [241]. The leaves extract of *Carcia papaya* and *Camellia sinensis* (green tea) extract were investigated as green corrosion inhibitors for α β (duplex) brass in 1M Nitric acid solution using weight loss and potential measurement techniques [138]. Extract of leaves and berries of *Solanum nigrum* were investigated as green inhibitor for zinc in 0.5N HCl [176] using weight loss, thermometric and gasometric methods. *Vernonia amygdalina* (bitter leaf) was tested for zinc plate corrosion inhibitor in 2M HCl solution by weight loss, gasometric and potentiostatic polarization [180].

A.Y. El-Etre et al. studied aqueous extract of *Lawsonia* (heena) leaves as corrosion inhibitor for C-steel, nickel and zinc in acidic, neutral and alkaline medium using polarization technique [73]. *Morinda tinctoria* leaves extract has shown corrosion inhibition property for mild steel in HCl medium using weight loss and AC impedance studies [118].

The corrosion controlling capacity of beet root extract was investigated in well water in the absence and presence of Zn^{+2} ion for carbon steel by mass loss method [205]. *Azadiractha indica*, ethanolic extract of leaves and seeds were tested as corrosion inhibitor for mild steel in H_2SO_4 solution using weight loss and gasometric techniques [68]. A.S. Founda et al. studied methanolic extract of barks and rhizomes of *curcum* plant as a green inhibitor for steel in 3.5% NaCl and 16ppm Na_2S solution by PDP, EIS, electro chemical frequency modulation (EFM) techniques [82]. Corrosion inhibition by *Ficus abutilifolia* plant extract on N-80 oil well tubular steel was studied by weight loss technique by G.Abubakar et al. [10] in 15% HCl solution. *Cassia auriculata* flowers extract was tested as corrosion inhibitor for Al and mild steel in 2M HCl solution by weight loss, polarization and impedance studies by A. Rajendran and C. Karthikeyan [192]. *Ginseng* root extract has been proved as eco-friendly corrosion inhibitor for AA 1060 aluminum alloy in HCl solution by weight loss method [164].

Hui Cang et al. studied *Aloes* leaves extract for mild steel corrosion in 1M HCl solution by weight loss PDP, EIS techniques [97]. S.M. Mahdi showed pomegranate peel powder as inhibitor for mild steel in 5% HCl and 5% H_2SO_4 solutions using weight loss method [141]. *Solanum trilobatum* was tested as green inhibitor for aluminum corrosion in 1M NaOH medium using weight loss, hydrogen evaluation, EIS and polarization methods [84]. F.S. de souza and A. Spinelli studied naturally occurring biological molecule caffeic acid as corrosion inhibitor for mild steel in 0.1 M H_2SO_4 solution using weight loss, PDP, EIS and Raman sopectroscopy [59]. M.Znini et al. revealed the corrosion inhibition effect of essential oil obtained from *Salvia aucheri mesatlantica* for mild steel corrosion in 0.5 M H_2SO_4 solution using weight loss and electrochemical polarization measurements [254].

A.S. Abdulrahman et al. have investigated corrosion inhibition of mild steel in sulphuric acid solution by leaves extract of *African prequentina* using gravimetric, gasometric and thermometric measurements [4].

Seed extract of *Psidium guajava* fruit (guava) was studied by K.P. Vinod Kumar et al. as inhibitor for carbon steel in HCl medium using weight loss measurement [120]. S. Leelavathi and R. Rajalakshmi revealed the corrosion mitigating property of leaves extract of *Dodonaea viscosa L.* on mild steel corrosion in 1M HCl and 0.5M H₂SO₄ using mass loss and electrochemical measurements [131]. Nasrin Soltani et al. studied leaves extract of *Salvia officinalis* as inhibitor for 304 stainless steel in 1M HCl solution using weight loss, PDP, EIS and Tafel polarization studies [224]. M. Sangeetha et al tested aqueous extract of asafoetida for protection of mild steel corrosion in sea water using weight loss method [195]. Bentiss et al. studied 4H-1,2,3-triazole derivatives as corrosion inhibitors for mild steel in normal HCl solution by using weight loss and AC impedance measurements and polarisation curves. Results showed that 4H-1,2,3-triazole derivatives obeys Langmuir adsorption model on mild steel surface [41].

The corrosion inhibition efficiency of pyridazine compounds in 0.5M H₂SO₄ medium were studied by Bouklah et al. using weight loss method at various temperatures and revealed that inhibition efficiency increases with increase in concentration. Pyridazine compounds followed Langmuir adsorption isotherm on mild steel surface [48]. Corrosion inhibition of Armco iron in HCl solution was studied by using four surfactants: tetradecyl trimethyl ammoniumiodide (TTAI), tetradecyl trimethyl ammoniumbromide (TTAB), hexadecyl trimethyl ammonium bromide (HTAB) and dodecyl trimethyl ammonium bromide (DTAB). They observed that protection efficiency increases with increase in inhibitor concentration and length of alkyl chain and these surfactants followed Langmuir adsorption isotherm on Armco iron surface [50].

Cristofari et al. studied essential oil extracted from *Pulicaria mauritanica* as corrosion inhibitor for mild steel in 0.5M H₂SO₄ medium. They employed weight loss, EIS, electrochemical polarization methods. Carvatan acetone was found predominant component in essential oil in 87.3%. 91.5% inhibition efficiency was found at 2g/L essential oil

concentration. Spontaneous adsorption of inhibitor was observed and adsorption followed Langmuir adsorption isotherm [56].

Eddy investigated corrosion prevention properties of ethanolic extract of *Garcinia kola* and *Cola nitida* using weight loss and thermometric methods for mild steel in H₂SO₄ medium. Physical adsorption mechanism was proposed from inhibition efficiency trend with temperature and Langmuir adsorption isotherm was followed by inhibitor [69]. Ekanem et al. studied pineapple leaves extract as mild steel corrosion inhibitor in HCl solution at 30⁰C- 60⁰C temperature range using weight loss and hydrogen evolution methods. Inhibition efficiency increases with increase in temperature. Extract adsorption followed Langmuir isotherm and chemisorption is also proposed by the trend of inhibition efficiency with temperature [71].

4-phenylsemicarbazide (4PSC) and semicarbazide (SC) were found significant corrosion inhibitors for mild steel in HCl solution by Ita and Offiong. They used weight loss and hydrogen gas evolution measurements and found that 4PSC showed 82% inhibition efficiency and SC showed 66% inhibition efficiency [103].

Mimosa tannin was tested as corrosion inhibitor for low carbon steel in sulphuric acid medium by using weight loss method in the range of 20⁰C to 60⁰C temperatures and observed that adsorption of tannin followed Temkin, Freundlich and Freundlich adsorption isotherms [147]. Tryptamine (TA) was found as effective corrosion inhibitor for ARMCO iron in 0.5 M deaerated H₂SO₄ solution in 25⁰C-55⁰ C temperature range. They employed potentiodynamic curves and electrochemical impedance spectroscopy (EIS) methods. TA adsorption followed Bockris – Swinkels' adsorption isotherm (X=1) [150].

Corrosion inhibition efficiency of aqueous extract of fenugreek leaves and seeds were studied by Ehteram A. Noor in HCl and H₂SO₄ solution for mild steel and revealed that both extract act as anodic type

inhibitors. He observed that inhibition efficiency was found greater in HCl than in H₂SO₄ solution. He employed electrochemical impedance spectroscopy and potentiodynamic polarization measurements for study [158].

Okafor et al. studied leaves (LV), root (RT) and seeds (SD) extract of *Azadirachta indica* as corrosion inhibitor for mild steel in H₂SO₄ solution using weight loss and gasometric techniques. Inhibition efficiency followed SD > RT > LV trend and increases with increase in extract concentrations. Adsorption followed Freundlich adsorption isotherm [171].

Leaves extract of *Bridelia retusa*, *Murraya koenigii*, *Embilica officinalis* were studied as corrosion inhibitor for mild steel in H₂SO₄ and HCl solutions respectively [178, 186, 198]. Sharma et al. have also studied mature leaves extract of *Azadirachta indica* as corrosion inhibitor for mild steel in 2N HNO₃ solution at 30⁰C and 60⁰C respectively and extract followed Frumkin adsorption isotherm [209].

Fruit extract of Shahjan (*Moringa olifera*) was investigated as a good corrosion inhibitor for mild steel corrosion in HCl solution using weight loss, EIS, linear polarization and potentiodynamic polarization techniques (Tafel). Inhibitor extract obeyed Langmuir adsorption isotherm [217].

The essential oils extracted from aerial parts of *Mentha spicata* L. and *Lavandula multifida* L. were observed as corrosion inhibitor for steel in 1M HCl and 0.5M H₂SO₄ solutions using weight loss method and electrochemical polarization measurements studies by Znini et al. In studies they found that these natural oils act as mixed type of inhibitors and followed Langmuir adsorption isotherm [255, 256].

Rajendran has revealed that flower extract of *Nerium oleander* contains anticorrosive property for mild steel and aluminium in 2M HCl at

$30^{\circ} \pm 1^{\circ} \text{C}$ and observed that inhibition percentage increases with increase in extract concentration [193].

Corrosion inhibition property of aqueous extract of water hyacinth leaves extract- Zn^{+2} system with and without TSC (Tri Sodium Citrate) was studied by Kavitha and Manjula [110] and Kavitha et al. [109] respectively in aqueous environment containing 60 ppm Cl^{-} ion for mild steel. Shanab et al. studied *Eichhornia crassipes* as corrosion inhibitor for Magnesium alloy (AZ31E) in 3.5% NaCl solution [207] while Ulaeto et al. reported leaves and roots extract of *Eichhornia crassipes* as corrosion inhibitor for mild steel in hydrochloric acid medium using gasometric technique [230] and Oloruntoba Daniel Toyin investigated corrosion inhibitive property of leaves extract of water hyacinth for 1014 steel in chloride environment [175].

Sudesh Kumar and Suraj Prakash Mathur had investigated ethanolic extract of leaves, latex and fruit of *Calotropis procera* as corrosion inhibitor for aluminium in sulphuric acid medium [121] while Bharthi et al. reported leaves extract of *Calotropis procera* as corrosion inhibitor for aluminium in 1 M HCl solution [43]. Sudesh kumar et al. also studied corrosion controlling property of alcoholic extracts of leaves, latex and fruit extract of *Calotropis procera* and *Calotropis gigantea* for mild steel in basic solution by mass loss method and thermometric method [122]. Raja and Sethuraman have also reported corrosion inhibitive property of *Calotropis procera* for mild steel in sulphuric acid medium [189].

Sharma et al. studied ethanolic extract of leaves, stem bark and fruit of *Lantana camara* was studied as corrosion inhibitor for aluminium in different concentrations of sulphuric acid solution [208], Petchiammal and Selvaraj have reported anticorrosive effect of fruit peel extract of *Lantana camara* in 1M HCl for mild steel and found maximum 85% inhibition efficiency [179]. Besides these Nkiko et al. also reported *Lantana camara* leaves extract as corrosion inhibitor for Zinc alloy in H_3PO_4 solution [157]

Although large amount of research studies have been done on corrosion inhibition of mild steel in aggressive media by various natural substances, but still there is thirst to search newer and better green corrosion inhibitors which are very less or not studied. To keep this in view, the present work has been undertaken which enlightens, “Studies on potential green corrosion inhibitors for mild steel in different media”, for which no reference could be found in literature reviewed so far.

CHAPTER - 2

MATERIALS, METHODS AND METHODOLOGY

Materials:

Selection of plants as corrosion inhibitors:

Aqueous extract of *Lantana camara* leaves (AELCL), *Nerium oleander* leaves (AENOL), *Calotropis procera* leaves (AECPL) and Water hyacinth (*Eichhornia crassipes*) (AEWHL), 1M HCl solution, 1M H₂SO₄ solution and mild steel cylindrical specimens of, borosil beaker (250 ml), volumetric flasks, measuring cylinders, different emery papers (Marks 80 to 120 grades), distilled water, electronic balance (citizens model CY204), thermostat (12 holes double walled), electronic oven (14') and desiccators (210 ml).

The detailed descriptions of the selected plants for corrosion studies of mild steel are explained below.

1. Lantana camara:

Plant classification

Kingdom : Plantae

Division : Magnoliophyta

Class : Magnoliopsida

Order : Lamiales

Family : Verbenaceae

Genus : Lantana

Species : Lantana camara L.

Lantana camara also known as wild-sage, big-sage (Malaysia), red-sage (Caribbean) and tick-berry (South Africa). It is a flowering plant of Verbenaceae family native to tropical and subtropical America but few taxa are indigenous to tropical Asia and Africa [105]. It is a low erect shrub of 2-4 meters in height. Leaves are ovate, bright green in color with rough and hairy surface and give pungent smell when crushed. It has flowers of various colours like white,

yellow, cream, orange, pink, purple, red. The fruit of *Lantana camara* L. is greenish blue-black colour, round shining with 5-7 mm in diameter.

Boiled leaves of *Lantana camara* reduce swellings and pain of the body. Lotion prepared from its astringent bark is used in cutiginous eruptions and leprous ulcers. Alkaloids obtained from its leaves reduce blood pressure, accelerate deep respiration and stimulate intestinal movements in experimental animals.

Lantana camara is an invasive species and a nutritious weed and well often out-compete other desirable species, leading to a reduction in bio-diversity. It excretes chemicals (allelopathy) which retards the growth of surrounding plants by inhibiting germination and root elongation [15]. It is toxic to livestock and form thickets, which greatly reduce productivity of agriculture land. The active substance which causes toxicity in grazing animals is pentacyclic triterpenoids which causes liver damage and photosensitivity [34].

The plant has been used to treat variety of disorders. In Asian countries, leaves were used to treat cuts, rheumatism and ulcers [200]. Traditionally it is used as tonic, in abdominal pains, as anthelmintic and insecticide [247]. The plant is reported to contain various compounds like triterpenoids [200, 35], flavonoids [200, 239], amino acids [247], saponins, steroids [200] etc.

2. Nerium Oleander:

Plant classification

Kingdom : Plantae

Division : Magnoliophyta

Class : Magnoliopsida

Order : Gentianales

Family : Apocynaceae

Genus : Nerium

Species : Nerium oleander L.

Its common name is Oleander or Kaner. It is an evergreen shrub, belongs to Apocynaceae family. It is also cultivated as ornamental plant. It is found in Mediterranean region, and in Southeast Asia and Southern Europe. It has long narrow dark green leaves with different colored flowers like white, pink, red, light yellow.

Nerium is one of the most poisonous plant and contain many toxic compounds which have been reported lethal to people and to infant or a child. The most significant of these toxins are Oleandrin and nerin, which are cardiac glycosides [36], which can cause numbness by blocking the receptors in skin. Its toxicity remains even after drying of Oleander. The leaves and flower have cardio tonic, diaphoretic, anticancer, diuretic, antifungal [244]. Oil from the root bar is used in skin diseases and leprosy. Seeds are poisonous and used in dropsy and rheumatism. The whole plant is said to have anticancer properties [5]. The most well known effect of oleander is due to two glycosides, nerin and an alkaloid olendrin, which have cardio stimulatory action [253] and to the glycosides, gentiobiosyl-olendrin, gentiobiosyn-nerigoside and gentiobiosyl-beaumontoside extracted from its leaves [144]. Its lymph is rich in minerals [30] and α -tocopherol, an important antioxidant [98]. Olender flowers in fresh and dried condition shows antinociceptive activity [252].

3. Calotropis procera:

Plant classification

Kingdom : Plantae

Division : Magnoliophyta

Class : Magnoliopsida

Order : Gentianales

Family : Asclepiadaceae

Genus : Calotropis

Species : Calotropis procera

Calotropis procera belongs to the Asclepiadaceae family. It has many common names like swallow wort in English, Madar in Hindi, Alarka in Sanskrit. Besides it, it is also known as Apple of Sodom, rubber bush etc. It grows in warm dry climate in sandy and salty soil. It can grow as weed in cultivated areas. It also grows in rubbish heap, waste land, in sand dunes and along roadside. Calotropis procera is found in Pakistan , Nepal, India, Afghanistan, Algeria, Iran, Iraq, Isreal, Kenya, Saudi Arabia, Nigeria , Oman , Vietnam , Kuwait, Yemen , United Zimbabwe and Arab Emirates .

Calotropis procera is erect, tall, large perennial shrub of height approximately 4-5 m and secretes milky latex when cut. Leaves are broadly ovate-oblong, opposite thick, green covered with fine pubescent hair on young. It has purple flowers. Phytochemical studies show that it contains several compounds. Its leaves and stock contains calotropin and calotropagenin. White flowers contain calotrophenyl acetate.

Chemical investigation shows that plant conatins cardiac glycosides catotropogenin , calotropin , uscharin , calotoxin and calactin [14]. It also has been investigated for cardenolides [204] and anthocyanins [16].

Calotropis procera shows medicinal properties. It shows anticancer and insecticidal activity. The flowers show hepatoprotective activity [206], anti-inflammatory, antipyretic, antimicrobial effects and larvicidal activity [146]. The latex is reported to show analgesic and wound healing activity [63], anti-inflammatory and anti-microbial activity [203] while roots show anti-fertility property [107].

4. Water Hyacinth:

Plant classification

Kingdom : Plantae

Division : Magnoliophyta

Class : Liliopsida

Order : Liliales

Family : Potentillaceae

Genus : Eichhornia Kunth

Species : Eichhornia crassipes

Water hyacinth (*Eichhornia crassipes*) is a perennial aquatic herb belongs to Potentillaceae family. It is free floating water plant. It has glossy green leathery leaves, inflated petioles and hairy roots. It has funnel shaped flowers having six petals of light bluish purple flower with yellow center.

It is native to South America and a worst and noxious aquatic weed. It grows rapidly and forms impenetrable mats which cover the whole waterways. It is an aggressive invader and forms impenetrable mats on the entire pond surface, block water transport, increase water evaporation and transpiration, block irrigation canals, decrease the oxygen and sunlight to the aquatic plants and aquatic animals and thus creates difficulties in survival of aquatic plants and animals and reduce the aquatic biodiversity. So water hyacinth is challenging the ecological stability of fresh water bodies [116] out competing all other species growing in the vicinity, posing a threat to aquatic biodiversity [177]. Its mats prevent the transfer of oxygen from air to water surface or decrease oxygen production by other plants and algae [242]. Low level of oxygen results in the release of phosphorus from sediments which accelerate eutrophication and lead to increase in water hyacinth or algal bloom [45]. Death and decay of water hyacinth vegetation deteriorates water quality and quantity of potable water and increases treatment costs of drinking water [149, 155,177].

Water hyacinth can uptake heavy metals like Cr, Co, Ni, Pb and Hg from industrial waste water [9, 142, 220, 235] and used for bio cleaning of water. It is highly tolerant to these. Beside this it can remove toxins like cyanides, which is

beneficial in gold mining operations [66]. Phytochemical studies showed presence of alkaloids [156], compounds of nutritional values like phenolic flavonoids, glutathione [143] and other metabolites.

Acids selected as different media:

1. Hydrochloric Acid (HCl)

Hydrochloric acid is a pungent smelling colourless solution of HCl gas in water. It is monoprotic acid which gives one H^+ ion in solution. It is highly corrosive acid. The name “Hydrochloric Acid” was coined by Joseph Louis Gay-Lussac, the French chemist in 1814. Hydrochloric acid is a binary mixture (two-component) of HCl and H_2O has a constant boiling azeotrope at 20.2% HCl and $108.6^\circ C$ ($227^\circ F$). It is prepared in solutions up to 38% HCl (concentrated grade). Higher concentrations just over 40% has high evaporation rate and thus storage and handling is difficult. 38% HCl has 1.189 kg/L density, BP $48^\circ C$ and viscosity 2.10 mPa.S. these above data are at $20^\circ C$ and 1 atm pressure. Hydrochloric acid is used in pickling of steel, removing rust from iron, production of organic and inorganic compounds such as vinyl chloride, bisphenol A and numerous pharmaceutical products, iron (III) chloride, polyaluminium chloride (PAC) (both used as flocculation and coagulation agents in sewage treatment), calcium chloride salt, nickel (II) chloride, zinc chloride etc.

2. Sulphuric acid (H_2SO_4):

Sulphuric acid is highly corrosive, diprotic acid. It is a mineral acid, having formula H_2SO_4 and molecular weight 98.079 g/mol. It is colourless or slightly yellow viscous liquid and soluble in water. It is also known as oil of vitriol. 98% sulphuric acid has 1.83 kg/L density and 18 mol/L concentration. Sulphuric acid when reacted with SO_3 forms oleum ($H_2S_2O_7$). 98% sulphuric acid has < 1 mm Hg vapor pressure at $40^\circ C$. Anhydrous H_2SO_4 is very polar liquid having a dielectric constant around 100 and shows high electrical conductivity due to autoprotolysis. It has wide range of applications like domestic acidic drain cleaner, as electrolyte in lead acid batteries, fertilizers production, oil refining,

mineral processing, waste water processing, as dehydrating agent, production of dyes, detergents, insecticides, antifreeze, in pharmaceutical industries etc.

Methods:

The leaves of *Lantana camara*, *Calotropis procera*, *Nerium oleander* and Water hyacinth (*Eichhornia crassipes*) were collected from local areas and pond of Kota city Rajasthan (India), city. These were washed and air-dried in shed for 6-7 days, crushed and grounded mechanically and converted into fine powdered form.

Preparation of AELCL

For preparation of AELCL (aqueous extract of the *Lantana camara* leaves): 20 g of dried and grounded *Lantana camara L.* leaves were heated between 70°C-80°C in 500 ml of distilled water for one hour in round bottom flask. The extract was left overnight and then filtered and made up to 500 ml with distilled water.

Preparation of AECPL:

Stock solution of AECPL (aqueous solution of *Calotropis procera* leaves): 20 grams of dried grounded leaves powder of *Calotropis procera L.* was heated between 70°C-80°C in 250 ml of distilled water for one hour in round bottom flask. The extract was left overnight and then filtered and made up to 250 ml with distilled water.

Preparation of AENOL:

For preparation of the stock solution of AENOL (aqueous extract of *Nerium oleander* leaves): 20g of dried grounded leaves powder of *Nerium olender L.* was heated between 70°C-80°C in 200 ml of distilled water for one hour in 250 ml round bottom flask with air condenser The extract was left overnight and then filtered and made up to 200 ml with distilled water.

Preparation of AEWHL:

For preparation of the stock solution of AEWHL (aqueous extract of water hyacinth (*Eichhoria crassipes*) leaves): 20g of dried grounded leaves powder of

Eichhoria crassipes was heated between 70°C-80°C in 500 mL of distilled water for one hour in round bottom flask. The extract was left overnight and then filtered and made up to 500 ml with distilled water.

Preparation of different acidic media:

Acidic media for corrosion studies of mild steel were prepared by AR grade HCl (Merck Ltd), and H₂SO₄ (Merck Ltd). 1M standard solution of each acid was prepared using de-ionized distilled water.

Determination of weight loss:

For corrosion studies of mild steel specimens gravimetric technique for weight loss described by Mattson [112] was used. For weight loss cylindrical mild steel specimens of various dimensions (5 cm in length and 0.80 cm in diameter), (4.7 cm in length and 0.50 cm diameter), (4.9 cm in length and 0.70 cm in diameter), (4.8 cm in length and 0.60 cm in diameter) were taken. The above specimens were abraded with different emery papers, degreased in acetone and washed with distilled water dried and the constant weight (W_1) was recorded by electronic balance.

Cylindrical mild steel specimens were hanged by plastic thread and glass rod in 100 ml of different acidic media in 250 ml borosil glass beaker, containing specific amount of aqueous extracts of leaves of four different plants.

After one hour of immersion time the specimens were removed from acidic media, washed with distilled water ,dried and again abraded with emery paper to remove the upper material and weighed accurately (W_2) by electronic balance. Weight loss (ΔW) is calculated by ($W_1 - W_2$). The different employed concentrations range of the aqueous extracts of leaves of the 4 plants were 2%-6% (v/v) for AELCL, 1%-8% (v/v) for AECPL, 1%-10% (v/v) for AENOL and 1%-5% (v/v) for AEWHL extract. The corrosion inhibition experiments were performed at four different temperature ranges (30°C, 40°C, 50°C, 60°C).

Determination of Corrosion Rates:

In 1M HCl and 1M H₂SO₄ values of Corrosion Rates (CR) for mild steel specimens in various concentrations of inhibitors at four different studied temperatures were calculated by following equation (1) [159].

$$C R = \left(\frac{\Delta W}{A t} \right) \quad (1)$$

Where ΔW is the weight loss calculated by the difference of initial weight (W_1) and final weight (W_2) of mild steel specimen after treating with different acidic media containing different concentrations of inhibitor solutions. A is the surface area of different specimen and t is immersion time in minute.

Determination of Inhibition Efficiency (IE %):

From the above calculated corrosion rate values (CR) the inhibition efficiencies for the mild steel specimens in 1M HCl and 1M H₂SO₄ solutions containing different amount of inhibitor solutions at various temperatures are calculated by the following equation (2) [159,246].

$$I E \% = \left(\frac{C R_{\text{blank}} - C R_{\text{inh}}}{C R_{\text{blank}}} \right) \times 100 \quad (2)$$

Where $C R_{\text{blank}}$ and $C R_{\text{inh}}$ are the corrosion rates in the absence and presence of the different inhibitors at various concentrations.

Determination of Kinetic Parameters:

Kinetic parameters K (rate constant) and B (reaction constant) are calculated by the straight lines obtained in the graph between the log of inhibitor concentrations and the log of corrosion rate values at different temperatures. The following equation (3) is used to determine the kinetic parameters [114,160].

$$\log C R = \log K + B \log C_{\text{inh}} \quad (3)$$

where K is the rate constant and equals to CR when the inhibitor concentration is unity. B is the reaction constant which is the measure of inhibitor effectiveness and $C R_{\text{inh}}$ is the concentration in (v/v %) (ml/ 100ml) of four different inhibitors.

Determination of the thermodynamic and activation parameters:

The thermodynamic and activation parameters like the Activation Energy (E_{act}), enthalpy of activation (ΔH^*) and entropy of activation (ΔS^*) were calculated for mild steel dissolution process,

Activation energy (E_{act}):

Activation energy was calculated using the following Arrhenius equation (4) [232,246].

$$\log CR = \log A - \left(\frac{E_{act}}{2.303 RT}\right) \quad (4)$$

Where A is the Arrhenius pre exponential factor, CR is corrosion rate, T is absolute temperature in Kelvin and R is the universal gas constant. The slope of graph plotted between log CR and 1/T gives the value of activation energy at various studied temperatures.

Enthalpy of activation (ΔH^*) and entropy of activation (ΔS^*):

The value of enthalpy of activation (ΔH^*) entropy of activation (ΔS^*) can be calculated by the following transition state equation (5) [232,246].

$$\log \left(\frac{CR}{T}\right) = \left[\log \left(\frac{R}{Nh}\right) + \left(\frac{\Delta S^*}{2.303 R}\right) \right] - \left[\frac{\Delta H^*}{2.303 RT}\right] \quad (5)$$

Where, CR is corrosion rate, N is Avogadro`s number, T is absolute temperature and R is the universal gas constant, h is Planck`s constant.

A plot between $\log (CR/T)$ and $(1/T)$ gives a straight line with slope of $\left(\frac{\Delta H^*}{2.303 RT}\right)$ and intercept of $\left[\log \left(\frac{R}{Nh}\right) + \left(\frac{\Delta S^*}{2.303 R}\right)\right]$ from which the values of enthalpy of activation (ΔH^*) and entropy of activation (ΔS^*) are calculated.

Absorption Isotherms:

Adsorption has significant role in corrosion inhibition processes. Inhibitors generally physically or chemically adsorbed on metal surface and slow down the metal dissolution process. To understand the nature of adsorption, the obtained

surface coverage θ were fitted in different adsorption isotherms like Langmuir adsorption isotherm, Temkin adsorption isotherm, Freundlich adsorption isotherm.

Many researchers have used the Langmuir adsorption isotherm to study the adsorption process. The mathematical expression for Langmuir adsorption isotherm is according to equation (6) [38, 83, 161, 185, 237]

$$\frac{C_{inh}}{\theta} = \frac{1}{K_{ads}} + C_{inh} \quad (6)$$

Rearranging the above equation (6)

$$\frac{\theta}{1-\theta} = K_{ads} C_{inh} \quad (7)$$

$$\text{Or } \log\left(\frac{\theta}{1-\theta}\right) = \log(K_{ads}) + \log(C_{inh}) \quad (8)$$

where C_{inh} is the inhibitor concentration in (ml/L) and K_{ads} (ml^{-1}L) is the equilibrium constant of adsorption, θ is the degree of surface coverage and is equal to $\text{IE}\% / 100$. A straight line is obtained between (C_{inh}/θ) and C_{inh} or between $\log(C_{inh}/\theta)$ and $\log C_{inh}$ values, if the adsorption process follows Langmuir adsorption isotherm.

Freundlich adsorption isotherm is given by the following equation (9) and (10)[117].

$$\theta = K_{ads} \cdot C_{inh} \quad (9)$$

$$\log\theta = \log(K_{ads}) + n \log C_{inh} \quad (10)$$

Where $\theta < n < 1$, θ is the degree of surface coverage and C_{inh} is the concentration of the inhibitor, K_{ads} is the equilibrium constant in the adsorption process. A straight line is obtained between the logarithm of degree of surface coverage (θ) and logarithm of inhibitor concentration C_{inh} in Freundlich isotherm.

Temkin adsorption is given by the following equation (11) [152, 172]

$$-2a\theta = \ln(K_{ads}) + \ln(C_{inh}) \quad (11)$$

Where a is the molecular interaction factor in adsorbed layer, K_{ads} is equilibrium constant and C_{inh} is the inhibitor concentration and θ is the degree of surface coverage.

Determination of Adsorption Parameters:

Gibbs Energy ΔG_{ads} :

The values of K_{ads} obtained from adsorption isotherms is related to Gibbs energy by the following equation (12) [115,159].

$$K_{ads} = \frac{1}{C_{H_2O}} \exp(-\Delta G_{ads} / RT) \quad (12)$$

It can also be written as

$$\Delta G_{ads} = -2.303RT \log (K_{ads} \cdot C_{H_2O}) \quad (13)$$

Where, C_{H_2O} is the concentration of water in (ml/L) in metal solution surface, R is Universal gas constant and T is the absolute temperature.

Determination of Enthalpy of Adsorption(ΔH_{ads}) and Entropy of Adsorption (ΔS_{ads}):

Enthalpy of adsorption (ΔH_{ads}) and entropy of adsorption (ΔS_{ads}) are calculated by the following basic equation (14) [72,159].

$$\Delta G_{ads} = \Delta H_{ads} - T \Delta S_{ads} \quad (14)$$

The intercept of the graph between the ΔG_{ads} and absolute temperature T , gives the values of ΔH_{ads} . Values of ΔS_{ads} were obtained by putting the values of ΔH_{ads} in equation (14) at different temperatures.

Methodology

For investigating the effective natural eco-friendly, cost effective natural corrosion inhibitors for mild steel 4 different plant species as *Lantana camara*, *Calotropis procera*, *Nerium oleander* and *Eichhoria crassipes* (water hyacinth) were selected. The plant leaves of these plants were collected from local land area and

ponds of Kota city, washed, air dried in shed for 6-7 days, crushed mechanically into fine powder and their aqueous extracts were prepared by heating (as specified above mentioned quantity of leaves powder)in distilled water using round bottom flask between 70°C-80°C for one hour. The extracts were left overnight and then filtered and made up to the mark by adding required quantity of distilled water. Analytical grade (Merck Ltd) hydrochloric acid and sulphuric acid were taken to prepare acidic media. 1M solution of each acid was prepared in distilled water for experimental studies. The weight loss method, described by Mattson [112] was used to calculate the corrosion rates. For this cylindrical mild steel specimen of different dimensions were taken for different plant species. The length and diameter of these specimens were (5cm and 0.80cm), (4.9cm and 0.70cm), (4.8cm and 0.60 cm), (4.7cm and 0.50cm). These cylindrical specimens were abraded with series of emery papers degreased with acetone and washed thoroughly with distilled water and finally dried in hot air till constant initial weight (W_1) is recorded from electronic balance(citizen model CY 204). These specimens were hanged with plastic thread and glass rod in 100 ml acidic solution for 1 hour in 250 ml borosil beaker in presence and absence of different concentrations (v/v %) of aqueous extracts of inhibitors at different temperatures. After one hour specimens were removed, washed with distill water, dried and again abraded with emery paper and weighed finally with electronic balance (W_2). Thus weight loss (W_1-W_2) is obtained in grams. The employed concentration range of different plant extracts were different for four different plant species and were expressed in (v/v %). These were 2%-6% (v/v) for AELCL, 1%-8% (v/v) for AECPL, 1%-10% (v/v) for AENOL, 1%-5% (v/v) for AEWHL. The experiments were repeated at 30°C, 40°C, 50°C, 60°C temperatures.

From the above obtained weight loss data, corrosion rates (CR) were calculated by using equation (1). Similarly inhibition efficiencies were calculated using equation (2), Kinetic parameters were calculated by using equation (3), thermodynamic and activation parameters were calculated using equations (4) and (5). The different adsorption isotherms were plotted by using the equations (8), (10) and (11). Gibbs energy of adsorption, enthalpy of adsorption and entropy of adsorption were calculated by equations (13) and (14).

CHAPTER - 3

OBSERVATIONS AND RESULTS

The results obtained from gravimetric (weight loss) method, are used for calculating Corrosion rates, Inhibition efficiencies, Kinetic parameters, Apparent activation energy (E_{act}), Enthalpy of activation ΔH^* , Entropy of activation (ΔS^*) and Gibbs Energy (ΔG_{ads}), Enthalpy of Adsorption (ΔH_{ads}) and Entropy of Adsorption (ΔS_{ads}). These data are summarized in tabular (Table 1 to 40) and graphical (Figure 1 to 62) form under well defined headings for four different plant extracts i.e. AECPL, AELCL, AENOL, AEWHL in two different selected acids. Concentrations of extracts prepared are expressed in % (v/v). Langmuir, Freundlich and Temkin adsorption isotherms are drawn for different plant materials.

Table 1. Mild steel corrosion rates in 1 M HCl solution in absence and presence of different concentrations of AECPL at different temperatures

C_{inh} in (v/v)%	CR x 10⁻³ (g cm⁻² min⁻¹)			
	30°C	40°C	50°C	60°C
0.0	0.69	1.37	2.33	3.07
1.0	0.59	1.21	2.17	2.88
2.0	0.41	1.08	1.94	2.81
3.0	0.38	0.99	1.93	2.74
5.0	0.33	0.86	1.86	2.64
8.0	0.27	0.72	1.57	2.56

Table 2. Inhibition efficiencies of AECPL at different concentrations and temperatures in 1 M HCl solution

C_{inh} in (v/v)%	IE (%)			
	30°C	40°C	50°C	60°C
1.0	14.49	11.67	06.86	06.18
2.0	40.57	21.16	16.73	08.46
3.0	44.92	27.73	17.16	10.74
5.0	52.17	37.22	20.17	14.00
8.0	60.86	47.44	32.61	16.61

Table 3. Kinetic parameters for mild steel corrosion in 1 M HCl solution with AECPL

Temperature (°C)	Kinetic Parameters	
	B	K x 10⁻³ (g cm⁻² min⁻¹)
30°C	-0.3584	0.5736
40°C	-0.2514	1.2755
50°C	-0.1363	2.2024
60°C	-0.0538	2.9080

Table 4. Activation and thermodynamic parameters for mild steel corrosion in 1M HCl solution with AECPL

C_{inh} in (v/v)%	E_{act} (kJ/mol)	ΔH^* (kJ/mol)	ΔS^* (J/mol/K)
0.0	41.26	38.83	-177.64
1.0	43.20	41.39	-170.56
2.0	52.93	50.41	-143.63
3.0	54.91	52.48	-137.55
5.0	57.86	54.99	-130.48
8.0	60.92	59.20	-118.53

Table5. Adsorption parameters for mild steel corrosion in 1M HCl solution with AECPL

Temperature (°C)	ΔG_{ads} (kJ/mol)	ΔH_{ads} (kJ/mol)	ΔS_{ads} (J/mol/K)
30°C	-13.76	-35.95	-73.23
40°C	-12.84		-73.83
50°C	-11.99		-74.17
60°C	-11.59		-73.15

Table 6. Mild steel corrosion rates in 1M H₂SO₄ solution in absence and presence of different concentrations of AECPL at different temperatures

C_{inh} in (v/v)%	CR x 10⁻³ (g cm⁻² min⁻¹)			
	30°C	40°C	50°C	60°C
0.0	0.64	1.55	1.73	2.88
1.0	0.57	1.48	1.63	2.66
2.0	0.51	1.41	1.55	2.59
3.0	0.46	1.32	1.44	2.51
5.0	0.40	1.22	1.37	2.43
8.0	0.31	1.15	1.29	2.30

Table7. Inhibition efficiencies of AECPL at different concentrations and temperatures in 1M H₂SO₄ solution

C_{inh} in (v/v)%	IE (%)			
	30°C	40°C	50°C	60°C
1.0	10.93	04.51	05.78	07.63
2.0	20.31	09.03	10.40	10.06
3.0	28.12	14.83	16.76	12.84
5.0	37.50	21.29	20.80	15.62
8.0	51.56	25.80	25.43	20.13

Table 8. Kinetic parameters for mild steel corrosion in 1M H₂SO₄ solution with AECPL

Temperature (°C)	Kinetic Parameters	
	B	K x 10⁻³ (gcm⁻² min⁻¹)
30°C	-0.2776	0.6055
40°C	-0.1264	1.5282
50°C	-0.1167	1.6730
60°C	-0.0671	2.7158

Table 9. Activation and thermodynamic parameters for mild steel corrosion in 1M H₂SO₄ solution with AECPL

C_{inh} in (v/v)%	E_{act} (kJ/mol)	ΔH* (kJ/mol)	ΔS* (J/mol/K)
0.0	40.77	38.96	-177.95
1.0	42.40	39.88	-175.59
2.0	44.92	42.49	-167.92
3.0	46.08	43.56	-165.22
5.0	49.21	46.78	-155.72
8.0	55.58	53.27	-136.40

Table10. Adsorption parameters for mild steel corrosion in 1M H₂SO₄ solution with AECPL

Temperature (°C)	ΔG_{ads} (kJ/mol)	ΔH_{ads} (kJ/mol)	ΔS_{ads} (J/mol/K)
30°C	-12.15	-69.11	-187.99
40°C	-10.27	-69.11, 19.13	-187.99, 93.93
50°C	-11.28	19.13	94.15
60°C	-12.15	19.13	93.93

Table11. Mild steel corrosion rates in 1M HCl solution in absence and presence of different concentrations of AELCL at different temperatures

C_{inh} in (v/v)%	CR x 10⁻³ (g cm⁻² min⁻¹)			
	30°C	40°C	50°C	60°C
0.0	1.00	1.50	2.16	2.70
2.0	0.61	1.10	2.00	2.60
3.0	0.50	0.83	1.90	2.57
4.0	0.33	0.66	1.80	2.54
6.0	0.11	0.50	1.70	2.40

Table12. Inhibition efficiencies of AELCL at different concentrations and temperatures in 1M HCl solution

C_{inh} in (v/v)%	IE (%)			
	30°C	40°C	50°C	60°C
2.0	40.00	26.66	07.40	03.70
3.0	50.00	44.66	12.03	04.81
4.0	70.00	56.00	16.66	05.92
6.0	90.00	66.66	21.29	11.11

Table 13. Kinetic parameters for mild steel corrosion in 1M HCl solution with AELCL

Temperature (°C)	Kinetic Parameters	
	B	K x 10 ⁻³ (g cm ⁻² min ⁻¹)
30°C	-1.5439	2.2289
40°C	-0.7379	1.8647
50°C	-0.1476	2.2496
60°C	-0.0836	2.8029

Table 14. Activation and thermodynamic parameters for mild steel corrosion in 1M HCl solution with AELCL

C_{inh} in (v/v)%	E_{act} (kJ/mol)	ΔH^* (kJ/mol)	ΔS^* (J/mol/K)
0.0	27.48	24.47	-221.99
2.0	39.80	37.86	-182.12
3.0	44.12	41.60	-171.58
4.0	55.20	52.68	-138.46
6.0	86.12	84.18	-43.23

Table15. Adsorption parameters for mild steel corrosion in 1 M HCl solution with AELCL

Temperature (°C)	ΔG_{ads} (kJ/mol)	ΔH_{ads} (kJ/mol)	ΔS_{ads} (J/mol/K)
30°C	-11.60	23.85	116.99
40°C	-12.77	23.85 , -89.62	116.99 , -245.53
50°C	-09.89	-89.62	-246.84
60°C	-07.85	-89.62	-245.56

Table16. Mild steel corrosion rates in 1 M H₂SO₄ solution in absence and presence of different concentrations of AELCL at different temperatures

C_{inh} in (v/v)%	CR x 10⁻³ (g cm⁻² min⁻¹)			
	30°C	40°C	50°C	60°C
0.0	0.98	1.59	2.42	2.94
2.0	0.92	1.32	2.27	2.70
3.0	0.79	1.09	2.19	2.22
4.0	0.35	0.82	1.40	1.95
6.0	0.34	0.81	1.37	1.84

Tables17. Inhibition efficiencies of AELCL at different concentrations and temperatures in 1 M H₂SO₄ solution

C_{inh} in (v/v)%	IE (%)			
	30°C	40°C	50°C	60°C
2.0	06.12	16.98	06.19	08.16
3.0	19.39	31.44	09.50	24.48
4.0	64.28	48.42	42.14	33.67
6.0	65.30	49.05	43.38	37.41

Table18. Kinetic parameters for mild steel corrosion in 1 M H₂SO₄ solution with AELCL

Temperature (°C)	Kinetic Parameters	
	B	K x 10 ⁻³ (g cm ⁻² min ⁻¹)
30°C	-1.0232	1.9592
40°C	-0.4931	1.8454
50°C	-0.5291	3.4119
60°C	-0.3591	3.4182

Table19. Activation and thermodynamic parameters for mild steel corrosion in 1M H₂SO₄ solution with AELCL

C_{inh} in (v/v)%	E_{act} (kJ/mol)	ΔH* (kJ/mol)	ΔS* (J/mol/K)
0.0	29.86	28.05	-210.30
2.0	29.41	26.41	-216.24
3.0	28.90	25.99	-218.79
4.0	47.67	44.67	-231.28
6.0	46.69	44.18	-229.52

Table20. Adsorption parameters for mild steel corrosion in 1 M H₂SO₄ solution with AELCL

Temperature (°C)	ΔG_{ads} (kJ/mol)	ΔH_{ads} (kJ/mol)	ΔS_{ads} (J/mol/K)
30°C	-05.18	20.28	84.03
40°C	-11.60		101.85
50°C	-06.42		82.66
60°C	-09.90		90.63

Table21. Mild steel corrosion rates in 1M HCl solution in absence and presence of different concentrations of AENOL at different temperatures

C_{inh} in (v/v)%	CR x 10⁻³ (g cm⁻² min⁻¹)			
	30°C	40°C	50°C	60°C
0.0	1.17	1.75	3.72	3.85
1.0	0.83	1.41	3.08	3.19
2.0	0.79	1.32	2.84	3.14
3.0	0.44	0.89	2.27	2.97
5.0	0.34	0.79	1.73	2.74
10.0	0.19	0.45	1.00	1.77

Table 22. Inhibition efficiencies of AENOL at different concentrations and temperatures in 1M HCl solution

C_{inh} in (v/v)%	IE (%)			
	30°C	40°C	50°C	60°C
1.0	29.05	19.42	17.20	17.14
2.0	32.47	24.57	23.65	18.44
3.0	62.39	49.14	38.97	22.85
5.0	70.94	54.85	53.49	28.83
10.0	83.76	74.28	73.11	54.02

Table 23. Kinetic parameters for mild steel corrosion in 1M HCl solution with AENOL

Temperature (°C)	Kinetic Parameters	
	B	K x 10⁻³ (g cm⁻² min⁻¹)
30°C	-0.6753	0.9831
40°C	-0.5013	1.6084
50°C	-0.5002	3.6132
60°C	-0.2466	3.6157

Table24. Activation and thermodynamic parameters for mild steel corrosion in 1M HCl solution with AENOL

C_{inh} in (v/v)%	E_{act} (kJ/mol)	ΔH* (kJ/mol)	ΔS* (J/mol/K)
0.0	33.58	30.93	-199.27
1.0	38.22	35.79	-186.02
2.0	38.58	36.06	-185.61
3.0	52.37	49.94	-144.85
5.0	56.19	53.76	-134.45
10.0	60.05	57.66	-126.74

Table 25. Adsorption parameters for mild steel corrosion in 1M HCl solution with AENOL

Temperature (°C)	ΔG_{ads} (kJ/mol)	ΔH_{ads} (kJ/mol)	ΔS_{ads} (J/mol/K)
30°C	-14.73	-27.04	-40.63
40°C	-13.97	-27.04	-41.76
50°C	-13.91	-27.04, -09.07	-40.65, 14.98
60°C	-14.06	-09.07	14.98

Table 26. Mild steel corrosion rates in 1M H₂SO₄ solution in absence and presence of different concentrations of AENOL at different temperatures

C_{inh} in (v/v)%	CR x 10⁻³ (g cm⁻² min⁻¹)			
	30°C	40°C	50°C	60°C
0.0	0.75	1.54	2.51	3.69
1.0	0.62	1.39	2.36	3.60
2.0	0.45	0.94	2.27	3.54
3.0	0.39	0.79	2.14	3.45
5.0	0.32	0.69	2.08	3.39
10.0	0.21	0.54	1.97	3.32

Table 27. Inhibition efficiencies of AENOL at different concentrations and temperatures in 1 M H₂SO₄ solution

C_{inh} in (v/v)%	IE (%)			
	30°C	40°C	50°C	60°C
1.0	17.33	09.74	05.98	02.44
2.0	40.00	38.96	09.56	04.07
3.0	48.00	48.70	14.74	06.50
5.0	57.33	55.19	17.13	08.13
10.0	72.00	64.94	21.51	10.03

Table 28. Kinetic parameters for mild steel corrosion in 1 M H₂SO₄ solution with AENOL

Temperature (°C)	Kinetic Parameters	
	B	K x 10 ⁻³ (g cm ⁻² min ⁻¹)
30°C	-0.4542	0.6266
40°C	-0.3977	1.2972
50°C	-0.0826	2.3708
60°C	-0.0414	3.6350

Table 29. Activation and thermodynamic parameters for mild steel corrosion in 1M H₂SO₄ solution with AENOL

C_{inh} in (v/v)%	E_{act} (kJ/mol)	ΔH* (kJ/mol)	ΔS* (J/mol/K)
0.0	43.17	40.32	-172.49
1.0	48.21	44.75	-159.45
2.0	55.97	48.03	-152.55
3.0	58.71	50.21	-146.74
5.0	63.21	54.59	-134.21
10.0	74.78	64.55	-105.03

Table 30. Adsorption parameters for mild steel corrosion in 1 M H₂SO₄ solution with AENOL

Temperature (°C)	ΔG_{ads} (kJ/mol)	ΔH_{ads} (kJ/mol)	ΔS_{ads} (J/mol/K)
30°C	-13.99	-64.62	-167.10
40°C	-13.55		-163.16
50°C	-11.38		-164.83
60°C	-09.20		-166.43

Table 31. Mild steel corrosion rates in 1M HCl solution in absence and presence of different concentrations of AEWHL at different temperatures

C_{inh} in (v/v)%	CR x 10⁻³ (g cm⁻² min⁻¹)			
	30°C	40°C	50°C	60°C
0.0	0.88	1.56	2.25	2.96
1.0	0.67	1.35	2.17	2.81
2.0	0.62	1.21	2.08	2.74
3.0	0.52	1.14	1.99	2.69
4.0	0.42	1.04	1.91	2.60
5.0	0.28	0.80	1.73	2.51

Table 32. Inhibition efficiencies of AEWHL at different concentrations and temperatures in 1M HCl solution

C_{inh} in (v/v)%	IE (%)			
	30°C	40°C	50°C	60°C
1.0	23.86	13.46	03.55	05.06
2.0	29.54	22.43	07.55	07.43
3.0	40.90	26.92	11.55	09.12
4.0	52.27	33.33	15.11	12.16
5.0	68.18	48.71	23.11	15.20

Table 33. Kinetic parameters for mild steel corrosion in 1M HCl solution with AEWHL

Temperature (°C)	Kinetic Parameters	
	B	K x 10 ⁻³ (g cm ⁻² min ⁻¹)
30°C	-0.4885	0.7675
40°C	-0.2762	1.4217
50°C	-0.1301	2.2387
60°C	-0.0651	2.8510

Table 34. Activation and thermodynamic parameters for mild steel corrosion in 1M HCl solution with AEWHL

C_{inh} in (v/v)%	E_{act} (kJ/mol)	ΔH* (kJ/mol)	ΔS* (J /K/mol)
0.0	33.69	31.01	-200.82
1.0	39.92	38.01	-179.88
2.0	42.17	39.50	-175.67
3.0	45.69	43.78	-162.88
4.0	51.33	48.27	-149.57
5.0	61.51	58.84	-117.92

Table 35. Adsorption parameters for mild steel corrosion in 1M HCl solution with AEHL

Temperature (°C)	ΔG_{ads} (kJ/mol)	ΔH_{ads} (kJ/mol)	ΔS_{ads} (J/K /mol)
30°C	-13.91	-79.90	-217.79
40°C	-12.92	-79.90	-213.99
50°C	-09.58	-79.90 , 31.76	-217.71 , 127.99
60°C	-10.86	31.76	127.99

Table 36. Mild steel corrosion rates in 1M H₂SO₄ solution in absence and presence of different concentrations of AEWHL at different temperatures

C_{inh} in (v/v)%	CR x 10⁻³ (g cm⁻² min⁻¹)			
	30°C	40°C	50°C	60°C
0.0	0.71	1.43	2.14	2.77
1.0	0.62	1.29	1.87	2.25
2.0	0.58	1.19	1.73	2.21
3.0	0.41	1.03	1.64	2.09
4.0	0.34	0.79	1.47	1.90
5.0	0.25	0.62	1.36	1.73

Table 37. Inhibition efficiencies of AEWHL at different concentrations and temperatures in 1M H₂SO₄ solution

C_{inh} in (v/v)%	IE (%)			
	30°C	40°C	50°C	60°C
1.0	12.67	09.79	12.61	18.77
2.0	18.30	16.78	19.15	20.21
3.0	42.25	27.97	23.36	24.54
4.0	52.11	44.75	31.30	31.40
5.0	64.78	56.64	36.44	37.54

Table 38. Kinetic parameters for mild steel corrosion in 1M H₂SO₄ solution with AEWHL

Temperature (°C)	Kinetic Parameters	
	B	K x 10 ⁻³ (g cm ⁻² min ⁻¹)
30°C	-0.5555	0.7194
40°C	-0.4369	1.4645
50°C	-0.1943	1.9534
60°C	-0.1627	2.3966

Table 39. Activation and thermodynamic parameters for mild steel corrosion in 1M H₂SO₄ solution with AEWHL

C_{inh} in (v/v)%	E_{act} (kJ/mol)	ΔH* (kJ/mol)	ΔS* (J/mol/K)
0.0	37.63	34.95	-189.31
1.0	35.62	32.35	-198.63
2.0	36.69	34.22	-193.32
3.0	45.08	42.61	-168.13
4.0	48.06	46.15	-158.40
5.0	55.22	52.51	-139.87

Table40. Adsorption parameters for mild steel corrosion in 1 M H₂SO₄ solution with AEHL

Temperature (°C)	ΔG_{ads} (kJ/mol)	ΔH_{ads} (kJ/mol)	ΔS_{ads} (J/mol/K)
30°C	-12.00	-13.52	-05.02
40°C	-11.95	-13.52, 31.44	-05.02, 138.63
50°C	-13.22	31.44	138.27
60°C	-14.72	31.44	138.62

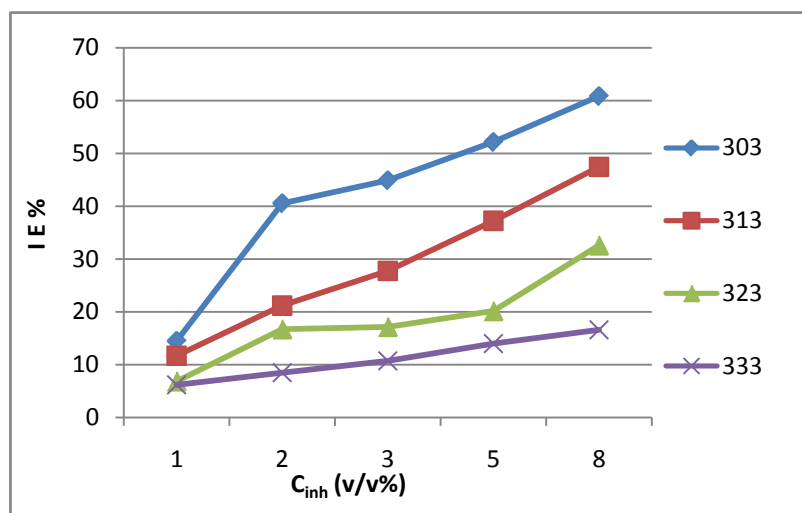


Figure 1. Variation in IE % for mild steel corrosion in 1M HCl at different concentrations of AECPL at different studied temperatures

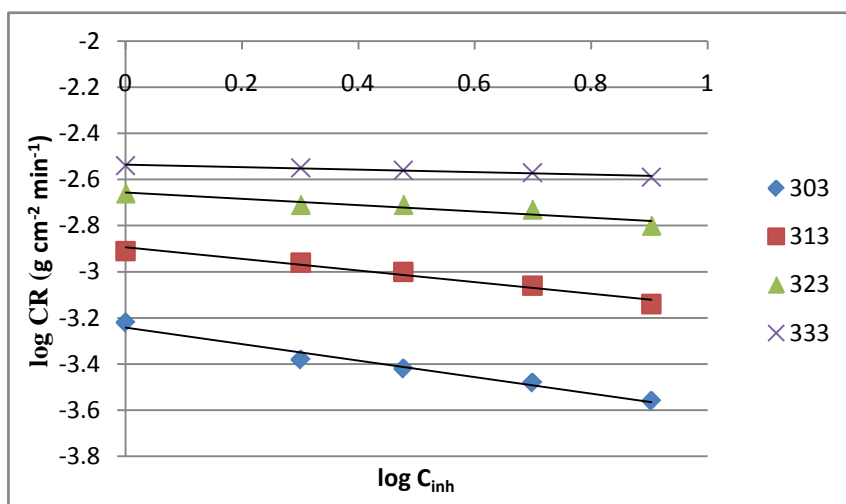


Figure 2. Variation of log CR with log C_{inh} for mild steel corrosion in 1M HCl in presence of different concentrations of AECPL at various studied temperatures

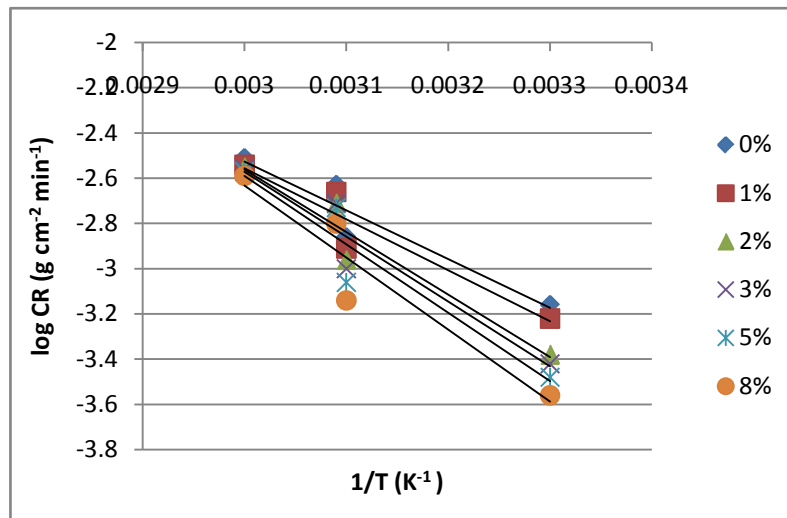


Figure 3. Arrhenius plots for mild steel corrosion in 1M HCl in absence and presence of various concentrations of AECPL

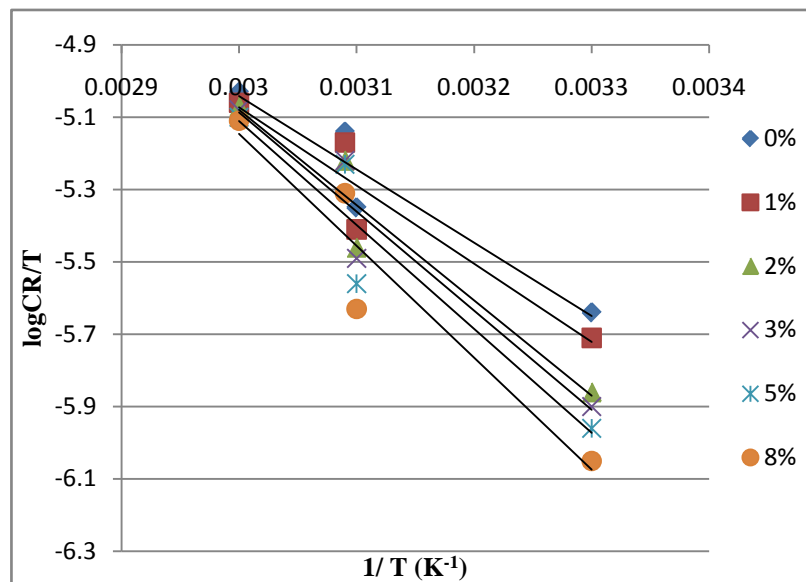


Figure 4. Transition-state plots for mild steel corrosion in 1M HCl in absence and presence of various concentrations of AECPL

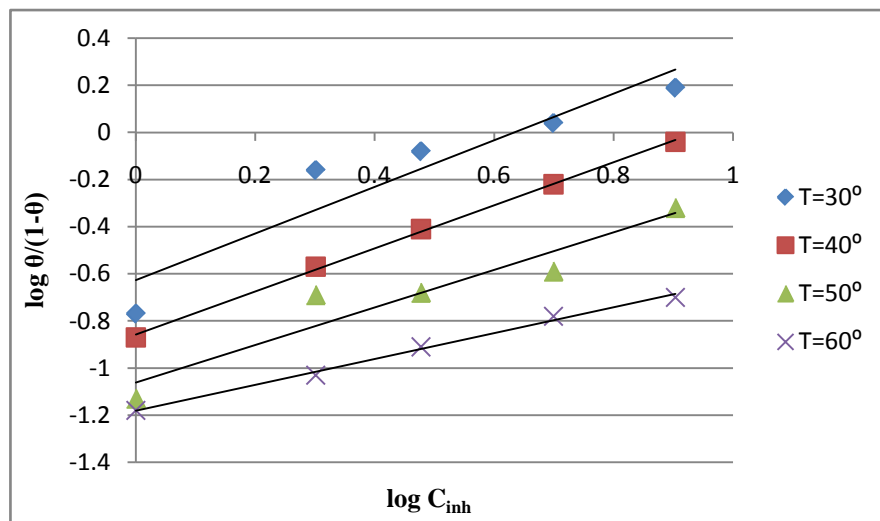


Figure 5. Langmuir adsorption isotherms of AECPL on mild steel surface in 1M HCl at different studied temperatures

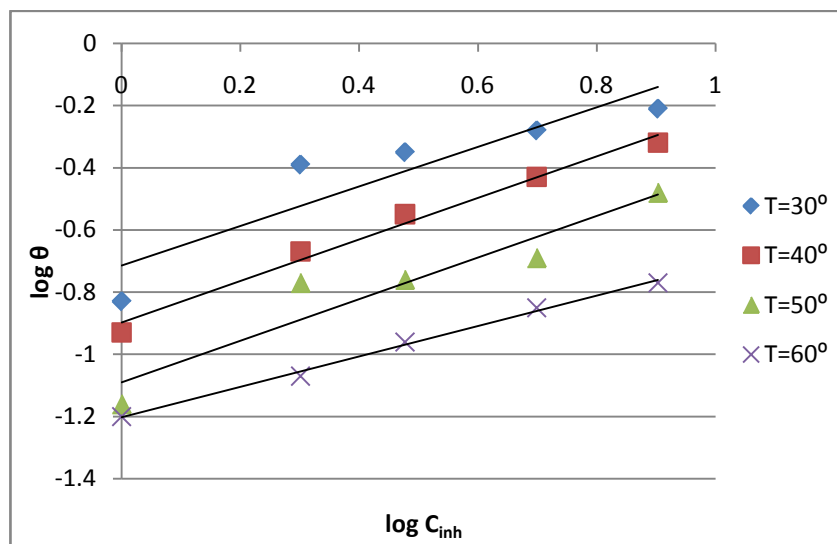


Figure 6. Freundlich adsorption isotherms of AECPL on mild steel surface in 1M HCl at different studied temperatures

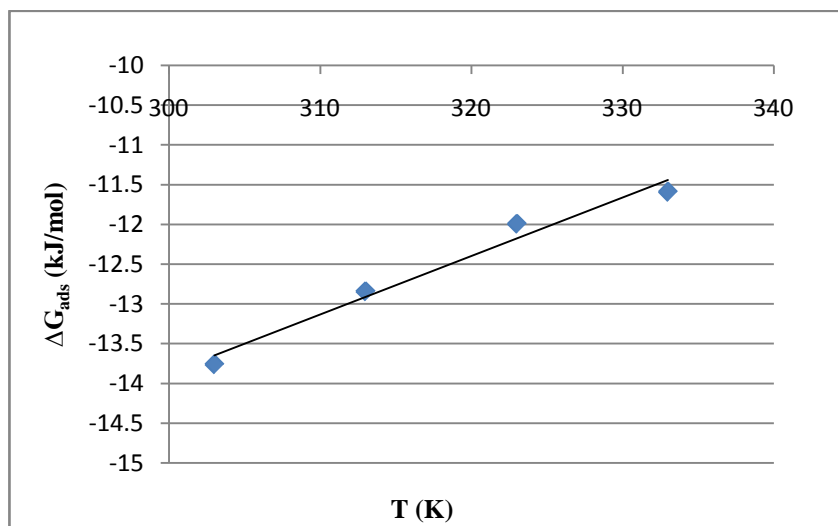


Figure 7. The variation of ΔG_{ads} (kJ/mol) with T (K) for mild steel corrosion in 1M HCl solution with AECPL

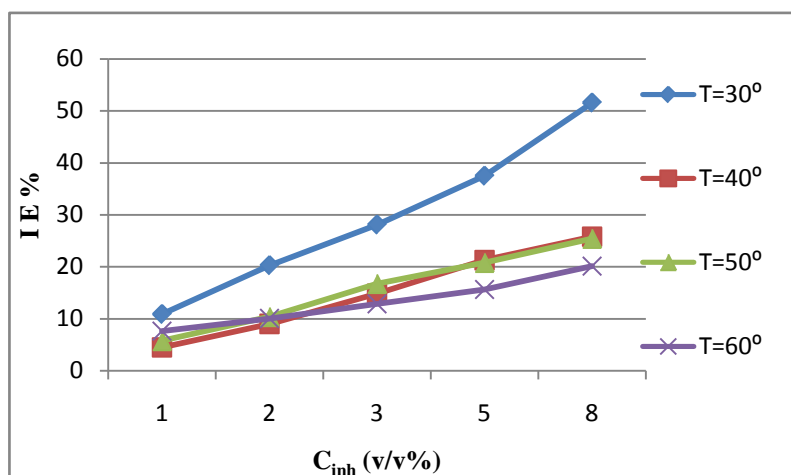


Figure 8. Variation in IE % for mild steel corrosion in 1M H₂SO₄ at different concentrations of AECPL at different studied temperatures

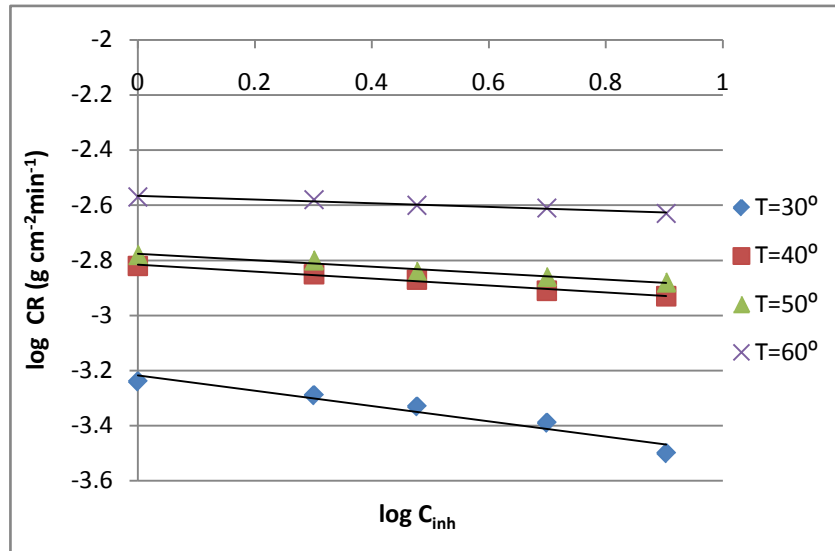


Figure 9. Variation of logCR with logC_{inh} for mild steel corrosion in 1M H₂SO₄ in presence of different concentrations of AECPL at various studied temperatures

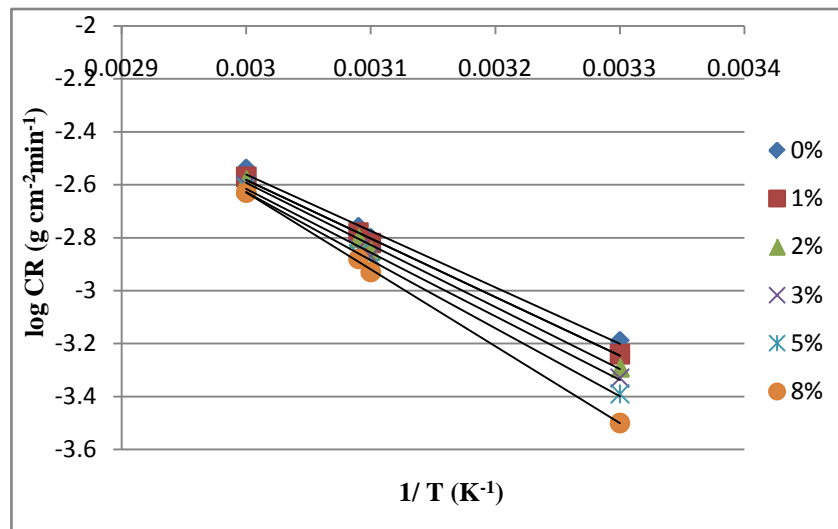


Figure10. Arrhenius plots for mild steel corrosion in 1M H₂SO₄ in absence and presence of various concentrations of AECPL

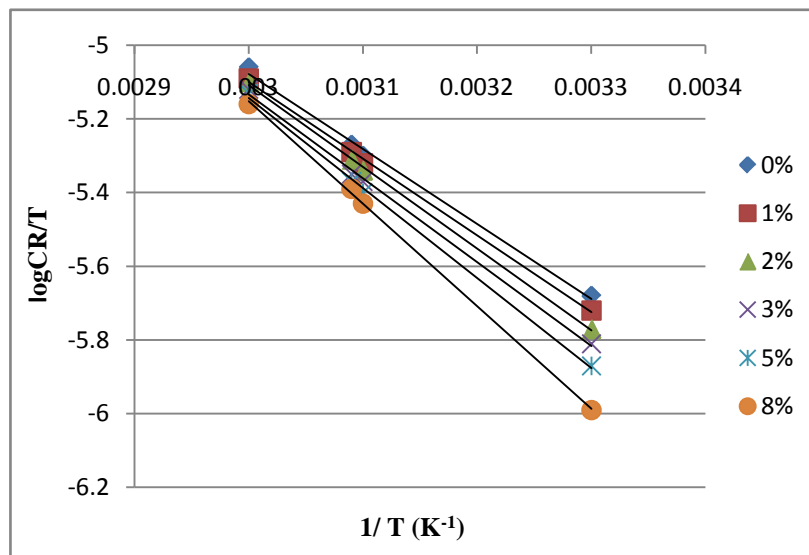


Figure 11. Transition-state plots for mild steel corrosion in 1M H₂SO₄ in absence and presence of various concentrations of AECPL

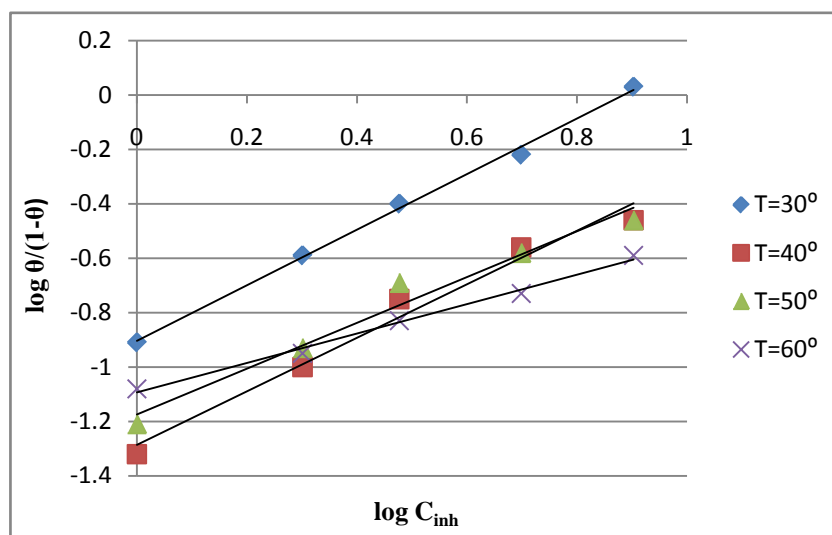


Figure 12. Langmuir adsorption isotherms of AECPL on mild steel surface in 1M H₂SO₄ at different studied temperatures

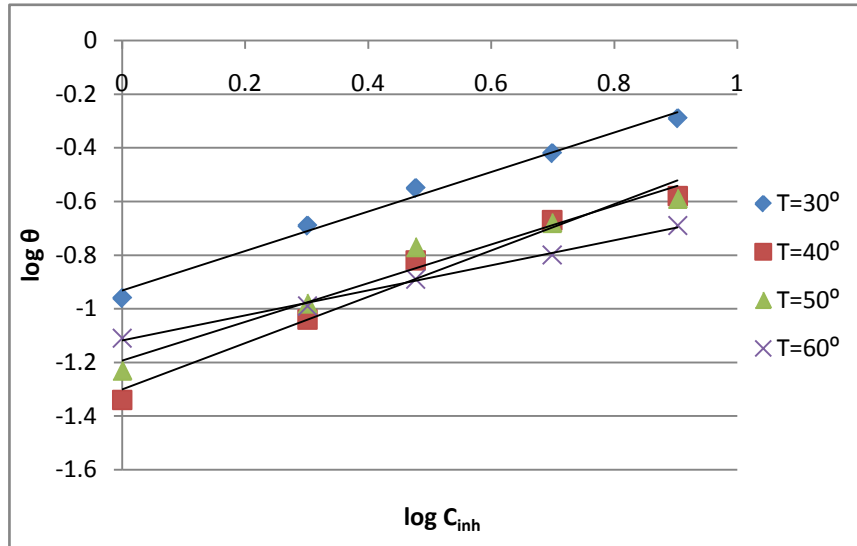


Figure 13. Freundlich adsorption isotherms of AECPL on mild steel surface in 1M H₂SO₄ at different studied temperature

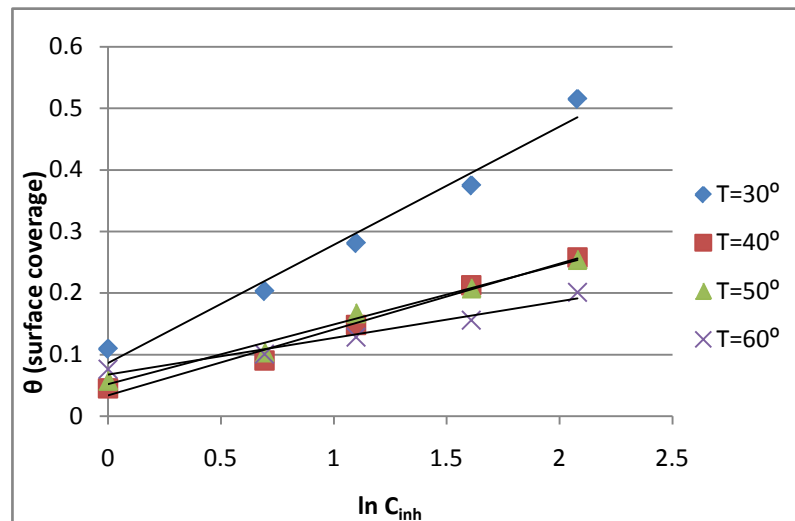


Figure 14. Temkin adsorption isotherms of AECPL on mild steel surface in 1M H₂SO₄ at different studied temperatures

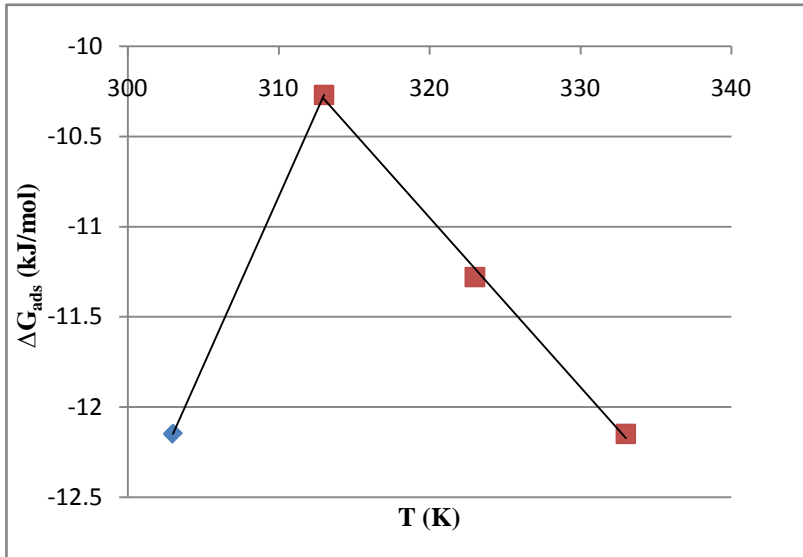


Figure 15. The variation of ΔG_{ads} (kJ/mol) with T (K) for mild steel corrosion in 1M H_2SO_4 solution with AECPL

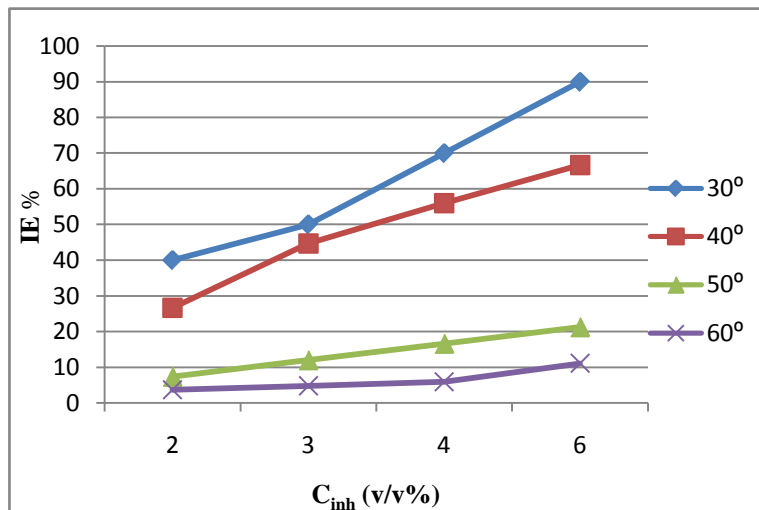


Figure 16. Variation in IE % for mild steel corrosion in 1M HCl at different concentrations of AELCL at different studied temperatures

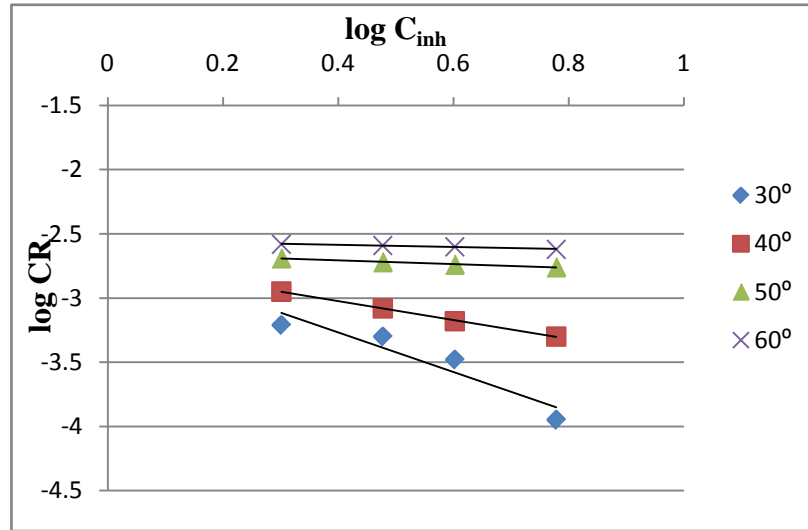


Figure 17. Variation of logCR with log C_{inh} for mild steel corrosion in 1 M HCl in presence of different concentrations of AELCL at various studied temperatures

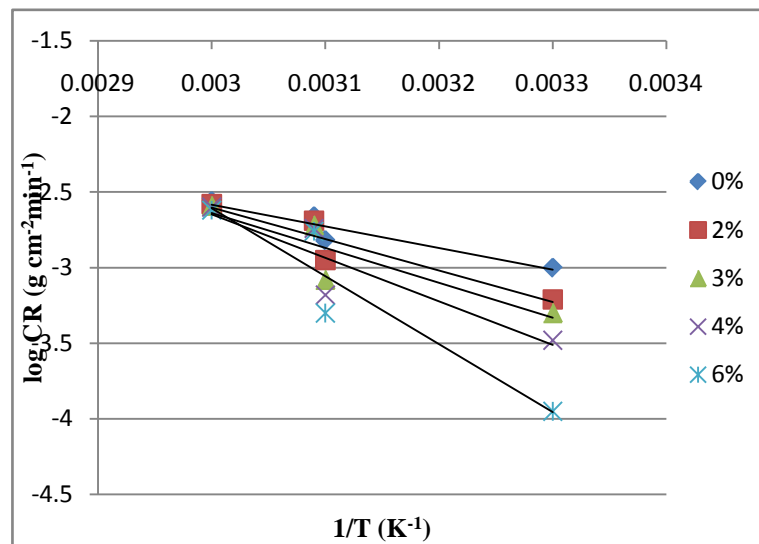


Figure 18. Arrhenius plots for mild steel corrosion in 1M HCl in absence and presence of various concentrations of AELCL

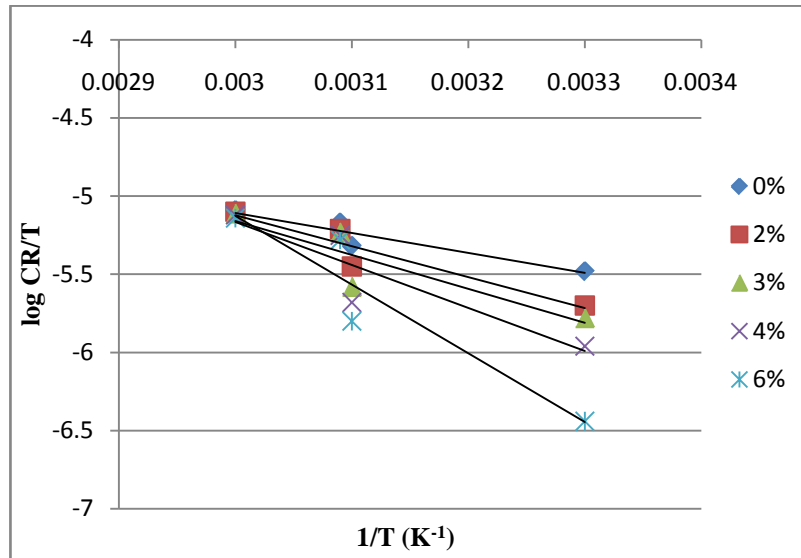


Figure 19. Transition-state plots for mild steel corrosion in 1M HCl in absence and presence of various concentrations of AELCL

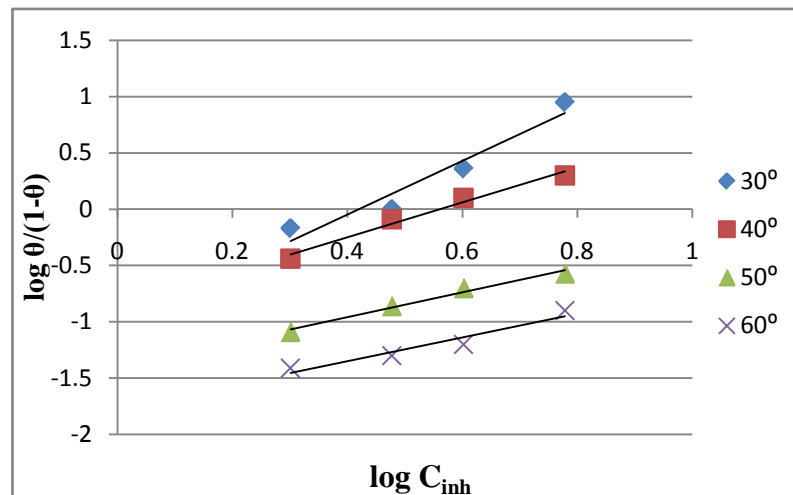


Figure 20. Langmuir adsorption isotherms of AELCL on mild steel surface in 1M HCl at different studied temperatures

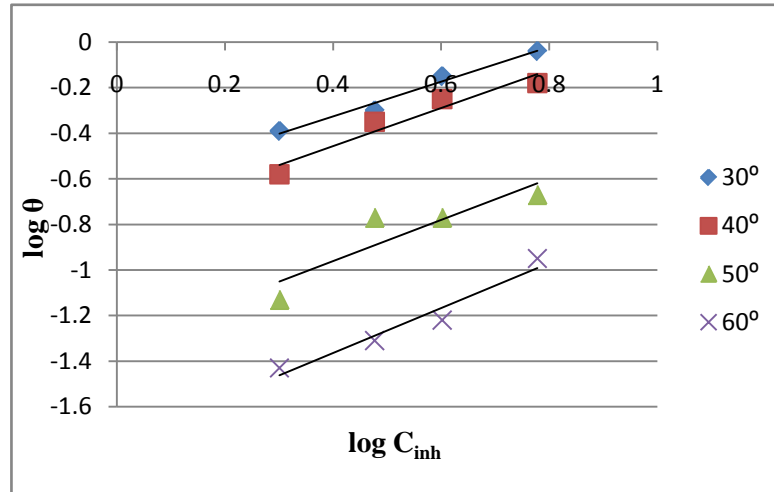


Figure 21. Freundlich adsorption isotherms of AELCL on mild steel surface in 1M HCl at different studied temperatures

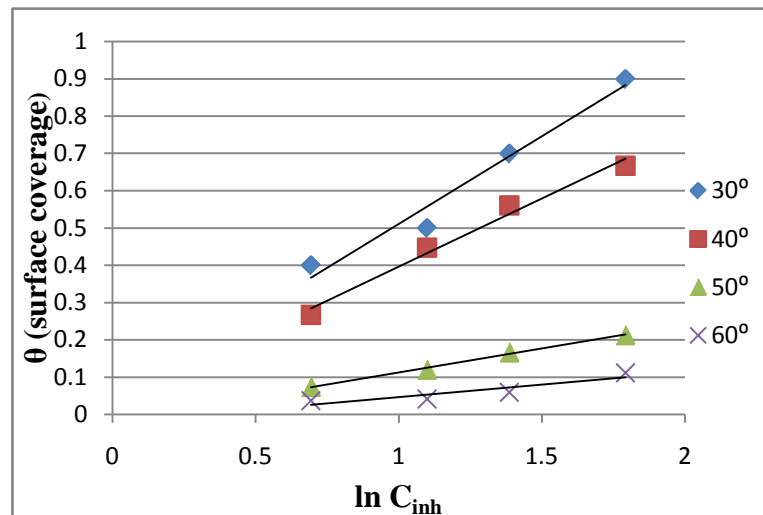


Figure 22. Temkin adsorption isotherms of AELCL on mild steel surface in 1M HCl at different studied temperatures

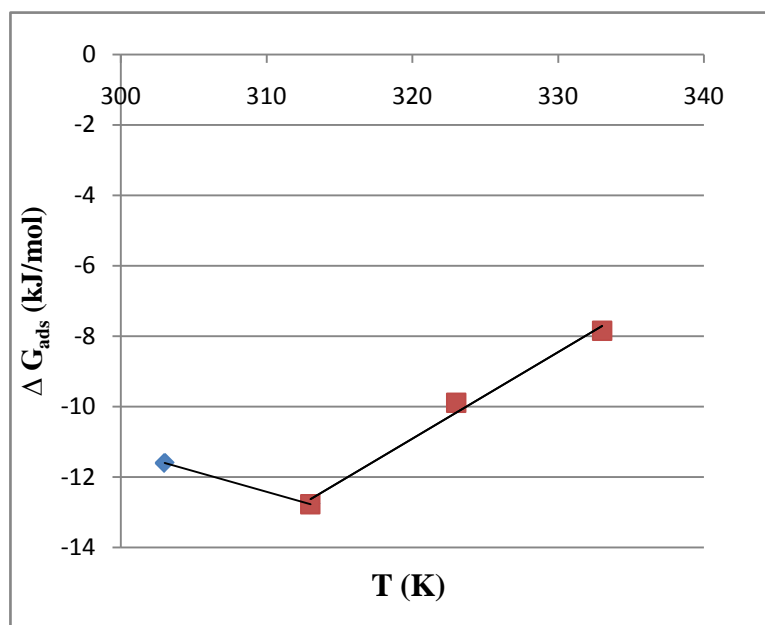


Figure 23. The variation of ΔG_{ads} (kJ/mol) with T (K) for mild steel corrosion in 1M HCl solution with AELCL

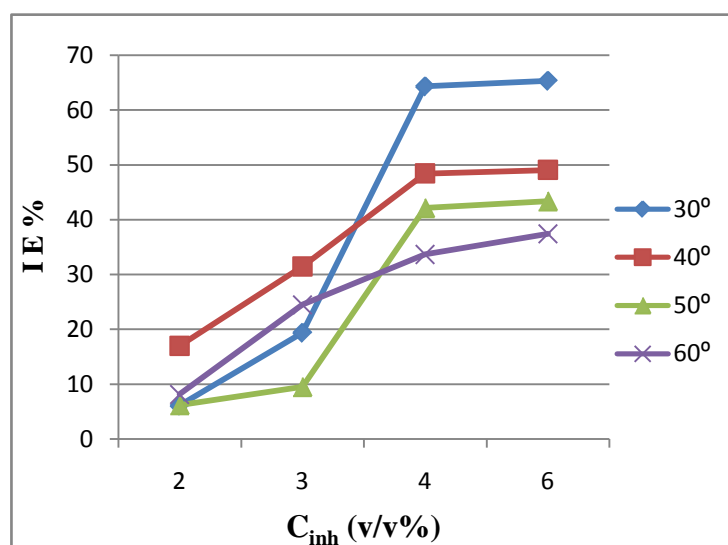


Figure 24. Variation in IE % for mild steel corrosion in 1M H₂SO₄ at different concentrations of AELCL at different studied temperatures

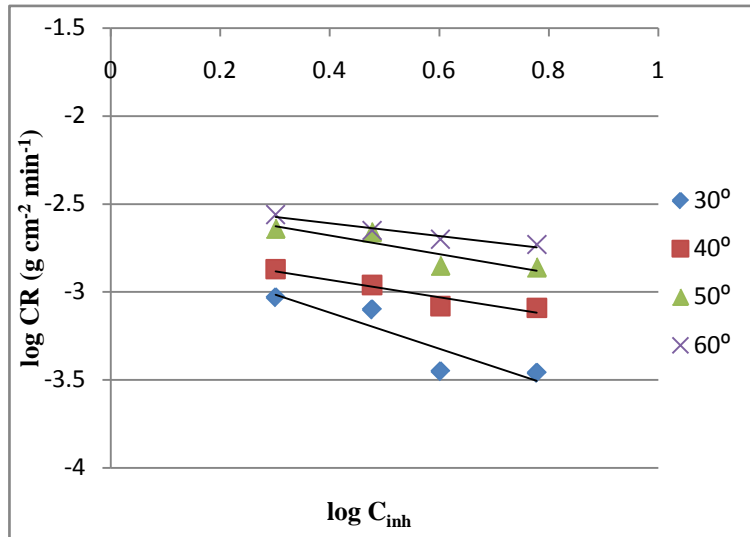


Figure 25. Variation of logCR with logC_{inh} for mild steel corrosion in 1M H₂SO₄ in presence of different concentrations of AELCL at various studied temperatures

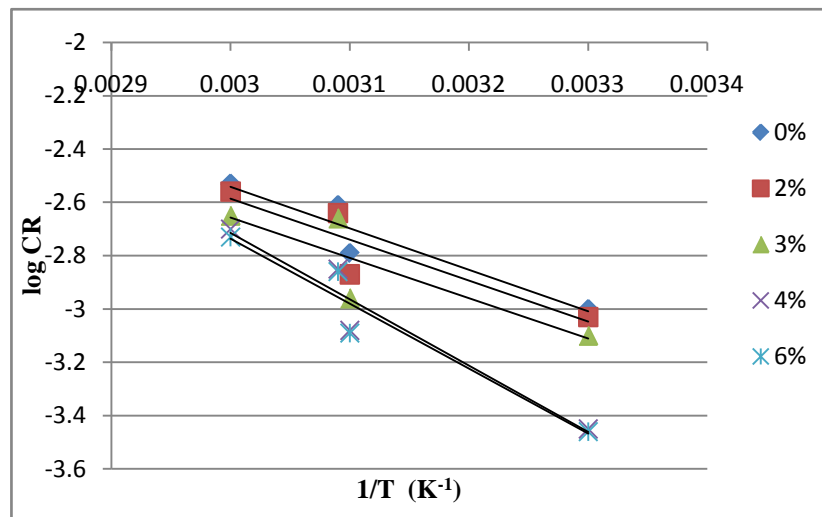


Figure 26. Arrhenius plots for mild steel corrosion in 1M H₂SO₄ in absence and presence of various concentrations of AELCL

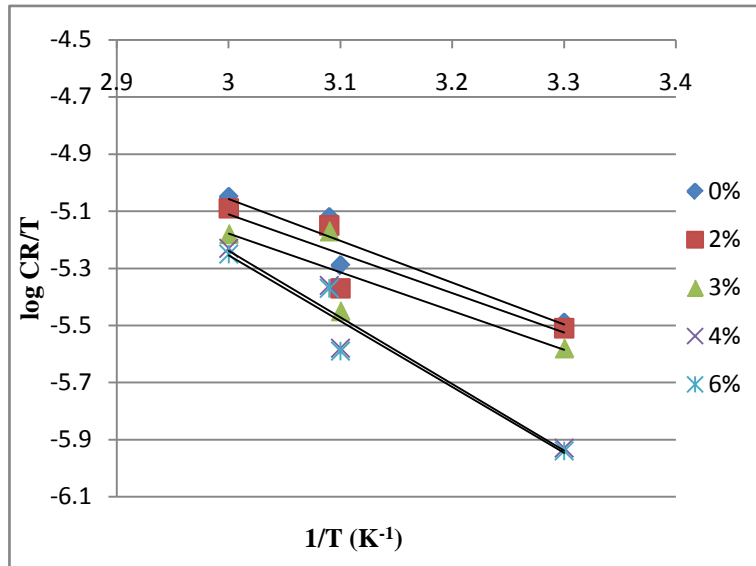


Figure 27. Transition-state plots for mild steel corrosion in 1M H₂SO₄ in absence and presence of various concentrations of AELCL

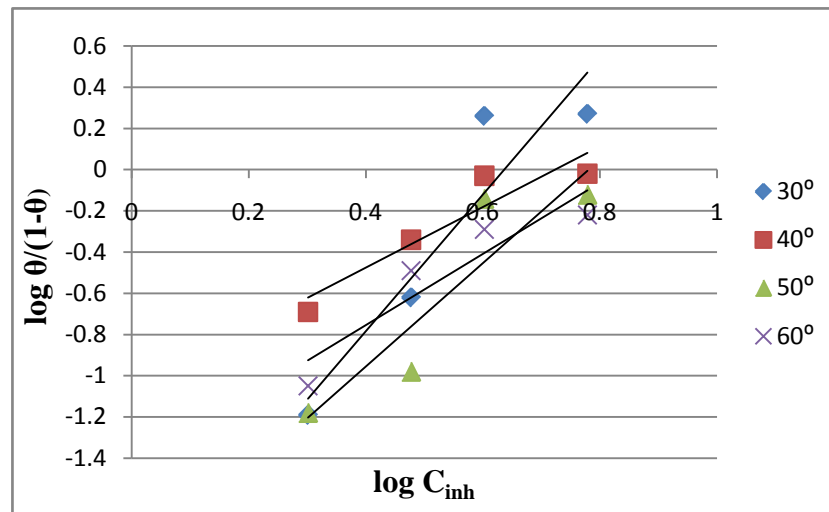


Figure 28. Langmuir adsorption isotherms of AELCL on mild steel surface in 1M H₂SO₄ at different studied temperatures

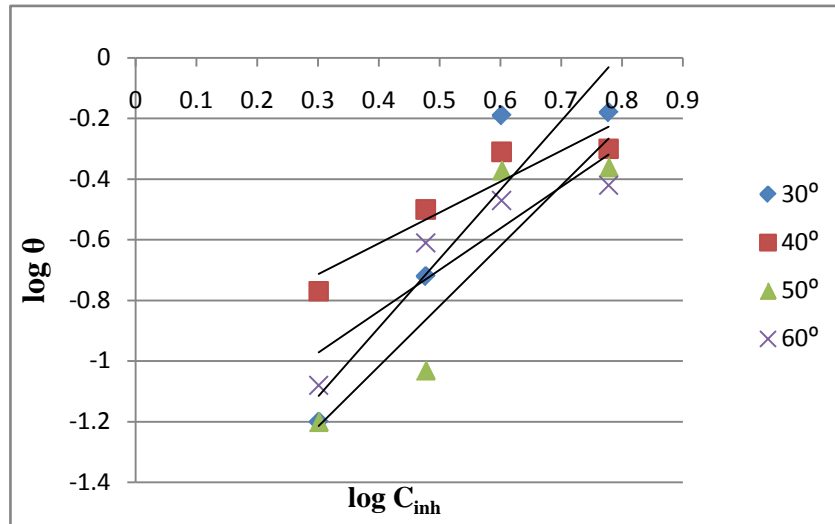


Figure 29. Freundlich adsorption isotherms of AELCL on mild steel surface in 1M H₂SO₄ at different studied temperatures

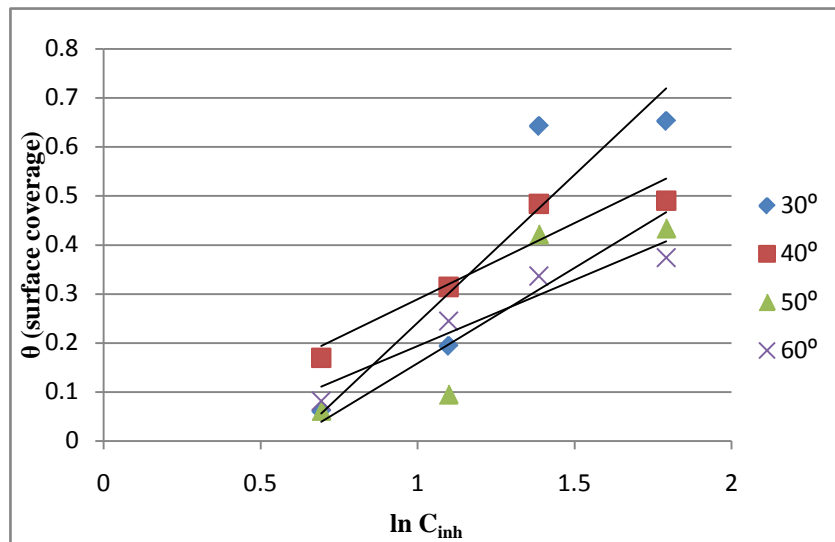


Figure 30. Temkin adsorption isotherms of AELCL on mild steel surface in 1M H₂SO₄ at different studied temperatures

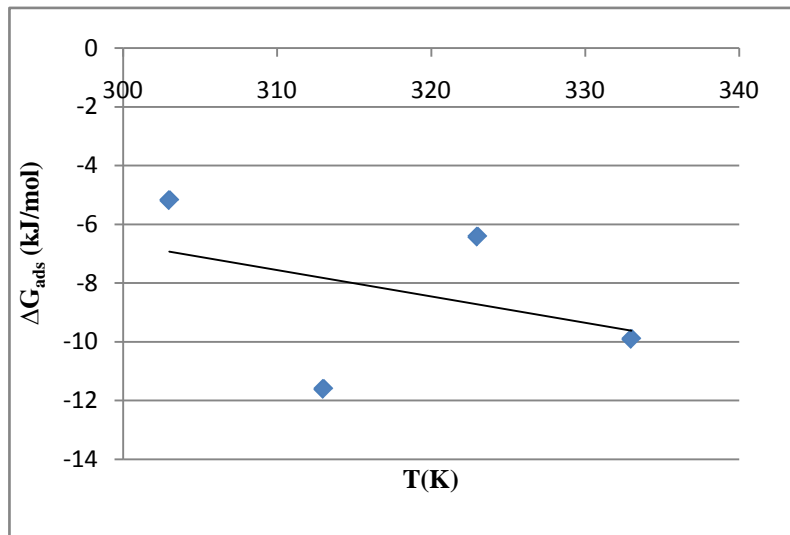


Figure 31. The variation of ΔG_{ads} (kJ/mol) with T (K) for mild steel corrosion in 1M H_2SO_4 solution with AELCL

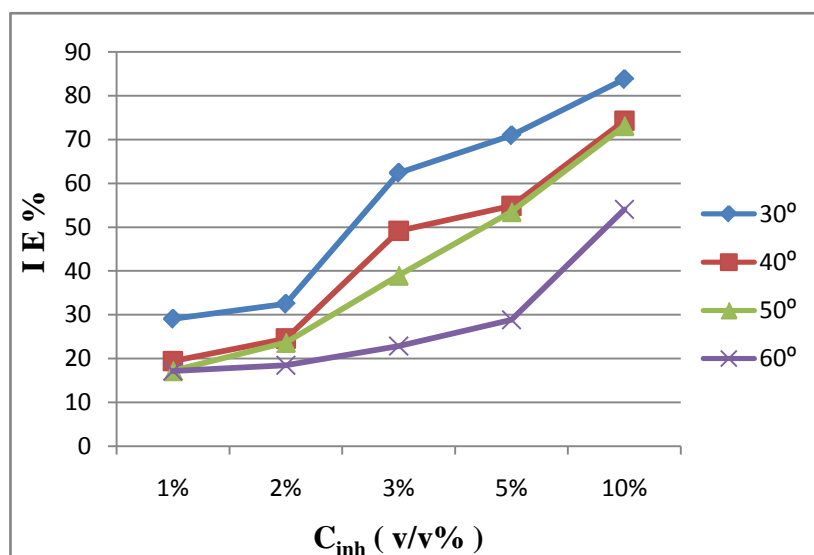


Figure32. Variation in IE % for mild steel corrosion in 1M HCl at different concentrations of AENOL at different studied temperatures

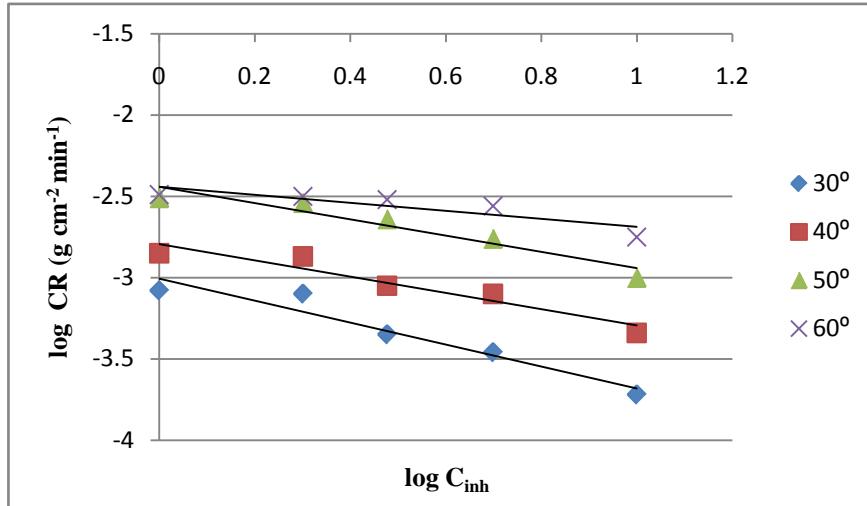


Figure 33. Variation of logCR with logC_{inh} for mild steel corrosion in 1M HCl in presence of different concentrations of AENOL at various studied temperatures

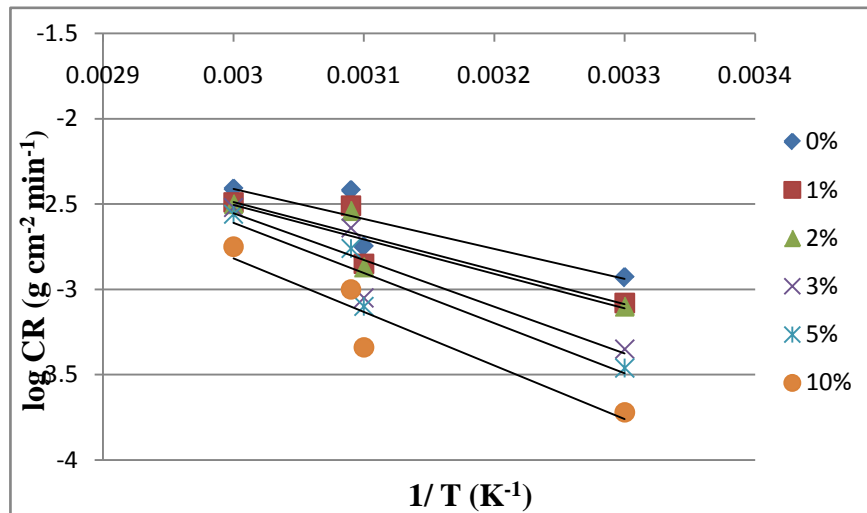


Figure 34. Arrhenius plots for mild steel corrosion in 1M HCl in absence and presence of various concentrations of AENOL

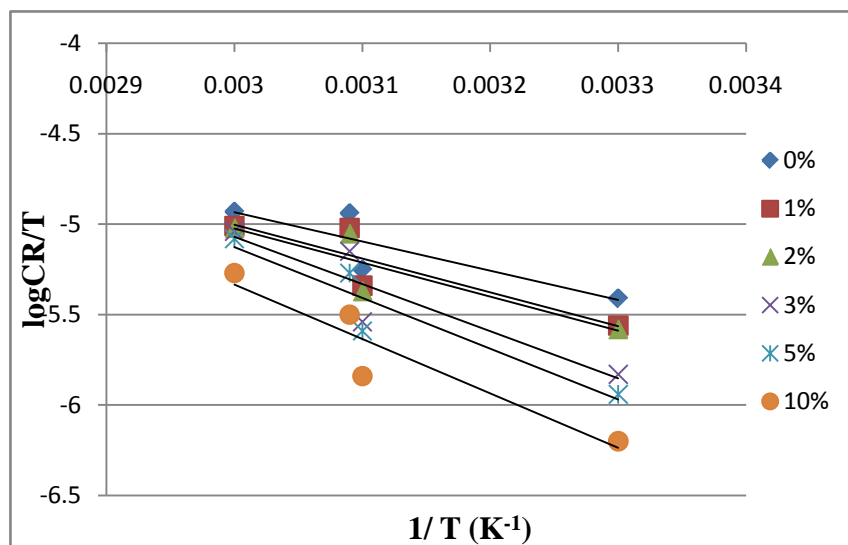


Figure 35. Transition-state plots for mild steel corrosion in 1M HCl in absence and presence of various concentrations of AENOL

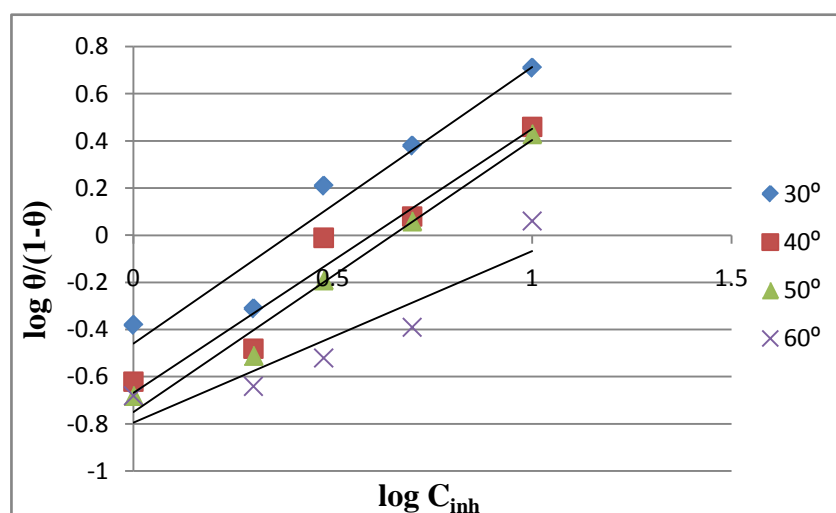


Figure 36. Langmuir adsorption isotherms of AENOL on mild steel surface in 1M HCl at different studied temperatures

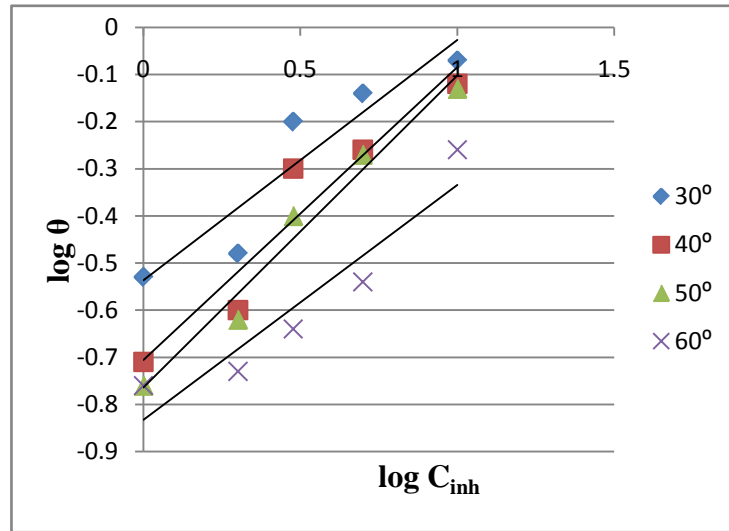


Figure37. Freundlich adsorption isotherms of AENOL on mild steel surface in 1M HCl at different studied temperatures

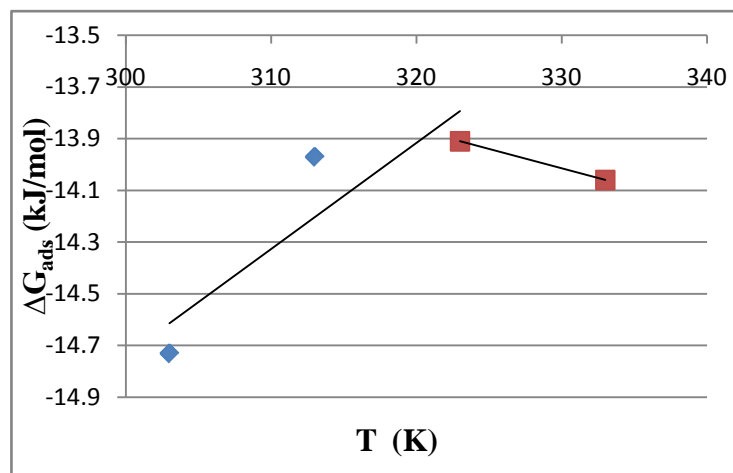


Figure 38. The variation of ΔG_{ads} (kJ/mol) with T (K) for mild steel corrosion in 1M HCl solution with AENOL

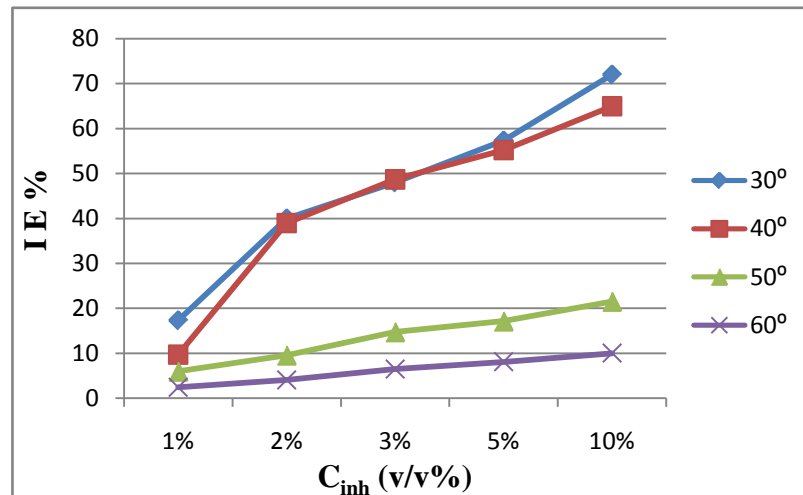


Figure 39. Variation in IE% for mild steel corrosion in 1M H₂SO₄ at different concentrations of AENOL at different studied temperatures

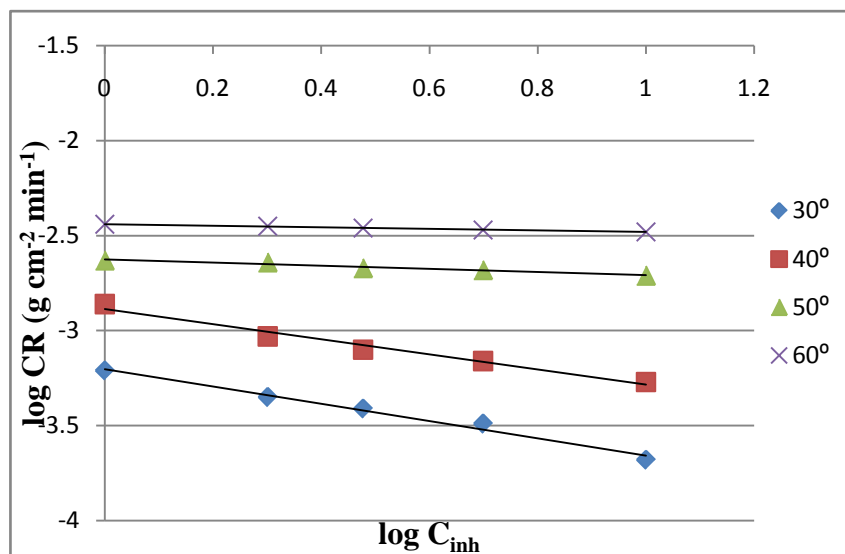


Figure 40. Variation of log CR with log C_{inh} for mild steel corrosion in 1M H₂SO₄ in presence of different concentrations of AENOL at various studied temperatures

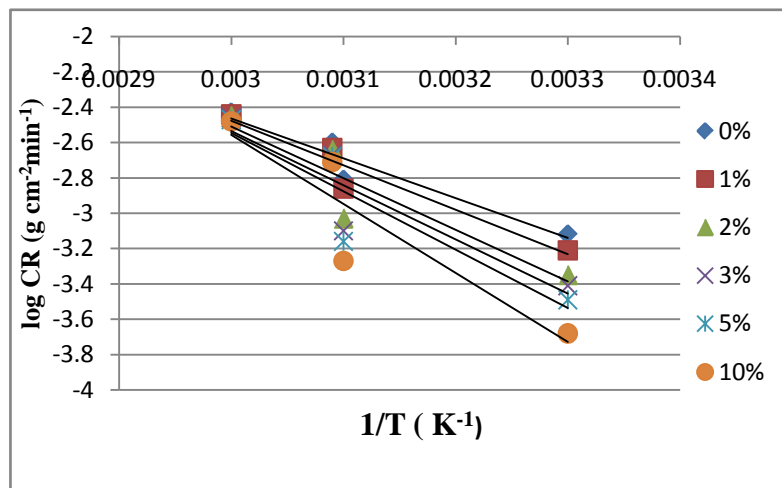


Figure 41. Arrhenius plots for mild steel corrosion in 1M H₂SO₄ in absence and presence of various concentrations of AENOL

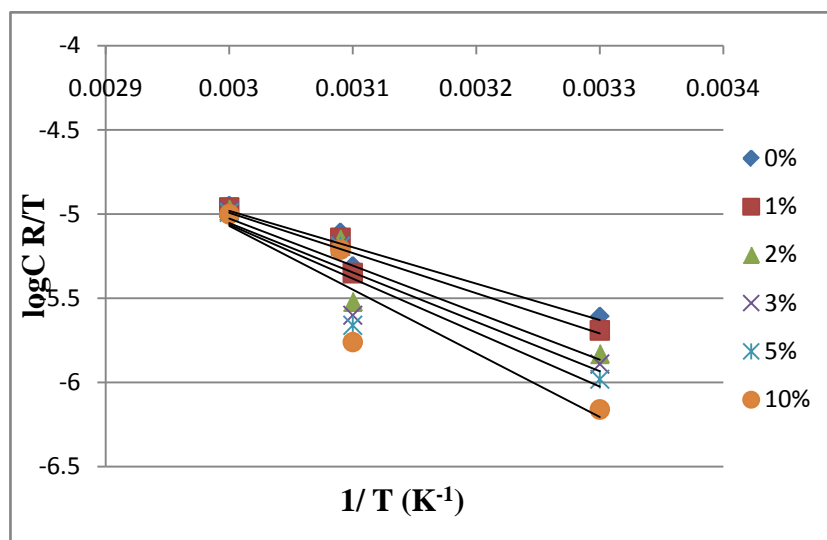


Figure 42. Transition-state plots for mild steel corrosion in 1M H₂SO₄ in absence and presence of various concentrations of AENOL

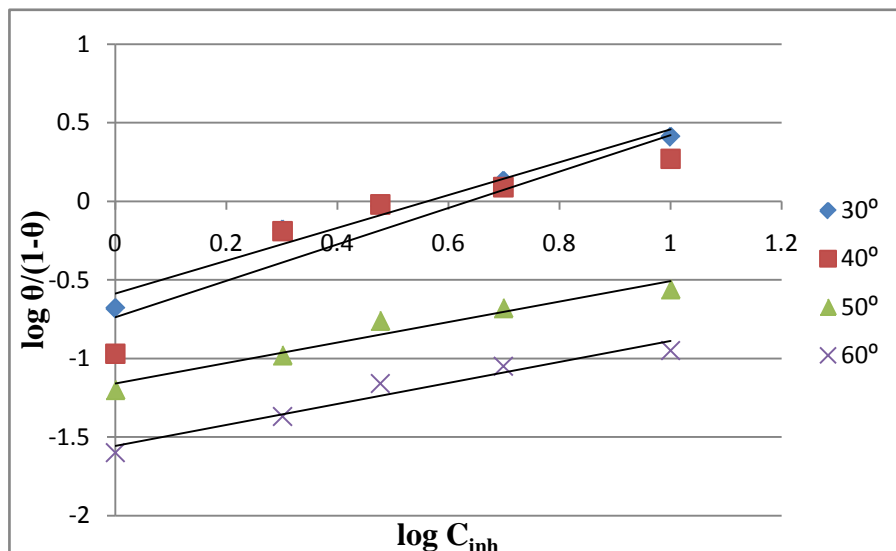


Figure 43. Langmuir adsorption isotherms of AENOL on mild steel surface in 1M H₂SO₄ at different studied temperatures

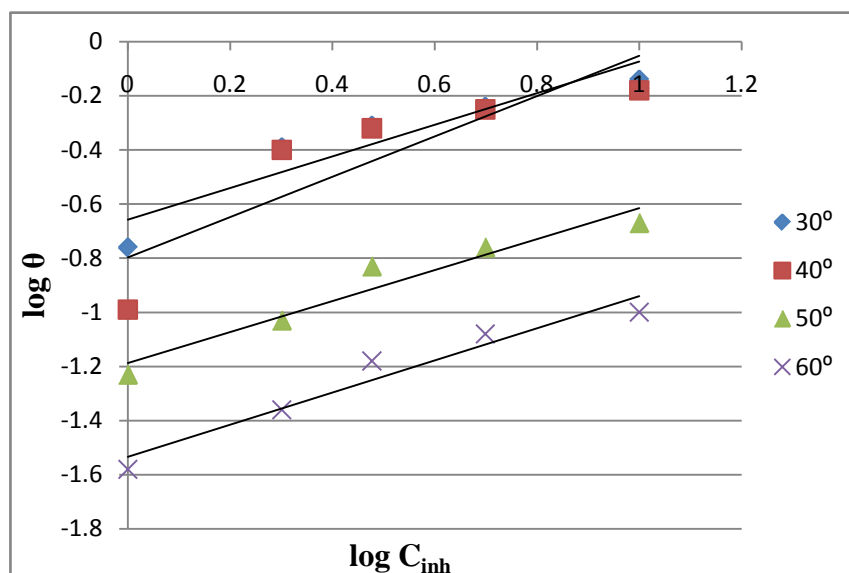


Figure 44. Freundlich adsorption isotherms of AENOL on mild steel surface in 1M H₂SO₄ at different studied temperatures

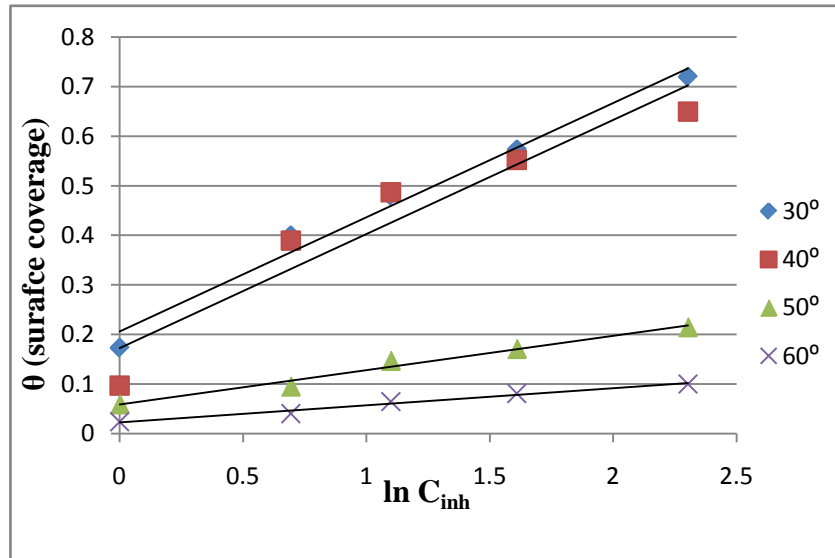


Figure 45. Temkin adsorption isotherms of AENOL on mild steel surface in 1M H₂SO₄ at different studied temperatures

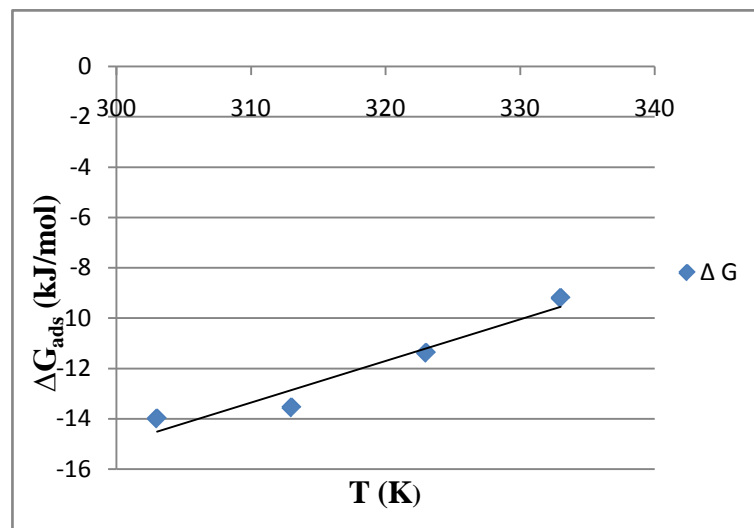


Figure 46. The variation of ΔG_{ads} (kJ/mol) with T (K) for mild steel corrosion in 1M H₂SO₄ solution with AENOL

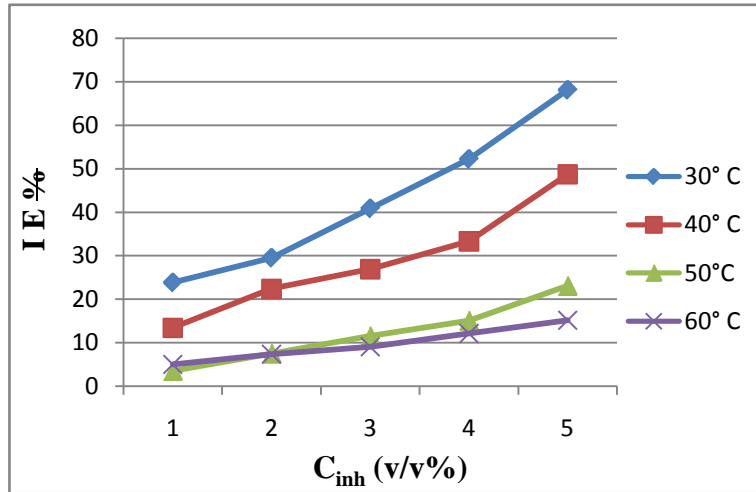


Figure 47. Variation in IE% for mild steel corrosion in 1M HCl at different concentrations of AEWHL at different studied temperatures

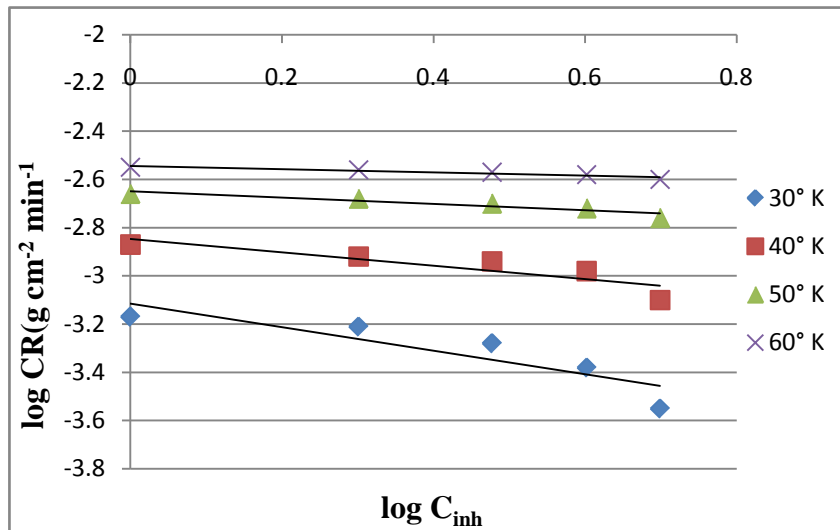


Figure 48. Variation of log CR with $\log C_{inh}$ for mild steel corrosion in 1M HCl in presence of different concentrations of AEWHL at various studied temperatures

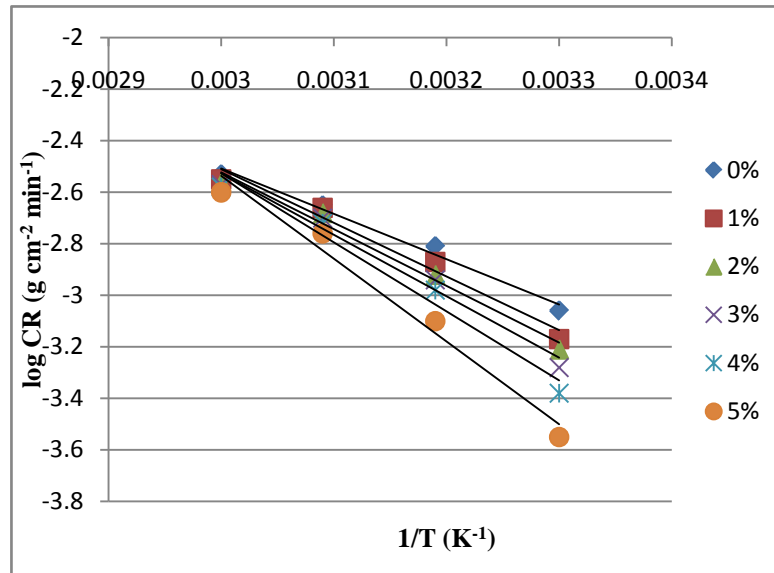


Figure 49. Arrhenius plots for mild steel corrosion in 1M HCl in absence and presence of various concentrations of AEWHL

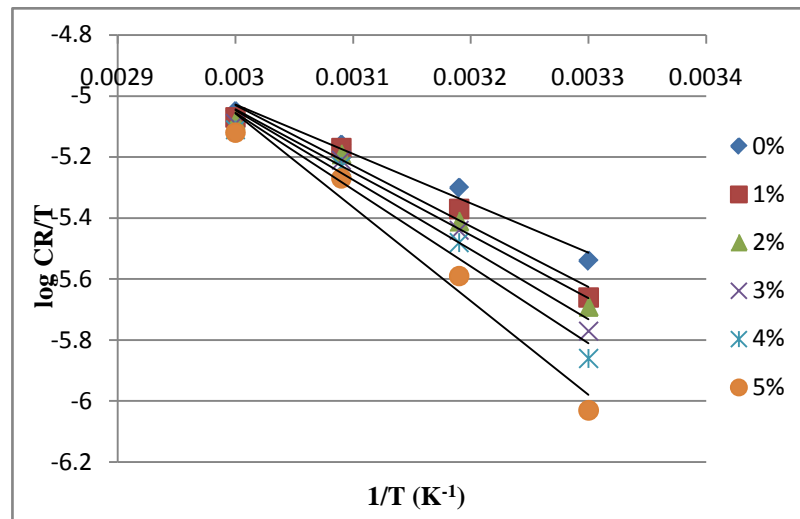


Figure 50. Transition-state plots for mild steel corrosion in 1M HCl in absence and presence of various concentrations of AEWHL

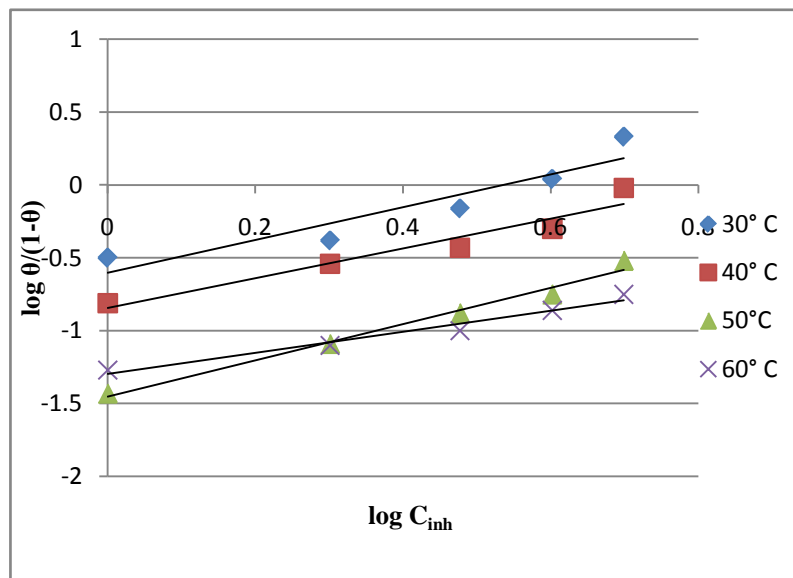


Figure 51. Langmuir adsorption isotherms of AEWHL on mild steel surface in 1M HCl at different studied temperatures

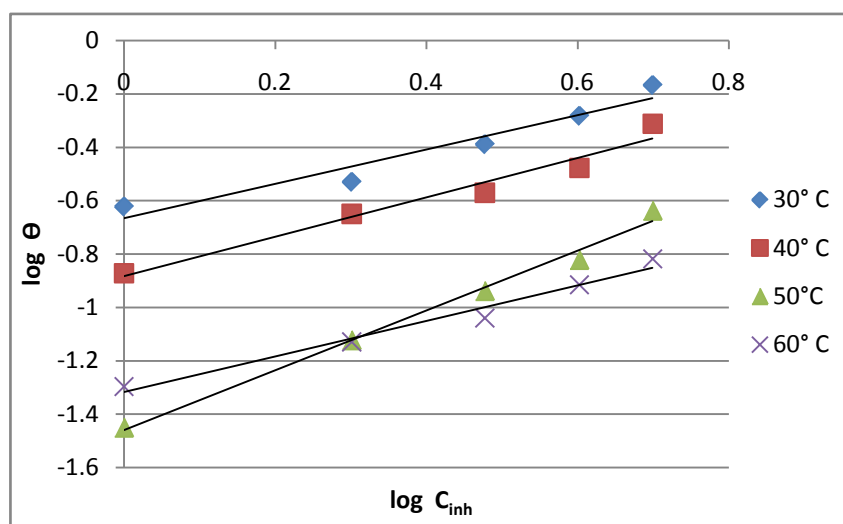


Figure 52. Freundlich adsorption isotherms of AEWHL on mild steel surface in 1M HCl at different studied temperatures

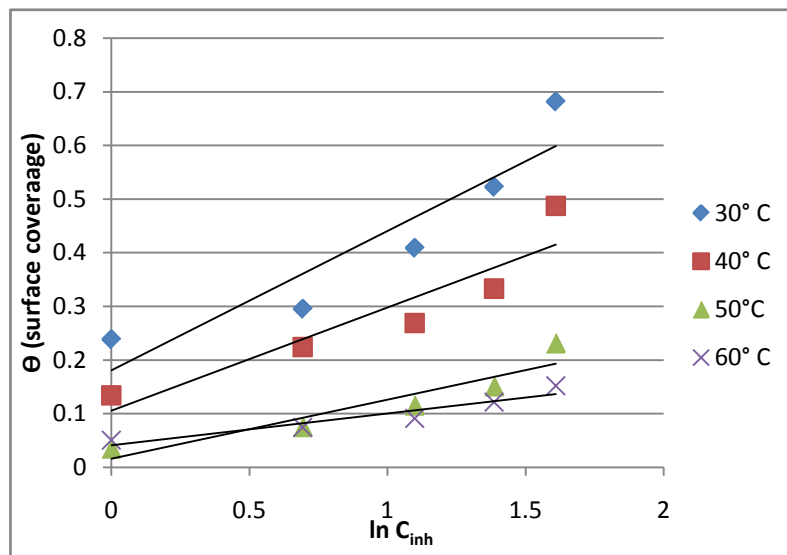


Figure 53. Temkin adsorption isotherms of AEWHL on mild steel surface in 1M HCl at different studied temperatures

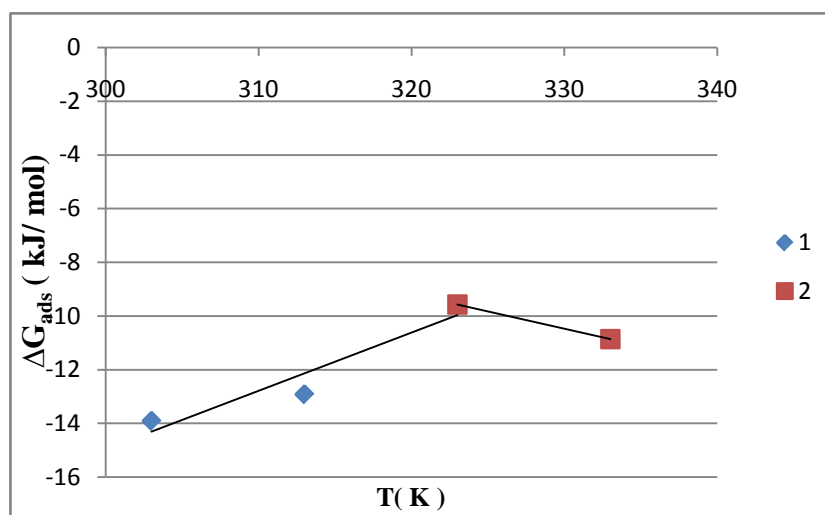


Figure 54. The variation of ΔG_{ads} (kJ/mol) with T (K) for mild steel corrosion in 1M HCl solution with AEWHL

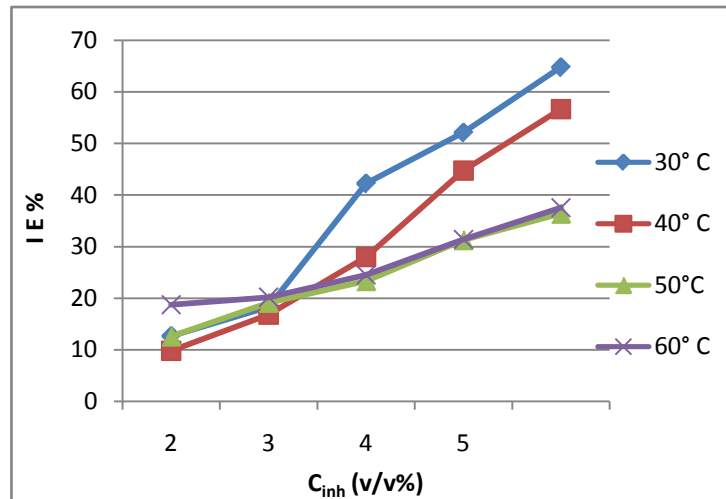


Figure 55. Variation in IE% for mild steel corrosion in 1M H₂SO₄ at different concentrations of AEWHL at different studied temperatures

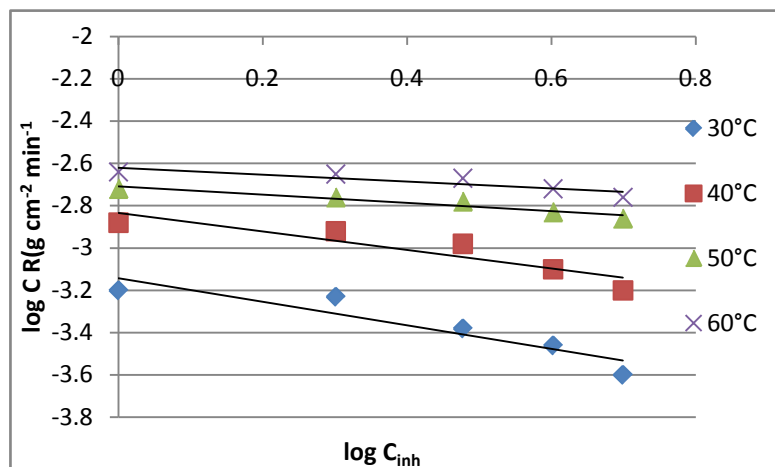


Figure 56. Variation of log CR with log C_{inh} for mild steel corrosion in 1M H₂SO₄ in presence of different concentrations of AEWHL at different studied temperatures

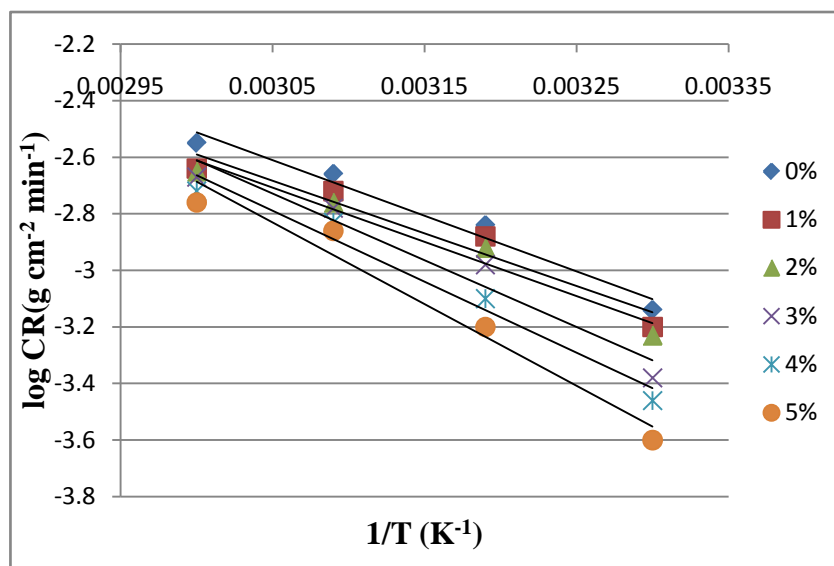


Figure 57. Arrhenius plots for mild steel corrosion in 1M H₂SO₄ in absence and presence of various concentrations of AEWHL

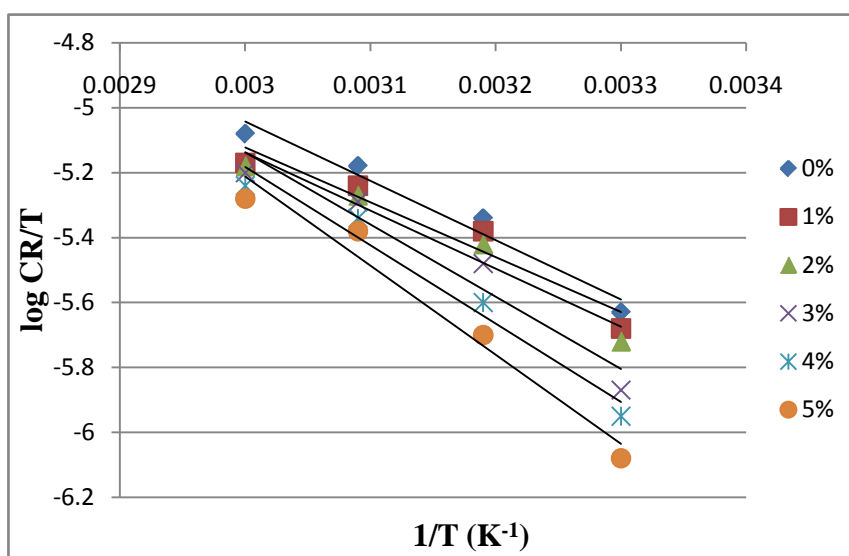


Figure 58. Transition-state plots for mild steel corrosion in 1M H₂SO₄ in absence and presence of various concentrations of AEWHL

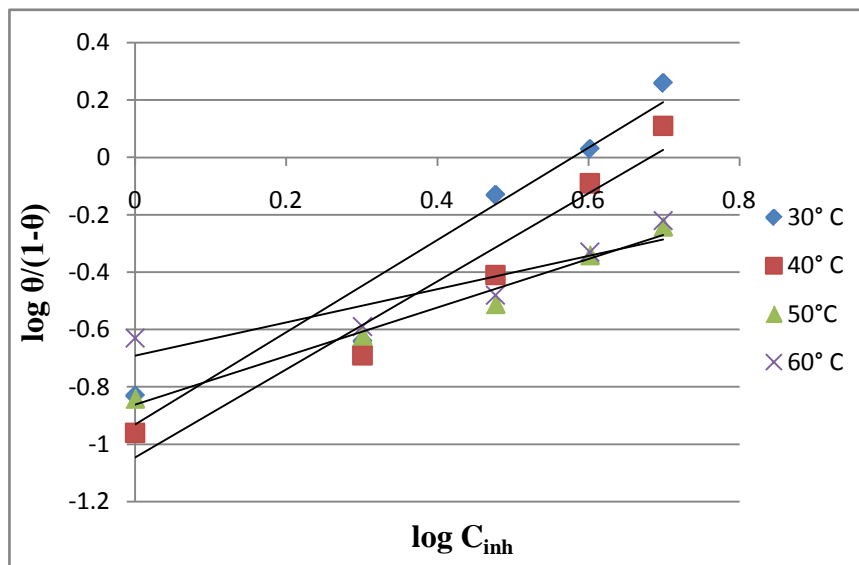


Figure 59. Langmuir adsorption isotherms of AEWHL on mild steel surface in 1M H₂SO₄ at different studied temperatures

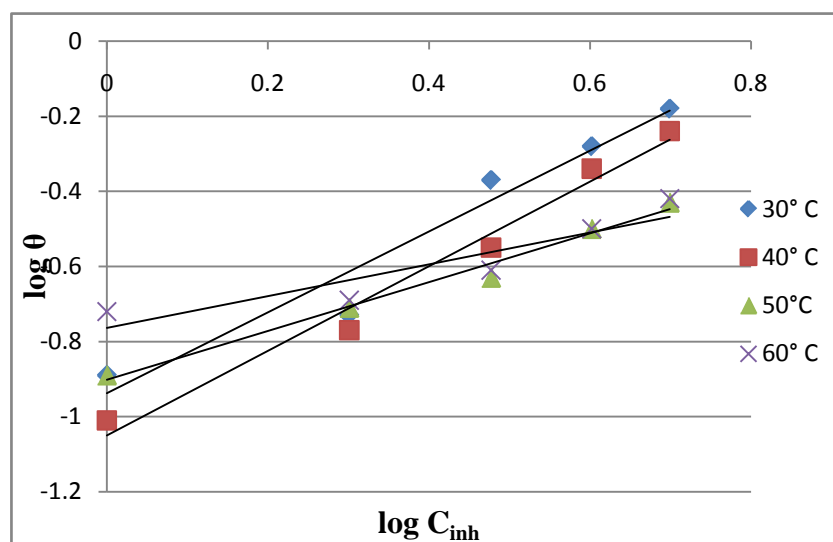


Figure 60. Freundlich adsorption isotherms of AEWHL on mild steel surface in 1M H₂SO₄ at different studied temperatures

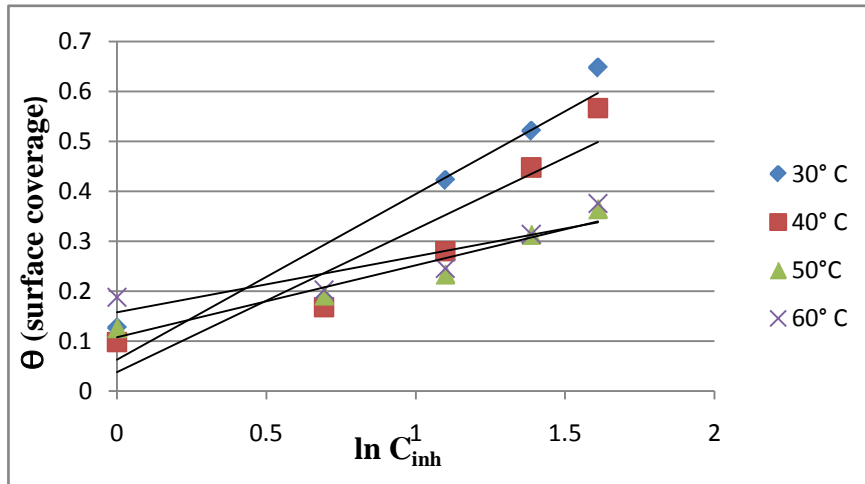


Figure 61. Temkin adsorption isotherms of AEWHL on mild steel surface in 1M H₂SO₄ at different studied temperatures

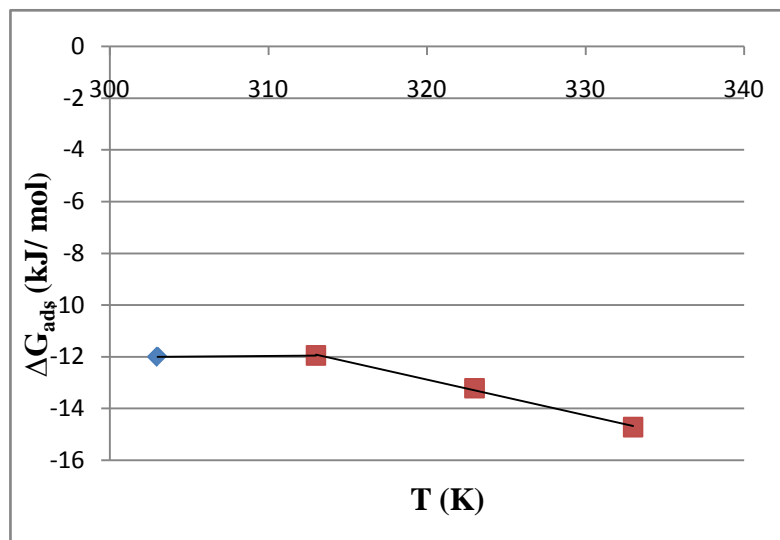


Figure 62. The variation of ΔG_{ads} (kJ/mol) with T (K) for mild steel corrosion in 1M H₂SO₄ solution with AEWHL

CHAPTER - 4

DISCUSSION ON FINDINGS AND CONCLUSIONS

Discussion on findings of present study for corrosion inhibition at mild steel surfaces is done and conclusions are drawn under eight main headings (4.1 to 4.8) according to different plant materials used viz: AECPL, AELCL, AENOL, AEWHL in two different aggressive media chosen. These discussions are enlisted below:

- 4.1 AQUEOUS EXTRACT OF CALOTROPIS PROCERA LEAVES IN 1M HCl
- 4.2 AQUEOUS EXTRACT OF CALOTROPIS PROCERA LEAVES IN 1M H₂SO₄
- 4.3 AQUEOUS EXTRACT OF LANTANA CAMARA LEAVES IN 1M HCl
- 4.4 AQUEOUS EXTRACT OF LANTANA CAMARA LEAVES IN 1M H₂SO₄
- 4.5 AQUEOUS EXTRACT OF NERIUM OLEANDER LEAVES IN 1M HCl
- 4.6 AQUEOUS EXTRACT OF NERIUM OLEANDER LEAVES IN 1M H₂SO₄
- 4.7 AQUEOUS EXTRACT OF WATER HYACINTH LEAVES IN 1M HCl
- 4.8 AQUEOUS EXTRACT OF WATER HYACINTH LEAVES IN 1M H₂SO₄

4.1 AQUEOUS EXTRACT OF CALOTROPIS PROCERA LEAVES IN 1M HCl

CORROSION RATES:

Corrosion rates were calculated by Eq.(1) [159]. Table1 shows that corrosion rates of mild steel decrease with increase in concentration of AECPL as inhibitor at all studied temperatures. This could be subjected to the adsorption of the phytoconstituents of inhibitor molecules with increase in concentration of inhibitor. The corrosion rate obeys Arrhenius type reaction, as it increases with rise in temperature [159].

INHIBITION EFFICIENCY:

From the obtained corrosion rates, inhibition efficiencies were calculated by using Eq.(2) [159,246]. Fig.1 represents the variation of IE% with different concentrations of AECPL at various studied temperatures. Data in Table2 show that IE% increase with increase in extract concentration, which is an indication of an increase in number of components of extract adsorbed on mild steel surface, which block the active sites of metal from acid attack and protect the metallic corrosion [162, 168]. Further the decrease in IE% with rise in temperature suggests electrostatic interaction (physical adsorption) of the extract molecules on mild steel surface [168]. This further indicates desorption of adsorbed inhibitor species at higher temperatures and metal dissolution takes place [83]. 60.86% inhibition efficiency is observed at 8% (v/v) concentration of inhibitor at 30°C.

KINETIC PARAMETERS:

Corrosion rates of steel specimens against concentration of inhibitor was calculated using kinetic relationship Eq.(3) [114, 160]. Fig 2 represents plot between log CR and log C_{inh} values at various studied temperatures. B and

were calculated by slope and intercept of straight lines of the graph. The obtained results in Table 3 can be discussed as follows [159].

- Negative values of B indicate that corrosion rate is inversely proportional to concentration of inhibitor. In other words the corrosion rates decrease with increase in concentration of inhibitor species.
- The high negative values of B reflect good inhibitive property of inhibitor. High negative value of B can be observed as steep slope in graph (Fig.2).
- Value of B is high at lower temperatures, indicates that inhibitive species is more effective at comparatively lower temperatures.
- The increase in K values with increase in temperature, indicating the increase in corrosion rates with temperatures.

THRMODYNAMIC AND ACTIVATION PARAMETERS:

Thermodynamic and activation parameters like apparent activation energy E_{act} , enthalpy of activation ΔH^* and entropy of activation ΔS^* were calculated for steel dissolution process. Activation energies E_{act} were calculated from the slopes of Arrhenius plots drawn between log CR and $1/T$ in Fig.3 in accordance with the Arrhenius Eq.(4) [246,232]. Table4 represents the calculated data of activation energies. The values of activation energies in presence of inhibitor were found higher than in uninhibited solution. This indicates the formation of higher energy barrier in corrosion reaction by inhibitor molecules. The increase in E_{act} for corrosion process further interpreted as physical adsorption of inhibitor species on mild steel surface [136, 166, 181]. Besides this according to Damaskin [58], the value of activation energy lesser than 80kJ/mol and even smaller than 5kJ/mol represents physical adsorption. This assertion supports the experimental results obtained in the present work. The values of enthalpies of activation ΔH^* and entropy of activation ΔS^* were calculated by transition state Eq.(5) [232, 246]. A plot of $\log (CR/T)$ versus $1/T$ gave a straight line with slope of $(-\Delta H^*/2.303R)$ and intercept of $[(\log R/Nh) + (\Delta S^*/2.303 R)]$ from which the values of ΔH^* and ΔS^* were calculated (Fig.4). These values are tabulated in

Table 4. Values of ΔH^* were found positive. Positive values indicate endothermic nature of steel dissolution process [37, 153, 246]. Endothermic process further indicates that mild steel dissolution reduces at lower temperatures and increases with increase in temperatures. Negative values of ΔS^* are indicative of formation of activated complex in rate determining step, which represents association rather than dissociation step, meaning the decrease in disorder takes place on going from reactants to activated complex [37, 85, 223]. It is also observed from data in Table 4 that E_{act} and ΔH^* vary in the same manner. Values of both E_{act} and ΔH^* increase with increase in concentration of inhibitor, suggesting that energy barrier is increases with increase in inhibitor concentration. This means that corrosion reaction will further be pushed to surface sites that are characterized by progressively higher values of E_{act} as the concentration of inhibitor becomes greater [37, 221, 227]. The values of activation energy were found larger than corresponding values of enthalpy of activation, indicate the involvement of a gaseous reaction, simply hydrogen evolution in corrosion process, associated with a decrease in total reaction volume [159].

ADSORPTION ISOTHERMS:

The nature of adsorption can be explained by understanding the process at metal/electrolyte interface. Further to understand the nature of adsorption, obtained surface coverage (θ) were fitted in different adsorption isotherms. Langmuir adsorption isotherm was drawn by using Eq. (8) [38, 83, 161, 185, 237]. Freundlich adsorption isotherm was also drawn using the Eq.(10) [117] and straight lines were obtained. These isotherms are shown in Fig.5 and Fig.6 respectively.

ADSORPTION PARAMETERS:

[Gibbs Energy of Adsorption][ΔG_{ads}], Enthalpy of Adsorption][ΔH_{ads}] and Entropy of Adsorption [ΔS_{ads}]

Values of K_{ads} were calculated by the intercept of Langmuir isotherm drawn according to the Eq.(8) between $\log (\theta/1- \theta)$ and $\log C_{inh}$ and by using this

Gibbs energy was calculated by using Eq. (13) [115, 159]. The values of ΔG_{ads} were tabulated in Table 5. ΔG_{ads} values have been found negative at all studied temperatures indicating spontaneous adsorption process of inhibitor molecules and strong interactions between inhibitor molecules and metal surface [1, 37, 49, 67, 213, 225, 226]. Increase in ΔG_{ads} values (becomes less negative) with the increase of temperature indicates the occurrence of exothermic process [159]. Table 5 shows increase in ΔG_{ads} values with temperature indicates exothermic process of adsorption of inhibitor molecules, which is unfavourable at higher temperature due to desorption of inhibitor from metal surface [159, 225]. Generally values of ΔG_{ads} upto -20 KJ/mol are consistent with electrostatic interactions (physical adsorption) between charged molecules and charged metal surface and values upto -40 KJ/mol or higher involve charge sharing or transfer from inhibitor molecules to metal surface to form coordinate type of bond (chemical adsorption) [37, 49, 90, 132, 163, 165, 233]. The values of ΔG_{ads} were found from -13.76 kJ/mol to -11.59 kJ/mol. The obtained values of ΔG_{ads} were found less than -20 kJ/mol indicated physical adsorption of inhibitor molecules. Further the value of ΔG_{ads} is more negative at lower temperatures indicating that corrosion inhibition process is more effective at lower temperatures. It has been observed that adsorption of negatively charged species is facilitated due to the positively charged metal. But positively charged species can also be adsorbed and protect the positively charged metal surface acting with a negatively charged intermediate such as acid anions, adsorbed on metal surface [37, 181, 233]. Obtained values of Gibbs energy were plotted against temperature (Fig. 7) according to the basic Eq. (14) [72, 159]. Intercept of graph between ΔG_{ads} versus T (Fig. 7) gives value of ΔH_{ads} and by putting the value of intercept in Eq. (14) values of ΔS_{ads} were obtained. These obtained adsorption parameters Gibbs free energy of adsorption (ΔG_{ads}), enthalpy of adsorption (ΔH_{ads}), entropy of adsorption (ΔS_{ads}), are listed in Table 5. Values of ΔH_{ads} have been found negative indicating the exothermic adsorption process [85, 134, 136, 162], which further indicates lower IE% at higher temperatures, due to desorption of inhibitor molecules. The exothermic process is attributed to either physical or

chemical adsorption or mixture of both [42]. In exothermic process, values of ΔH_{ads} predict physisorption or chemisorption. For physisorption values of ΔH_{ads} is lower than 40kJ/mol while for chemisorption it approaches to 100 kJ/mol [39, 251]. Values of ΔH_{ads} in Table 5 indicate physisorption. Negative values of ΔS_{ads} indicate decrease in entropy of adsorption process. This behavior can be explained as follows: Before the adsorption of inhibitor molecules onto mild steel surface, inhibitor molecules might freely move in bulk solution (inhibitor molecules were chaotic). But with the process of adsorption, inhibitor molecules were orderly adsorbed onto the steel surface as a result decrease in entropy is observed [132, 133].

A more interesting behavior is observed in Table5 that negative ΔS_{ads} value is accompanied with negative ΔH_{ads} value. This further agrees that when the adsorption is an exothermic process, it must be accompanied by a decrease in the entropy change and vice versa [159, 228].

CONCLUSIONS:

1. Result showed that AECPL is good corrosion inhibitor for mild steel in 1M HCl solution.
2. Corrosion rates increase with increase in temperature and decrease with increase in inhibitor concentration.
3. Inhibition efficiency increases at lower temperature suggests the physisorption process of inhibitor on mild steel surface.
4. Apparent activation energy increases with increase in inhibitor concentrations also suggests physisorption.
5. Enthalpy of adsorption comes out to be negative and lower than 40 kJ/mol, which shows exothermic and physical adsorption process of inhibitor on mild steel surface.
6. The values of Gibbs free energies calculated were negative shows spontaneity of corrosion inhibition process of mild steel in 1 M HCl in AECPL.

4.2 AQUEOUS EXTRACT OF CALOTROPIS PROCERA LEAVES IN **1M H₂SO₄**

CORROSION RATES:

Corrosion rates were calculated by Eq.(1) [159]. Table6 shows that corrosion rates of mild steel decrease with increase in concentration of AECPL as inhibitor at all studied temperatures. This could be subjected to the adsorption of the phyto-constituents of inhibitor molecules with increase in concentration of inhibitor. The corrosion rate obeys Arrhenius type reaction, as it increases with rise in temperature [159].

INHIBITION EFFICIENCY:

From the obtained corrosion rates, inhibition efficiencies were calculated by using Eq.(2) [159,246]. Fig.8 represents the variation of IE% with different concentrations of AECPL at various studied temperatures. Data in Table 7 show that IE% increases or decreases with increasing temperatures at different studied extract concentrations of AECPL. This indicates the comprehensive adsorption (physical and chemical) of inhibitor species on mild steel surface [159]. Such type of observations were found in previous study by Noor [159]. Further it has been observed that IE% were increase with increase in inhibitor concentration. 51.56% inhibition efficiency is observed at 8% (v/v) concentration of inhibitor at 30°C.

KINETIC PARAMETERS:

Corrosion rates of steel specimens against concentration of inhibitor were calculated using kinetic relationship as Eq.(3) [114,160]. Fig 9 represents plot between log CR and log C_{inh} values at various studied temperatures. B and K were calculated by slope and intercept of straight lines of the graph.

The obtained results in Table 8 can be discussed as follows [159]:

- Negative values of B indicate that corrosion rate is inversely proportional to concentration of inhibitor. In other words the corrosion rates decrease with increase in concentration of inhibitor species.
- The high negative values of B reflect good inhibitive property of inhibitor. High negative value of B can be observed as steep slope in graph Fig.(9).
- Value of B is high at lower temperatures, indicates that inhibitive species is more effective at comparatively lower temperatures.
- The increase in K values with increase in temperature, indicating the increase in corrosion rates with temperatures.

THRMODYNAMIC AND ACTIVATION PARAMETERS:

Thermodynamic and activation parameters like apparent activation energy E_{act} , enthalpy of activation ΔH^* entropy of activation ΔS^* were calculated for steel dissolution process. Activation energies E_{act} were calculated from the slopes of Arrhenius plots drawn between log CR and $1/T$ in Fig.10 in accordance with the Arrhenius Eq. (4) [232, 246]

Table 9 represents the calculated data of activation energies. The values of activation energies in presence of inhibitor were found higher than in uninhibited solution. This indicates the formation of higher energy barrier in corrosion reaction by inhibitor molecules. The increase in E_{act} for corrosion process further interpreted as physical adsorption of inhibitor species on mild steel surface [136,166, 181]. Besides this according to Damaskin [58], the value of activation energy lesser than 80 kJ /mol and even smaller than 5 kJ/mol represents physical adsorption. This assertion supports the experimental results obtained in the present work. The values of enthalpy of activation ΔH^* and entropy of activation ΔS^* were calculated by transition state Eq.(5) [232, 246]. A plot of $\log (CR/T)$ vs $1/T$ gave a straight line with slope of $(-\Delta H^*/2.303R)$ and intercept of $[(\log R/Nh) + (\Delta S^*/2.303 R)]$ from which the values of ΔH^* and ΔS^* were calculated (Fig.11). These values are tabulated in Table 9 Values of ΔH^* were found positive. Positive values indicate endothermic nature of steel dissolution process [37, 153, 246]. Endothermic process further indicates that mild steel dissolution reduces at lower

temperatures and increases with increase in temperatures. Negative values of ΔS^* are indicative of formation of activated complex in rate determining step, which represents association rather than dissociation step, meaning the decrease in disorder takes place on going from reactants to activated complex [37, 85, 223].

It is also observed from data in Table 9 that E_{act} and ΔH^* vary in the same manner. Values of both E_{act} and ΔH^* increase with increase in concentration of inhibitor, suggesting that energy barrier is increases with increase in inhibitor concentration. This means that corrosion reaction will further be pushed to surface sites that are characterized by progressively higher values of E_{act} as the concentration of inhibitor becomes greater [37, 221, 227]. The values of activation energy were found larger than corresponding values of enthalpy of activation, indicate the involvement of a gaseous reaction, simply hydrogen evolution in corrosion process, associated with a decrease in total reaction volume [159].

ADSORPTION ISOTHERMS:

The nature of adsorption can be explained by understanding the process at metal/electrolyte interface. Further to understand the nature of adsorption, obtained surface coverage (θ) were fitted in different adsorption isotherms. Langmuir adsorption isotherm was plotted using Eq. (8) [38, 83, 161, 185, 237]. Freundlich and Temkin isotherm were also plotted using following Eq.(10) [117] & Eq.(11) [152, 172] and straight lines were observed. These isotherms are shown in Fig.12, Fig.13 and Fig.14 respectively.

ADSORPTION PARAMETERS:

[Gibbs Energy of Adsorption][ΔG_{ads}], Enthalpy of Adsorption][ΔH_{ads}] and Entropy of Adsorption [\Delta S_{ads}] :

Values of K_{ads} were calculated by the intercept of Langmuir isotherm drawn according to the Eq.(8) between $\log(\theta/1-\theta)$ and $\log C_{inh}$ and using this Gibbs energy was calculated by using Eq.(13) [115, 159]. The values of ΔG_{ads} were tabulated in Table10 ΔG_{ads} values has been found negative at all studied temperatures indicating spontaneous adsorption process of inhibitor molecules on

metal surface and strong interactions between inhibitor molecules and metal surface [1, 37, 49, 67, 213, 225, 226]. Generally values of ΔG_{ads} upto -20 kJ/mol are consistent with electrostatic interactions (physical adsorption) between charged molecules and charged metal surface and values upto -40 kJ/mol or higher involve charge sharing or transfer from inhibitor molecules to metal surface to form coordinate type of bond (chemical adsorption) [37, 49, 90, 132, 163, 165, 233]. The values of ΔG_{ads} were found from -10.27 kJ/mol to -12.15 kJ/mol. The obtained values of ΔG_{ads} were found less than -20 kJ/mol indicated physical adsorption of inhibitor molecules. It has been observed that adsorption of negatively charged species is facilitated due to the positively charged metal. But positively charged species can also be adsorbed and protect the positively charged metal surface acting with a negatively charged intermediate such as acid anions, adsorbed on metal surface [37, 181, 233]. Obtained values of Gibbs energy were plotted against temperature in accordance with the following basic Eq.(14) [72, 159]. Fig.15 shows the graph between ΔG_{ads} and T (K). Intercept of graph between ΔG_{ads} vs T give value of ΔH_{ads} and by putting the value of intercept in Eq.(14) values of ΔS_{ads} were obtained. These obtained adsorption parameters Gibbs free energy of adsorption (ΔG_{ads}), enthalpy of adsorption (ΔH_{ads}) and entropy of adsorption (ΔS_{ads}) are listed in Table 10. A segmented line of two opposite slopes was obtained in Fig.15 indicating two sets of adsorption sites having different ΔH_{ads} values. Similar type of results have been found in previous study between ΔG_{ads} and T(K) by E.A. Noor [159]. The calculated ΔH_{ads} values have been found negative and positive indicating both exothermic adsorption process [85, 134, 136, 162] and endothermic adsorption process [94, 237] respectively, depend upon the specific temperature range. Such type of comprehensive adsorption processes were obtained in previous study [159]. The exothermic process is attributed to either physical or chemical adsorption or mixture of both [42], while the endothermic process is attributed to chemisorption [65]. In exothermic process, values of ΔH_{ads} predict physisorption or chemisorption. For physisorption values of ΔH_{ads} is lower than 40 kJ/mol while for chemisorption it approaches to 100 kJ/mol [39, 251]. Negative values of ΔH_{ads} in Table 10 indicate chemisorption as it is greater than 40 kJ/mol.

Negative values of ΔS_{ads} indicate decrease in entropy of adsorption process. This behaviour can be explained as follows: Before the adsorption of inhibitor molecules onto mild steel surface, inhibitor molecules might freely move in bulk solution (inhibitor molecules were chaotic). But with the process of adsorption, inhibitor molecules were orderly adsorbed onto the steel surface as a result decrease in entropy is observed [132, 133]. The obtained positive values of ΔS_{ads} are the algebraic sum of the entropies of adsorption of organic molecules and the desorption of water molecules [78, 137]. Therefore the positive values of entropy of adsorption is the result of the substitution process, which can be attributed to the increase in the solvent entropy and more positive water desorption entropy [29, 151].

A more interesting behaviour is observed in Table10 that negative ΔS_{ads} value is accompanied with negative ΔH_{ads} value. This further agrees that when the adsorption is an exothermic process, it must be accompanied by a decrease in the entropy change and vice versa [159, 228].

CONCLUSIONS:

1. Result showed that AECPL is good corrosion inhibitor for mild steel in 1M H₂SO₄ solution.
2. Corrosion rates increase with increase in temperature and decrease with increase in inhibitor concentration.
3. Inhibition efficiency increases or decreases with increase in temperatures at given concentrations of inhibitor suggests comprehensive adsorption process.
4. Apparent activation energy increases with increase in inhibitor concentrations also suggests physisorption.
5. Enthalpy of adsorption comes out to be negative and positive suggests exothermic and endothermic adsorption process.
6. The values of Gibbs free energies calculated were negative show spontaneity of corrosion inhibition process of mild steel in 1M H₂SO₄ in AECPL.

4.3 AQUEOUS EXTRACT OF LANTANA CAMARA LEAVES IN 1M HCl

CORROSION RATES:

Corrosion rates were calculated by Eq.(1)[159]. Table 11 shows that corrosion rates of mild steel decrease with increase in concentration of AELCL as inhibitor at all studied temperatures. This could be subjected to the adsorption of the phytoconstituents of inhibitor molecules with increase in concentration of inhibitor. The corrosion rate obeys Arrhenius type reaction, as it increases with rise in temperature [159].

INHIBITION EFFICIENCY:

From the obtained corrosion rates, inhibition efficiencies were calculated using Eq.(2)[159,246]. Fig.16 represents the variation of IE% with different concentrations of AELCL at various studied temperatures. Data in Table 12 show that IE% increases with increase in extract concentration, which is an indication of an increase in number of components of extract adsorbed on mild steel surface, which block the active sites of metal from acid attack and protect the metallic corrosion [162,168]. Further the decrease in IE% with rise in temperature suggests electrostatic interaction (physical adsorption) of the extract molecules on mild steel surface. This further indicates desorption of adsorbed inhibitor species at higher temperatures and metal dissolution takes place [83]. 90% inhibition efficiency is observed at 30°C at 6% (v/v) concentration of inhibitor.

KINETIC PARAMETERS:

Corrosion rates of steel specimens against concentration of inhibitor were calculated using kinetic relationship Eq.(3)[114,160]. Fig.17 represents plot between log CR and log C_{inh} values at various studied temperatures. B and K

were calculated by slope and intercept of straight lines of the graph. The obtained results in Table13 can be discussed as follows [159].

- Negative values of B indicate that corrosion rate is inversely proportional to concentration of inhibitor. In other words the corrosion rates decrease with increase in concentration of inhibitor species.
- The high negative values of B reflect good inhibitive property of inhibitor. High negative value of B can be observed as steep slope in graph [Fig.17].
- Value of B is high at lower temperatures, indicates that inhibitive species is more effective at comparatively lower temperatures.
- The increase in K values with increase in temperature, indicating the increase in corrosion rates with temperatures.

THRMODYNAMIC AND ACTIVATION PARAMETERS:

Thermodynamic and activation parameters like apparent activation energy E_{act} , enthalpy of activation ΔH^* and entropy of activation ΔS^* were calculated for steel dissolution process. Activation energies E_{act} were calculated from the slopes of Arrhenius plots drawn between $\log CR$ and $1/T$ in Fig.18 in accordance with the Arrhenius Eq.(4)[232,246]. Table14 represents the calculated data of activation energies. The values of activation energies in presence of inhibitor were found higher than in uninhibited solution. This indicates the formation of higher energy barrier in corrosion reaction by inhibitor molecules. The increase in E_{act} for corrosion process further interpreted as physical adsorption of inhibitor species on mild steel surface [136, 166, 181]. Besides this according to Damaskin [58], the value of activation energy lesser than 80kJ/mol and even smaller than 5kJ/mol represents physical adsorption. This assertion supports the experimental results obtained in the present work upto the 4% (v/v) concentration of inhibitor. But at concentration 6% (v/v) of inhibitor 86.12 kJ/mol activation energy is observed, indicating chemical adsorption. The values of enthalpy of activation ΔH^* and entropy of activation ΔS^* were calculated by transition state Eq.(5). A plot of $\log (CR/T)$ versus $1/T$ in Fig.19 gave a straight line with slope of $(-\Delta H^*/2.303R)$ and intercept of $[(\log R/Nh) + (\Delta S^*/2.303R)]$ from which the values of ΔH^* and ΔS^*

were calculated. These values are tabulated in Table 14. Values of ΔH^* were found positive. Positive values indicate endothermic nature of steel dissolution process [37, 153, 246]. Endothermic process further indicates that mild steel dissolution reduces at lower temperatures and increases with increase in temperatures. Negative values of ΔS^* are indicative of formation of activated complex in rate determining step, which represents association rather than dissociation step, meaning the decrease in disorder takes place on going from reactants to activated complex [37, 85, 223]. It is also observed from data in Table 14 that E_{act} and ΔH^* vary in the same manner. Values of both E_{act} and ΔH^* increase with increase in concentration of inhibitor, suggesting that energy barrier is increases with increase in inhibitor concentration. This means that corrosion reaction will further be pushed to surface sites that are characterized by progressively higher values of E_{act} as the concentration of inhibitor becomes greater [37, 221, 227]. The values of activation energy were found larger than corresponding values of enthalpy of activation, indicate the involvement of a gaseous reaction, simply hydrogen evolution in corrosion process, associated with a decrease in total reaction volume [159].

ADSORPTION ISOTHERMS:

The nature of adsorption can be explained by understanding the process at metal/electrolyte interface. Further to understand the nature of adsorption, obtained surface coverage (θ) were fitted in different adsorption isotherms. Langmuir adsorption isotherm was drawn by using Eq.(8) [38,83,161,185,237]. Freundlich and Temkin adsorption isotherms were also drawn according to Eq.(10) [117] and Eq.(11) [152,172] and straight lines were obtained. These isotherms are shown in Fig.20, Fig.21 and Fig.22 respectively.

ADSORPTION PARAMETERS:

Gibbs Energy of Adsorption[ΔG_{ads}], **Enthalpy of Adsorption**[ΔH_{ads}] and **Entropy of Adsorption** [ΔS_{ads}]

Values of K_{ads} were calculated by the intercept of Langmuir isotherm drawn according to the Eq.(8) between $\log(\theta/1-\theta)$ and $\log C_{inh}$ and by using this Gibbs energy was calculated by using Eq.(13) [115,159]. The values of ΔG_{ads} were tabulated in Table15. ΔG_{ads} values has been found negative at all studied temperatures indicating spontaneous adsorption process of inhibitor molecules on metal surface and strong interactions between inhibitor molecules and metal surface [1, 37, 49, 67, 213, 225, 226]. Increase in ΔG_{ads} values (becomes less negative) with the increase of temperature indicates the occurrence of exothermic process [159]. Data in Table15 shows increase in ΔG_{ads} values with temperature indicates exothermic process of adsorption of inhibitor molecules, which is unfavourable at higher temperature due to desorption of inhibitor from metal surface [159, 225]. Generally values of ΔG_{ads} upto -20 kJ/mol are consistent with electrostatic interactions (physical adsorption) between charged molecules and charged metal surface and values upto -40 kJ/mol or higher involve charge sharing or transfer from inhibitor molecules to metal surface to form coordinate type of bond (chemical adsorption) [37, 49, 90, 132, 163, 165, 233]. The values of ΔG_{ads} were found from -11.60 kJ/mol to -7.85 kJ/mol. The obtained values of ΔG_{ads} were found less than -20 kJ/mol indicated physical adsorption of inhibitor molecules. Further the value of ΔG_{ads} is more negative at lower temperatures indicating that corrosion inhibition process is more effective at lower temperatures. Obtained values of Gibbs energy were plotted against temperature in Fig.23 according to the basic Eq.(14)[72,159]. Intercept of graph between ΔG_{ads} versus T in Fig.23 gives value of ΔH_{ads} and by putting the value of intercept in Eq.(14) values of ΔS_{ads} were obtained. These obtained adsorption parameters Gibbs free energy of adsorption (ΔG_{ads}), enthalpy of adsorption (ΔH_{ads}) and entropy of adsorption (ΔS_{ads}) are listed in Table15. A segmented line of two opposite slopes was obtained in Fig.23 indicating two sets of adsorption sites having different ΔH_{ads} values. Similar type of results have been found in previous study between ΔG_{ads} and T(K) by E.A. Noor [159]. The calculated ΔH_{ads} values have been found negative and positive indicating both exothermic adsorption process [85, 134, 136, 162] and endothermic adsorption process [94, 237] respectively, depend upon the specific temperature range. Similar type of

comprehensive adsorption processes were obtained in previous study [159]. Exothermic process is attributed to either physical or chemical adsorption or mixture of both [42], while the endothermic process is attributed to chemisorption [65]. In exothermic process, values of ΔH_{ads} predict physisorption or chemisorption. For physisorption values of ΔH_{ads} is lower than 40 kJ/mol while for chemisorption it approaches to 100 kJ/mol [39, 251]. Values of ΔH_{ads} in Table 15 indicate both physisorption and chemisorption process. Negative values of ΔS_{ads} indicate decrease in entropy of adsorption process. This behavior can be explained as follows: Before the adsorption of inhibitor molecules onto mild steel surface, inhibitor molecules might freely move in bulk solution (inhibitor molecules were chaotic). But with the process of adsorption, inhibitor molecules were orderly adsorbed onto the steel surface as a result decrease in entropy is observed [132, 133]. The obtained positive values of ΔS_{ads} are the algebraic sum of the entropies of adsorption of organic molecules and desorption of water molecules [78, 137]. Therefore the positive values of entropy of adsorption is the result of the substitution process, which can be attributed to the increase in the solvent entropy and more positive water desorption entropy [29, 151].

A more interesting behavior is observed in Table15 that negative ΔS_{ads} value is accompanied with negative ΔH_{ads} value and positive ΔS_{ads} value is accompanied with positive ΔH_{ads} value. This further agrees that when the adsorption is an exothermic process, it must be accompanied by a decrease in the entropy change and vice versa [159, 228]. It has been observed that adsorption of negatively charged species is adsorbed due to the positively charged metal. But positively charged species can also be adsorbed and protect the positively charged metal surface acting with a negatively charged intermediate such as acid anions, adsorbed on metal surface [37, 181, 233].

CONCLUSIONS:

1. Result showed that AELCL is good corrosion inhibitor for mild steel in 1M HCl solution.
2. Corrosion rates increase with increase in temperature and decrease with increase in inhibitor concentration.

3. Inhibition efficiencies increases at lower temperature suggest the physisorption process of inhibitor on mild steel surface.
4. Apparent activation energy increases with increase in inhibitor concentrations also suggests physisorption but chemisorptions is observed at 6 % (v/v) concentration.
5. Enthalpy of adsorption comes out to be positive and negative both at specific temperatures and its values indicate both chemisorption and physisorption process.
6. The values of Gibbs free energies calculated were negative shows spontaneity of corrosion inhibition process of mild steel in 1M HCl in AELCL.

4.4 AQUEOUS EXTRACT OF LANTANA CAMARA LEAVES IN 1M **H₂SO₄**

CORROSION RATES:

Corrosion rates were calculated by using Eq.(1)[159]. Table16 shows that corrosion rates of mild steel decrease with increase in concentration of AELCL as inhibitor at all studied temperatures. This could be subjected to the adsorption of the phyto-constituents of inhibitor molecules with increase in concentration of inhibitor. The corrosion rate obeys Arrhenius type reaction, as it increases with rise in temperature [159].

INHIBITION EFFICIENCY:

From the obtained corrosion rates, inhibition efficiencies were calculated by using Eq.(2)[159,246]. Fig.24 represents the variation of IE% with different concentrations of AELCL at various studied temperatures. Data in Table 17 show that IE% increases or decreases with increasing temperatures at different studied extract concentrations of AELCL. This indicates the comprehensive adsorption (physical and chemical adsorption) of inhibitor species on mild steel surface [159]. Such type of observations were found in previous study by E.A. Noor [159]. Further it has been observed that IE% were increase with increase in inhibitor concentration. 65.30% inhibition efficiency is observed at 30°C at 6% (v/v) concentration of inhibitor.

KINETIC PARAMETERS:

Corrosion rates of mild steel specimens were calculated by using the kinetic relationship according to Eq.(3)[114,160]. Fig 25 represents plot between log CR and log C_{inh} values at various studied temperatures. B and K were calculated by slope and intercept of straight lines of the graph. The obtained results in Table 18 can be discussed as follows [159].

- Negative values of B indicate that corrosion rate is inversely proportional to concentration of inhibitor. In other words the corrosion rates decrease with increase in concentration of inhibitor species.
- The high negative values of B reflect good inhibitive property of inhibitor. High negative value of B can be observed as steep slope in graph [Fig.25].
- Value of B is high at lower temperatures, indicates that inhibitive species is more effective at comparatively lower temperatures.
- The increase in K values with increase in temperature, indicating the increase in corrosion rates with temperatures.

THRMODYNAMIC AND ACTIVATION PARAMETERS:

The thermodynamic and activation parameters like apparent activation energy E_{act} , enthalpy of activation ΔH^* entropy of activation ΔS^* were calculated for steel dissolution process. Activation energies E_{act} were calculated from the slopes of Arrhenius plots drawn between $\log CR$ and $1/T$ in Fig.26 in accordance with the Arrhenius Eq.(4)[232,246]. Table19 represents the calculated data of activation energies. The values of activation energies in presence of inhibitor were found higher than in uninhibited solution. This indicates the formation of higher energy barrier in corrosion reaction by inhibitor molecules. The increase in E_{act} for corrosion process further interpreted as physical adsorption of inhibitor species on mild steel surface [136, 166, 181]. Besides this According to Damaskin [58], the value of activation energy lesser than 80kJ /mol and even smaller than 5kJ/mol represents physical adsorption. This assertion supports the experimental results obtained in the present work. The values of enthalpy of activation ΔH^* and entropy of activation ΔS^* were calculated by using transition state Eq.(5)[232,246]. A plot of $\log (CR/T)$ vs $1/T$ gave a straight line with slope of $(-\Delta H^*/2.303R)$ and intercept of $[(\log R/Nh) + (\Delta S^*/2.303R)]$ from which the values of ΔH^* and ΔS^* were calculated (Fig.27). These values are tabulated in Table19. Values of ΔH^* were found positive. Positive values indicate endothermic nature of steel dissolution process [37, 153, 246]. Endothermic process further indicates that mild steel dissolution reduces at lower

temperatures and increases with increase in temperatures. Negative values of ΔS^* are indicative of formation of activated complex in rate determining step, which represents association rather than dissociation step, meaning that the decrease in disorder takes place on going from reactants to activated complex [37, 85, 223].

It is also observed from data in Table 19 that E_{act} and ΔH^* vary in the same manner. Values of both E_{act} and ΔH^* increase with increase in concentration of inhibitor, suggesting that energy barrier is increases with increase in inhibitor concentration. This means that corrosion reaction will further be pushed to surface sites that are characterized by progressively higher values of E_{act} as the concentration of inhibitor becomes greater [37,221,227]. The values of activation energy were found larger than corresponding values of enthalpy of activation, indicate the involvement of a gaseous reaction, simply hydrogen evolution in corrosion process, associated with a decrease in total reaction volume [159].

ADSORPTION ISOTHERMS:

The nature of adsorption can be explained by understanding the process at metal/electrolyte interface. Further to understand the nature of adsorption, obtained surface coverage (θ) were fitted in different adsorption isotherms. The mathematical expressions for Langmuir adsorption isotherm can be expressed by the Eq.(8) [38,83,161,185,237]. Freundlich and Temkin adsorption isotherms were also drawn according to Eq.(10)[117] and Eq.(11)[152,172] and straight lines were obtained in Fig.28, Fig. 29 and Fig.30 respectively.

ADSORPTION PARAMETERS:

Gibbs Energy of Adsorption [ΔG_{ads}], Enthalpy of Adsorption [ΔH_{ads}] and Entropy of Adsorption [ΔS_{ads}]:

Values of K_{ads} were calculated by the intercept of Langmuir isotherm drawn according to the Eq.(8) between $\log(\theta/1-\theta)$ and $\log C_{inh}$ and by using this

Gibbs energy of adsorption was calculated by using Eq.(13)[115,159]. The values of ΔG_{ads} were tabulated in Table20. ΔG_{ads} values has been found negative at all studied temperatures indicating spontaneous adsorption process of inhibitor molecules on metal surface and strong interactions between inhibitor molecules and metal surface [1, 37, 49, 67, 213, 225, 226]. Generally values of ΔG_{ads} upto -20 kJ/mol are consistent with electrostatic interactions (physical adsorption) between charged molecules and charged metal surface and values upto -40kJ/mol or higher involve charge sharing or transfer from inhibitor molecules to metal surface to form coordinate type of bond (chemical adsorption) [37, 49, 90, 132, 163, 165, 233]. The values of ΔG_{ads} were found from -5.18kJ/mol to -11.60 kJ/mol. The obtained values of ΔG_{ads} were found less than -20kJ/mol indicated physical adsorption of inhibitor molecules. Obtained values of Gibbs energy were plotted against temperature in Fig.31 accordance with the following basic Eq.(14)[72,159]. Intercept of graph between ΔG_{ads} vs T gives value of ΔH_{ads} and by putting the value of intercept in Eq.(14) values of ΔS_{ads} were obtained. These obtained adsorption parameters Gibbs free energy of adsorption (ΔG_{ads}), enthalpy of adsorption (ΔH_{ads}) and entropy of adsorption (ΔS_{ads}) are listed in Table20. The calculated ΔH_{ads} values have been found positive indicating endothermic adsorption process [94, 237] at given temperature range. The endothermic process is attributed to chemisorption [65]. Positive values of ΔH_{ads} in Table20 indicate chemisorption. The obtained positive values of ΔS_{ads} are the algebraic sum of the entropies of adsorption of organic molecules and desorption of water molecules [78, 137]. Therefore the positive values of entropy of adsorption are the result of the substitution process, which can be attributed to the increase in the solvent entropy and more positive water desorption entropy [29, 151].

A more interesting behaviour is observed in Table 20 that positive ΔS_{ads} value is accompanied with positive ΔH_{ads} value. This further agrees that when the adsorption is an exothermic process, it must be accompanied by a decrease in the entropy change and vies versa [159, 228]. It has been observed that adsorption of negatively charged species is facilitated due to the positively charged metal. But positively charged species can also be adsorbed and

protect the positively charged metal surface acting with a negatively charged intermediate such as acid anions, adsorbed on metal surface [37, 181, 233].

CONCLUSIONS:

1. Result showed that AELCL is good corrosion inhibitor for mild steel in 1M H₂SO₄ solution.
2. Corrosion rates increase with increase in temperature and decrease with increase in inhibitor concentration.
3. Inhibition efficiency increases or decreases with increase in temperatures at given concentrations of inhibitor suggesting comprehensive adsorption process.
4. Apparent activation energy increases with increase in inhibitor concentrations also suggests physisorption.
5. Enthalpy of adsorption comes out to be negative and positive suggests exothermic and endothermic adsorption process which further suggests chemisorption.
6. The values of Gibbs free energies calculated were negative show spontaneity of corrosion inhibition process of mild steel in 1M H₂SO₄ in AELCL.

4.5 AQUEOUS EXTRACT OF NERIUM OLEANDER LEAVES IN 1M HCl

CORROSION RATES:

Corrosion rates were calculated by applying Eq.(1)[159]. Table 21 shows that corrosion rates of mild steel decrease with increase in concentration of AENOL as inhibitor at all studied temperatures. This could be subjected to the adsorption of the phyto-constituents inhibitor molecules with increase in concentration of inhibitor. The corrosion rate obeys Arrhenius type reaction, as it increases with rise in temperature [159].

INHIBITION EFFICIENCY:

From the obtained corrosion rates, inhibition efficiencies were calculated by using Eq.(2)[159,246]. Fig.32 represents the variation of IE% with different concentrations of AENOL at various studied temperatures. Data in Table 22 shows that IE% increase with increase in extract concentration, which is an indication of an increase in number of components of extract adsorbed on mild steel surface, which block the active sites of metal from acid attack and protect the metallic corrosion [162,168]. Further the decrease in IE% with rise in temperature suggests electrostatic interaction (physical adsorption) of the extract molecules on mild steel surface. This further indicates desorption of adsorbed inhibitor species at higher temperatures and metal dissolution takes place [83]. It can be observed that 83.76% inhibition efficiency is obtained at 30°C temperature at 10% (v/v) concentration of AENOL.

KINETIC PARAMETERS:

Corrosion rates of mild steel specimens were calculated by using the kinetic relationship as Eq.(3)[114,160]. Fig33 represents plot between $\log CR$ and $\log C_{inh}$ values at various studied temperatures. B and K were calculated by slope and intercept of straight lines of the graph. The obtained results in Table 23 can be discussed as follows [159].

- Negative values of B indicate that corrosion rate is inversely proportional to concentration of inhibitor. In other words the corrosion rates decrease with increase in concentration of inhibitor species.
- The high negative values of B reflect good inhibitive property of inhibitor. High negative value of B can be observed as steep slope in graph (Fig.33).
- Value of B is high at lower temperatures, indicates that inhibitive species is more effective at comparatively lower temperatures.
- The increase in K values with increase in temperature, indicating the increase in corrosion rates with temperatures.

THRMODYNAMIC AND ACTIVATION PARAMETERS:

The thermodynamic and activation parameters like apparent activation energy E_{act} , enthalpy of activation ΔH^* and entropy of activation ΔS^* were calculated for mild steel dissolution process. Activation energy E_{act} were calculated from the slopes of Arrhenius plots drawn between $\log CR$ and $1/T$ in Fig.34 in accordance with the by applying Arrhenius Eq.(4)[246,232]. Table 24 represents the calculated data of activation energies. The values of activation energies in presence of inhibitor were found higher than in uninhibited solution. This indicates the formation of higher energy barrier in corrosion reaction by inhibitor molecules. The increase in E_{act} for corrosion process further interpreted as physical adsorption of inhibitor species on mild steel surface [136,166,181]. Besides this According to Damaskin [58], the value of activation energy lesser than 80kJ/mol and even smaller than 5kJ/mol represents physical adsorption. This assertion supports the experimental results obtained in the present work. The values of enthalpy of activation ΔH^* and entropy of activation ΔS^* were calculated by using the transition state Eq.(5)[232,246]. A plot of $\log (CR/T)$ versus $1/T$ gave a straight line with slope of $(-\Delta H^*/2.303R)$ and intercept of $[(\log R/Nh) + (\Delta S^*/2.303 R)]$ from which the values of ΔH^* and ΔS^* were calculated (Fig.35). These values are tabulated in Table 24. Values of ΔH^* were found positive. Positive values indicate endothermic nature of steel dissolution process [37,153,246]. Endothermic process further indicates that mild steel dissolution reduces at

lower temperatures and increases with increase in temperatures. Negative values of ΔS^* are indicative of formation of activated complex in rate determining step, which represents association rather than dissociation step, meaning the decrease in disorder takes place on going from reactants to activated complex [37, 85, 223]. It is also observed from data in Table 24 that E_{act} and ΔH^* vary in the same manner. Values of both E_{act} and ΔH^* increase with increase in concentration of inhibitor, suggesting that energy barrier is increases with increase in inhibitor concentration. This means that corrosion reaction will further be pushed to surface sites that are characterized by progressively higher values of E_{act} as the concentration of inhibitor becomes greater [37,221,227]. The values of activation energy were found larger than corresponding values of enthalpy of activation, indicate the involvement of a gaseous reaction, simply hydrogen evolution in corrosion process, associated with a decrease in total reaction volume [159].

ADSORPTION ISOTHERMS:

The nature of adsorption can be explained by understanding the process at metal/electrolyte interface. Further to understand the nature of adsorption, obtained surface coverage (θ) were fitted in different adsorption isotherms. Langmuir adsorption isotherm was drawn by using the Eq.(8)[38,83,161,185,237]. Freundlich adsorption isotherm was also drawn according to Eq.(10)[117] and straight lines were obtained. These isotherms are shown in Fig.36 and Fig.37 respectively.

ADSORPTION PARAMETERS:

[Gibbs Energy of Adsorption][ΔG_{ads}], Enthalpy of Adsorption][ΔH_{ads}] and Entropy of Adsorption [ΔS_{ads}] :

Values of K_{ads} were calculated by the intercept of straight lines of Langmuir isotherm drawn according to the Eq.(8) between $\log (\theta /1- \theta)$ and $\log C_{inh}$ and by using this Gibbs energy of adsorption was calculated by using the Eq.(13) [115, 159]. The values of ΔG_{ads} are tabulated in Table25. ΔG_{ads} values has

been found negative at all studied temperatures indicating spontaneous adsorption process of inhibitor molecules on metal surface and strong interactions between inhibitor molecules and metal surface [1, 37, 49, 67, 213, 225, 226]. Generally values of ΔG_{ads} upto -20 kJ/mol are consistent with electrostatic interactions (physical adsorption) between charged molecules and charged metal surface and values upto -40 kJ/mol or higher involve charge sharing or transfer from inhibitor molecules to metal surface to form coordinate type of bond (chemical adsorption) [37, 49, 90, 132, 163, 165, 233]. The values of ΔG_{ads} were found from -13.91kJ/mol to -14.73 kJ/mol. The obtained values of ΔG_{ads} were less than -20 kJ/mol indicated physical adsorption of inhibitor molecules. It has been observed that adsorption of negatively charged species is facilitated due to the positively charged metal. But positively charged species can also be adsorbed and protect the positively charged metal surface acting with a negatively charged intermediate such as acid anions, adsorbed on metal surface [37, 181, 233]. Obtained values of Gibbs energy were plotted against temperature in Fig.38 in accordance with the Eq. (14) [72, 159]. Intercept of graph between ΔG_{ads} vs T give value of ΔH_{ads} and by putting the value of intercept in Eq.(14) values of ΔS_{ads} were obtained. These obtained adsorption parameters Gibbs free energy of adsorption (ΔG_{ads}), enthalpy of adsorption (ΔH_{ads}) and entropy of adsorption (ΔS_{ads}) are listed in Table25. A segmented line of two opposite slopes was obtained in Fig. 38 indicating two sets of adsorption sites having different ΔH_{ads} values. Similar type of segmented lined graph has been formed in previous study between ΔG_{ads} and T (K) by E.A. Noor [159]. Values of ΔH_{ads} has been found negative indicating the exothermic adsorption process [85, 134, 136, 162], which further indicates lower IE% at higher temperatures, due to desorption of inhibitor molecules. The exothermic process is attributed to either physical or chemical adsorption or mixture of both [42]. In exothermic process, values of ΔH_{ads} predict physisorption or chemisorption. For physisorption values of ΔH_{ads} is lower than 40kJ/mol while for chemisorption it approaches to 100kJ/mol [39,251]. Values of ΔH_{ads} in Table25 indicate physisorption. Negative values of ΔS_{ads} indicate decrease in entropy of

adsorption process. This behavior can be explained as follows: Before the adsorption of inhibitor molecules onto mild steel surface, inhibitor molecules might freely move in bulk solution (inhibitor molecules were chaotic). But with the process of adsorption, inhibitor molecules were orderly adsorbed onto the steel surface as a result decrease in entropy is observed [132, 133]. A more interesting behaviour is observed in Table 25 that negative ΔS_{ads} value is accompanied with negative ΔH_{ads} value. This further agrees that when the adsorption is an exothermic process, it must be accompanied by a decrease in the entropy change and vice versa [159, 228]. The obtained positive values of ΔS_{ads} are the algebraic sum of the adsorption of organic molecules and the desorption of water molecules [78, 137]. Therefore the positive values of entropy of adsorption is the result of the substitution process, which can be attributed to the increase in the solvent entropy and more positive water desorption entropy [29, 151].

CONCLUSIONS:

1. Result showed that AENOL is good corrosion inhibitor for mild steel in 1M HCl solution.
2. Corrosion rates increase with increase in temperature and decrease with increase in inhibitor concentration.
3. Inhibition efficiencies increases at lower temperature suggest the physisorption process of inhibitor on mild steel surface.
4. Apparent activation energy increases with increase in inhibitor concentrations also suggests physisorption.
5. Enthalpy of adsorption comes out to be negative and lower than 40 kJ/mol, which shows exothermic and physical adsorption process of inhibitor.
6. The values of Gibbs free energies calculated were negative shows spontaneity of corrosion inhibition process of mild steel in 1M HCl in AENOL.

4.6 AQUEOUS EXTRACT OF NERIUM OLEANDER LEAVES IN 1M

H₂SO₄

CORROSION RATES:

Corrosion rates were calculated by applying Eq.(1)[159]. Table 26 shows that corrosion rates of mild steel decrease with increase in concentration of AENOL as inhibitor at all studied temperatures. This could be subjected to the adsorption of the phyto-constituents of inhibitor molecules with increase in concentration of inhibitor. The corrosion rate obeys Arrhenius type reaction, as it increases with rise in temperature [159].

INHIBITION EFFICIENCY:

From the obtained corrosion rates, inhibition efficiencies were calculated by using Eq.(2)[159,246]. Fig.39 represents the variation of IE% with different concentrations of AENOL at various studied temperatures. Data in Table27 show that IE% increase with increase in extract concentration, which is an indication of an increase in number of components of extract adsorbed on mild steel surface, which block the active sites of metal from acid attack and protect the metallic corrosion [162, 168]. Further the decrease in IE% with rise in temperature suggests electrostatic interaction (physical adsorption) of the extract molecules on mild steel surface. This further indicates desorption of adsorbed inhibitor species at higher temperatures and metal dissolution takes place [83]. It can be observed that 72% inhibition efficiency is obtained at 30°C temperature at 10% (v/v) concentration of AENOL.

KINETIC PARAMETERS:

Corrosion rates of mild steel specimens were calculated by using the kinetic relationship as Eq.(3)[114,160]. Fig.40 represents plot between logCR and logC_{inh} values at various studied temperatures. B and K were calculated by slope and intercept of straight lines of the graph. The obtained results in Table28 can be discussed as follows [159].

- Negative values of B indicate that corrosion rate is inversely proportional to concentration of inhibitor. In other words the corrosion rates decrease with increase in concentration of inhibitor species.
- The high negative values of B reflect good inhibitive property of inhibitor. High negative value of B can be observed as steep slope in graph (Fig.40).
- Value of B is high at lower temperatures, indicates that inhibitive species is more effective at comparatively lower temperatures.
- The increase in K values with increase in temperature, indicating the increase in corrosion rates with temperatures.

THRMODYNAMIC AND ACTIVATION PARAMETERS:

The thermodynamic and activation parameters like apparent activation energy E_{act} , enthalpy of activation ΔH^* entropy of activation ΔS^* were calculated for mild steel dissolution process. Activation energies E_{act} were calculated from the slopes of Arrhenius plots drawn between $\log CR$ and $1/T$ in Fig.41 in accordance with the Arrhenius Eq.(4) [232,246] . The slope of $\log CR$ versus $1/T$ gives the values of activation energies at studied concentrations. Table29 represents the calculated data of activation energies. The values of activation energies in presence of inhibitor were found higher than in uninhibited solution. This indicates the formation of higher energy barrier in corrosion reaction by inhibitor molecules. The increase in E_{act} for corrosion process further interpreted as physical adsorption of inhibitor species on mild steel surface [136, 166, 181]. Besides this according to Damaskin [58], the value of activation energy lesser than 80kJ/mol and even smaller than 5kJ/mol represents physical adsorption. This assertion supports the experimental results obtained in the present work. The values of enthalpy of activation ΔH^* and entropy of activation ΔS^* were calculated by using the transition state Eq.(5) [232, 246]. A plot of $\log (CR/T)$ vs $1/T$ gave a straight line in Fig.42 with slope of $(-\Delta H^*/2.303R)$ and intercept of $[(\log R/Nh) + (\Delta S^*/2.303 R)]$ from which the values of ΔH^* and ΔS^* were calculated. These values are tabulated in Table 29. Values of ΔH^* were found positive. Positive values indicate endothermic nature of steel dissolution process [37, 153, 246].

Endothermic process further indicates that mild steel dissolution reduces at lower temperatures and increases with increase in temperatures. Negative values of ΔS^* are indicative of formation of activated complex in rate determining step, which represents association rather than dissociation step, meaning that the decrease in disorder takes place on going from reactants to activated complex [37, 85, 223].

It is also observed from data in Table 29 that E_{act} and ΔH^* vary in the same manner. Values of both E_{act} and ΔH^* increase with increase in concentration of inhibitor, suggesting that energy barrier increases with increase in inhibitor concentration. This means that corrosion reaction will further be pushed to surface sites that are characterized by progressively higher values of E_{act} as the concentration of inhibitor becomes greater [37,221,227]. The values of activation energy were found larger than corresponding values of enthalpy of activation, indicate the involvement of a gaseous reaction, simply hydrogen evolution in corrosion process, associated with a decrease in total reaction volume [159].

ADSORPTION ISOTHERMS:

The nature of adsorption can be explained by understanding the process at metal/electrolyte interface. Further to understand the nature of adsorption, obtained surface coverage (θ) were fitted in different adsorption isotherms. **Langmuir isotherm** was best fit and drawn by using the Eq.(8) [38,83,161,185,237]. Freundlich and Temkin adsorption isotherms were also drawn according to Eq.(10) [117] & Eq.(11) [152,172] and straight lines were obtained. These isotherms are shown in Fig.43, Fig.44 and Fig.45 respectively.

ADSORPTION PARAMETERS:

[Gibbs Energy of Adsorption][ΔG_{ads}], Enthalpy of Adsorption][ΔH_{ads}] and Entropy of Adsorption [\Delta S_{ads}] :

Values of K_{ads} were calculated by the intercept of straight lines of Langmuir isotherm drawn according to the Eq.(8) between $\log(\theta/1-\theta)$ and $\log C_{inh}$ and

by using this Gibbs energy of adsorption was calculated by using the Eq. (13) [115, 159]. The values of ΔG_{ads} are tabulated in Table30. ΔG_{ads} values has been found negative at all studied temperatures indicating spontaneous adsorption process of inhibitor molecules on metal surface and strong interactions between inhibitor molecules and metal surface [37, 49, 67, 213, 225, 226]. Generally values of ΔG_{ads} upto -20kJ/mol are consistent with electrostatic interactions (physical adsorption) between charged molecules and charged metal surface and values upto -40kJ/mol or higher involve charge sharing or transfer from inhibitor molecules to metal surface to form coordinate type of bond (chemical adsorption) [37, 49, 90, 132, 163, 165]. The values of ΔG_{ads} were found from -13.99kJ/mol to -9.20kJ/mol. The obtained values of ΔG_{ads} were less than -20kJ/mol indicated physical adsorption of inhibitor molecules. It has been observed that adsorption of negatively charged species is facilitated due to the positively charged metal. But positively charged species can also be adsorbed and protect the positively charged metal surface acting with a negatively charged intermediate such as acid anions, adsorbed on metal surface [37, 181, 233]. Obtained values of Gibbs energy were plotted against temperature in Fig.46 according to the Eq.(14) [72,159]. Intercept of graph between ΔG_{ads} versus T give value of ΔH_{ads} and by putting the value of intercept in Eq.(14) values of ΔS_{ads} were obtained. These obtained adsorption parameters Gibbs free energy of adsorption (ΔG_{ads}), enthalpy of adsorption (ΔH_{ads}), entropy of adsorption (ΔS_{ads}), are listed in Table30. Values of ΔH_{ads} has been found negative indicating the exothermic adsorption process [85, 134, 136, 162], which further indicates lower IE% at higher temperatures, due to desorption of inhibitor molecules. The exothermic process is attributed to either physical or chemical adsorption or mixture of both [42]. In exothermic process, values of ΔH_{ads} predict physisorption or chemisorption. For physisorption values of ΔH_{ads} is lower than 40kJ/mol while for chemisorption it approaches to 100kJ/mol [39,251]. Values of ΔH_{ads} in Table30 indicate chemisorptions as it is larger than 40 kJ/mol. Negative values of ΔS_{ads} indicate decrease in entropy of adsorption process. This behavior can be explained as follows: Before the

adsorption of inhibitor molecules onto mild steel surface, inhibitor molecules might freely move in bulk solution (inhibitor molecules were chaotic). But with the process of adsorption, inhibitor molecules were orderly adsorbed onto the steel surface as a result decrease in entropy is observed [132, 133]. A more interesting behaviour is observed in Table 30 that negative ΔS_{ads} value is accompanied with negative ΔH_{ads} value. This further agrees that when the adsorption is an exothermic process, it must be accompanied by a decrease in the entropy change and vice versa [159, 228].

CONCLUSIONS:

1. Result showed that AENOL is good corrosion inhibitor for mild steel in 1M H₂SO₄ solution.
2. Corrosion rates increase with increase in temperature and decrease with increase in inhibitor concentration.
3. Inhibition efficiencies increases at lower temperature suggest the physisorption process of inhibitor on mild steel surface.
4. Apparent activation energy increases with increase in inhibitor concentrations also suggests physisorption.
5. Enthalpy of adsorption comes out to be negative and higher than 40 kJ/mol, which shows exothermic and chemical adsorption process of inhibitor.
6. The values of Gibbs free energies calculated were negative shows spontaneity of corrosion inhibition process of mild steel in 1M H₂SO₄ in AENOL.

4.7 AQUEOUS EXTRACT OF WATER HYACINTH LEAVES IN 1M HCl

CORROSION RATES:

Corrosion rates were calculated by using Eq.(1) [159]. Table31 shows that corrosion rates of mild steel decrease with increase in concentration of AEWHL as inhibitor at all studied temperatures. This could be subjected to the adsorption of the phyto-constituents of inhibitor molecules with increase in concentration of inhibitor. The corrosion rate obeys Arrhenius type reaction, as it increases with rise in temperature [159].

INHIBITION EFFICIENCY:

From the obtained corrosion rates, inhibition efficiencies were calculated using Eq.(2) [159,246]. Fig.47 represents the variation of IE% with different concentrations of AEWHL at various studied temperatures. Data in Table 32 show that IE% increase with increase in extract concentration, which is an indication of an increase in number of components of extract adsorbed on mild steel surface, which block the active sites of metal from acid attack and protect the metallic corrosion [162,168]. Further the decrease in IE% with rise in temperature suggests electrostatic interaction (physical adsorption) of the extract molecules on mild steel surface [168]. This further indicates desorption of adsorbed inhibitor species at higher temperatures and metal dissolution takes place [83]. 68.18% inhibition efficiency is observed at 5% (v/v) concentration of inhibitor at 30°C.

KINETIC PARAMETERS:

Assuming that corrosion rates of steel specimens against concentration were calculated by kinetic relationship as Eq.(3) [114,160]. Fig 48 represents plot between $\log CR$ and $\log C_{inh}$ values at various studied temperatures. B and K were calculated by slope and intercept of straight lines of the graph.

The obtained results in Table33 can be discussed as follows [159]:

- Negative values of B indicate that corrosion rate is inversely proportional to concentration of inhibitor. In other words the corrosion rates decrease with increase in concentration of inhibitor species.
- The high negative values of B reflect good inhibitive property of inhibitor. High negative value of B can be observed as steep slope in graph (Fig.48).
- Value of B is high at lower temperatures, indicates that inhibitive species is more effective at comparatively lower temperatures.
- The increase in K values with increase in temperature, indicating the increase in corrosion rates with temperatures.

THERMODYNAMIC AND ACTIVATION PARAMETERS:

Thermodynamic and activation parameters like apparent activation energy E_{act} , enthalpy of activation ΔH^* and entropy of activation ΔS^* were calculated for steel dissolution process. Activation energies E_{act} were calculated from the slopes of Arrhenius plots drawn between $\log CR$ and $1/T$ in Fig.49 in accordance with the Arrhenius Eq.(4) [232,246]. Table34 represents the calculated data of activation energies. The values of activation energies in presence of inhibitor were found higher than in uninhibited solution. This indicates the formation of higher energy barrier in corrosion reaction by inhibitor molecules. The increase in E_{act} for corrosion process further interpreted as physical adsorption of inhibitor species on mild steel surface [136, 166, 181]. Besides this according to Damaskin [58], the value of activation energy lesser than 80kJ/mol and even smaller than 5kJ/mol represents physical adsorption. This assertion supports the experimental results obtained in the present work.

The values of enthalpy of activation ΔH^* and entropy of activation ΔS^* were calculated by transition state Eq.(5) [232,246]. A plot of $\log(CR/T)$ versus $1/T$ in Fig.50 gave a straight line with slope of $(-\Delta H^*/2.303R)$ and intercept of $[(\log R/Nh) + (\Delta S^*/2.303 R)]$ from which the values of ΔH^* and ΔS^* were calculated. These values are tabulated in Table34. Values of ΔH^* were found positive. Positive values indicate endothermic nature of steel dissolution process [37,153,246]. Endothermic process further indicates that mild steel dissolution

reduces at lower temperatures and increases with increase in temperatures. Negative values of ΔS^* are indicative of formation of activated complex in rate determining step, which represents association rather than dissociation step, meaning that the decrease in disorder takes place on going from reactants to activated complex [37, 85, 223].

It is also observed from data in Table34 that E_{act} and ΔH^* vary in the same manner. Values of both E_{act} and ΔH^* increase with increase in concentration of inhibitor, suggesting that energy barrier is increases with increase in inhibitor concentration. This means that corrosion reaction will further be pushed to surface sites that are characterized by progressively higher values of E_{act} as the concentration of inhibitor becomes greater [37, 221, 227]. The values of activation energy were found larger than corresponding values of enthalpy of activation, indicate the involvement of a gaseous reaction, simply hydrogen evolution in corrosion process, associated with a decrease in total reaction volume [159].

ADSORPTION ISOTHERMS:

The nature of adsorption can be explained by understanding the process at metal/electrolyte interface. Further to understand the nature of adsorption, obtained surface coverage (θ) were fitted in different adsorption isotherms. Langmuir adsorption isotherm was found best fit and plotted according to the Eq.(8) [38,83,161,185,237]. Freundlich and Temkin adsorption isotherms were also drawn according to Eq.(10) [117] and Eq.(11) [152,172] and straight lines were obtained. These isotherms are shown in Fig.51, Fig.52 and Fig.53 respectively.

ADSORPTION PARAMETERS:

[Gibbs Energy of Adsorption][ΔG_{ads}], Enthalpy of Adsorption][ΔH_{ads}] and Entropy of Adsorption [\Delta S_{ads}] :

Values of K_{ads} were calculated by the intercept of Langmuir isotherm drawn according to the Eq.(8) between $\log(\theta/1-\theta)$ and $\log C_{inh}$ and by using this Gibbs energy was calculated by the Eq.(13) [115,159]. The values of ΔG_{ads} were

tabulated in Table35. ΔG_{ads} values has been found negative at all studied temperatures indicating spontaneous adsorption process of inhibitor molecules on metal surface and strong interactions between inhibitor molecules and metal surface [1, 37, 49, 67, 213, 225, 226]. Generally values of ΔG_{ads} upto -20 kJ/mol are consistent with electrostatic interactions [physical adsorption] between charged molecules and charged metal surface and values upto -40 kJ/mol or higher involve charge sharing or transfer from inhibitor molecules to metal surface to form coordinate type of bond (chemical adsorption) [37, 49, 90, 132, 163, 165, 233]. The values of ΔG_{ads} were found from -13.91kJ/mol to -9.58kJ/mol. The obtained values of ΔG_{ads} were found less than -20kJ/mol indicated physical adsorption of inhibitor molecules. It has been observed that adsorption of negatively charged species is facilitated due to the positively charged metal. But positively charged species can also be adsorbed and protect the positively charged metal surface acting with a negatively charged intermediate such as acid anions, adsorbed on metal surface [37, 181, 233]. Obtained values of Gibbs energy were plotted against temperature in Fig.54 in accordance with the following basic Eq.(14) [72,159]. Intercept of graph between ΔG_{ads} versus T in Fig.54 gives value of ΔH_{ads} and by putting the value of intercept in Eq.(14) values of ΔS_{ads} were obtained. These obtained adsorption parameters Gibbs free energy of adsorption (ΔG_{ads}), enthalpy of adsorption (ΔH_{ads}) and entropy of adsorption (ΔS_{ads}), are listed in Table35. A segmented line of two opposite slopes was obtained in Fig.54 indicating two sets of adsorption sites having different ΔH_{ads} values. Similar type of results have been found in previous study between ΔG_{ads} and T(K) by E.A. Noor [159]. The calculated ΔH_{ads} values have been found negative and positive indicating both exothermic adsorption process [85,134,136,162] and endothermic adsorption process [94,237] respectively, depend upon the specific temperature range. Similar type of comprehensive adsorption processes were obtained in previous study [159]. Exothermic process is attributed to either physical or chemical adsorption or mixture of both [42], while the endothermic process is attributed to chemisorption [65]. In exothermic process, values of ΔH_{ads} predict physisorption or chemisorption. For physisorption values of ΔH_{ads} is lower than

40kJ/mol while for chemisorption it approaches to 100kJ/mol [39,251]. Values of ΔH_{ads} in Table 35 indicate both physisorption and chemisorption.

Negative values of ΔS_{ads} indicate decrease in entropy of adsorption process. This behaviour can be explained as follows: Before the adsorption of inhibitor molecules onto mild steel surface, inhibitor molecules might freely move in bulk solution (inhibitor molecules were chaotic). But with the process of adsorption, inhibitor molecules were orderly adsorbed onto the steel surface as a result decrease in entropy is observed [132, 133]. The obtained positive values of ΔS_{ads} are the algebraic sum of the adsorption of organic molecules and the desorption of water molecules [78,137]. Therefore the positive values of entropy of adsorption is the result of the substitution process, which can be attributed to the increase in the solvent entropy and more positive water desorption entropy [29, 151]. A more interesting behaviour is observed in Table 35 that negative ΔS_{ads} value is accompanied with negative ΔH_{ads} value. This further agrees that when the adsorption is an exothermic process, it must be accompanied by a decrease in the entropy change and vice versa [159, 228].

CONCLUSIONS:

1. Result showed that AEWHL is good corrosion inhibitor for mild steel in 1M HCl solution.
2. Corrosion rates increase with increase in temperature and decrease with increase in inhibitor concentration.
3. Inhibition efficiencies increases at lower temperature suggest the physisorption process of inhibitor on mild steel surface.
4. Apparent activation energy increases with increase in inhibitor concentrations also suggests physisorption.
5. Enthalpy of adsorption comes out to be negative and positive showing comprehensive (physical and chemical) adsorption of inhibitor molecules on mild steel surface.
6. The values of Gibbs free energies calculated were negative shows spontaneity of corrosion inhibition process of mild steel in 1M HCl in AEWHL.

4.8 AQUEOUS EXTRACT OF WATER HYACINTH LEAVES IN 1M

H₂SO₄

CORROSION RATES:

Corrosion rates were calculated by using Eq.(1)[159]. Table36 shows that corrosion rates of mild steel decrease with increase in concentration of AEWHL as inhibitor at all studied temperatures. This could be subjected to the adsorption of the phyto-constituents of inhibitor molecules with increase in concentration of inhibitor. The corrosion rate obeys Arrhenius type reaction, as it increases with rise in temperature [159].

INHIBITION EFFICIENCY:

From the obtained corrosion rates, inhibition efficiencies were calculated by using Eq.(2) [159,246]. Fig.55 represents the variation of IE% with different concentrations of AEWHL at various studied temperatures. Data in Table37 show that IE% increases or decreases with increasing temperatures at different studied extract concentrations of AEWHL. This indicates the comprehensive adsorption (physical and chemical adsorption) of inhibitor species on mild steel surface [159]. Such type of observation was found in previous study by Noor [159]. Further it has been observed that IE% were increase with increase in inhibitor concentration 64.78% inhibition efficiency is observed at 5% (v/v) concentration of inhibitor at 30°C.

KINETIC PARAMETERS:

Corrosion rates of mild steel specimens were calculated using the kinetic relationship according to Eq.(3) [114,160]. Fig 56 represents plot between logCR and logC_{inh} values at various studied temperatures. B and K were calculated by slope and intercept of straight lines of the graph.

The obtained results in Table 38 can be discussed as follows [159].

- Negative values of B indicate that corrosion rate is inversely proportional to concentration of inhibitor. In other words the corrosion rates decrease with increase in concentration of inhibitor species.
- The high negative values of B reflect good inhibitive property of inhibitor. High negative value of B can be observed as steep slope in graph [Fig.56].
- Value of B is high at lower temperatures, indicates that inhibitive species is more effective at comparatively lower temperatures.
- The increase in K values with increase in temperature, indicating the increase in corrosion rates with temperatures.

THERMODYNAMIC AND ACTIVATION PARAMETERS:

Thermodynamic and activation parameters like apparent activation energy E_{act} , enthalpy of activation ΔH^* entropy of activation ΔS^* were calculated for steel dissolution process. Activation energies E_{act} were calculated from the slopes of Arrhenius plots drawn between $\log CR$ and $1/T$ in Fig.57 according to the Arrhenius Eq.(4) [232,246]. Table39 represents the calculated data of activation energies. The values of activation energies in presence of inhibitor were found higher than in uninhibited solution. This indicates the formation of higher energy barrier in corrosion reaction by inhibitor molecules. The increase in E_{act} for corrosion process further interpreted as physical adsorption of inhibitor species on mild steel surface [136, 166, 181]. Besides this according to Damaskin [58], the value of activation energy lesser than 80kJ/mol and even smaller than 5kJ/mol represents physical adsorption. This assertion supports the experimental results obtained in the present work. The values of enthalpy of activation ΔH^* and entropy of activation ΔS^* were calculated by using transition state Eq.(5) [232, 246]. A plot of $\log (CR/T)$ versus $1/T$ in Fig.58 gave a straight line with a slope of $(-\Delta H^*/2.303R)$ and intercept of $[(\log R/Nh) + (\Delta S^*/2.303R)]$ from which the values of ΔH^* and ΔS^* were calculated (Fig.58). These values are tabulated in Table 39. Values of ΔH^* were found positive. Positive values indicate endothermic nature of steel dissolution process [37, 153, 246]. Endothermic process further indicates that mild steel dissolution reduces at lower temperatures and increases with increase in temperatures. Negative values of ΔS^* are indicative of formation

of activated complex in rate determining step, which represents association rather than dissociation step, meaning that the decrease in disorder takes place on going from reactants to activated complex [37, 85, 223].

It is also observed from data in Table 39 that E_{act} and ΔH^* vary in the same manner. Values of both E_{act} and ΔH^* increase with increase in concentration of inhibitor, suggesting that energy barrier is increases with increase in inhibitor concentration. This means that corrosion reaction will further be pushed to surface sites that are characterized by progressively higher values of E_{act} as the concentration of inhibitor becomes greater [37, 221, 227]. The values of activation energy were found larger than corresponding values of enthalpy of activation, indicate the involvement of a gaseous reaction, simply hydrogen evolution in corrosion process, associated with a decrease in total reaction volume [159].

ADSORPTION ISOTHERMS:

The nature of adsorption can be explained by understanding the process at metal/electrolyte interface. Further to understand the nature of adsorption, obtained surface coverage (θ) were fitted in different adsorption isotherms. The mathematical expressions for Langmuir adsorption isotherm can be expressed by the Eq.(8) [38,83,161,185,237]. Freundlich and Temkin adsorption isotherms were also drawn according to Eq.(10) [117] and Eq.(11) [152, 172] and straight lines were obtained in Fig.59, Fig.60 and Fig.61 respectively.

ADSORPTION PARAMETERS:

[Gibbs Energy of Adsorption][ΔG_{ads}], Enthalpy of Adsorption][ΔH_{ads}] ,Entropy of Adsorption [ΔS_{ads}] :

Values of K_{ads} were calculated by the intercept of Langmuir isotherm drawn according to the Eq.(8) between $\log(\theta/1-\theta)$ and $\log C_{inh}$ and by using this Gibbs energy of adsorption was calculated by using Eq.(13) [115,159]. The values of ΔG_{ads} were tabulated in Table40. ΔG_{ads} values has been found negative at all studied temperatures indicating spontaneous adsorption process of inhibitor molecules on metal surface and strong interactions between inhibitor molecules

and metal surface [1, 37, 49, 67, 225, 226]. Generally values of ΔG_{ads} upto -20kJ/mol are consistent with electrostatic interactions (physical adsorption) between charged molecules and charged metal surface and values upto -40kJ/mol or higher involve charge sharing or transfer from inhibitor molecules to metal surface to form coordinate type of bond (chemical adsorption) [37,49,90,132, 163,165,233]. The values of ΔG_{ads} were found from -11.95kJ/mol to-14.72kJ/mol. The obtained values of ΔG_{ads} were found less than -20kJ/mol indicated physical adsorption of inhibitor molecules. It has been observed that adsorption of negatively charged species is facilitated due to the positively charged metal. But positively charged species can also be adsorbed and protect the positively charged metal surface acting with a negatively charged intermediate such as acid anions, adsorbed on metal surface [37,181,233]. Obtained values of Gibbs energy were plotted against temperature in Fig.62 in accordance with the basic Eq.(14) [72,159]. Intercept of graph between ΔG_{ads} versus T gives value of ΔH_{ads} and by putting the value of intercept in Eq.(14) values of ΔS_{ads} were obtained. These obtained adsorption parameters Gibbs free energy of adsorption (ΔG_{ads}), enthalpy of adsorption (ΔH_{ads}) and entropy of adsorption (ΔS_{ads}) are listed in Table40. A segmented line of two opposite slopes was obtained in Fig.62 indicating two sets of adsorption sites having different ΔH_{ads} values. Similar type of results have been found in previous study between ΔG_{ads} and T(K) by E.A. Noor [159]. The calculated ΔH_{ads} values have been found negative and positive indicating both exothermic adsorption process [85, 134, 136, 162] and endothermic adsorption process [94, 237] respectively, depending upon the specific temperature range. Similar type of comprehensive adsorption processes were obtained in previous study [159]. The exothermic process is attributed to either physical or chemical adsorption or mixture of both [42], while the endothermic process is attributed to chemisorption [65]. In exothermic process, values of ΔH_{ads} predict physisorption or chemisorption. For physisorption values of ΔH_{ads} is lower than 40kJ/mol while for chemisorption it approaches to 100 kJ/mol [39, 251]. Values of ΔH_{ads} in Table 40 indicate physisorption. Negative values of ΔS_{ads} indicate decrease in entropy of adsorption process. This behaviour can be explained as follows: Before the adsorption of inhibitor molecules onto mild steel surface, inhibitor molecules

might freely move in bulk solution (inhibitor molecules were chaotic). But with the process of adsorption, inhibitor molecules were orderly adsorbed onto the steel surface as a result decrease in entropy is observed [132, 133]. The obtained positive values of ΔS_{ads} are the algebraic sum of the adsorption of organic molecules and the desorption of water molecules [78,137]. Therefore the positive values of entropy of adsorption is the result of the substitution process, which can be attributed to the increase in the solvent entropy and more positive water desorption entropy [29, 151]. A more interesting behaviour is observed in Table 40 that negative ΔH_{ads} value is accompanied with negative ΔS_{ads} value. This further agrees that when the adsorption is an exothermic process, it must be accompanied by a decrease in the entropy change and vice versa [159, 228].

CONCLUSIONS:

1. Result showed that AEWHL is good corrosion inhibitor for mild steel in 1M H_2SO_4 solution.
2. Corrosion rates increase with increase in temperature and decrease with increase in inhibitor concentration.
3. Inhibition efficiency increases or decreases with increase in temperatures at given concentrations of inhibitor suggesting comprehensive adsorption process.
4. Apparent activation energy increases with increase in inhibitor concentrations also suggests physisorption.
5. Enthalpy of adsorption comes out to be negative and positive suggests exothermic and endothermic adsorption process.
6. The values of Gibbs free energies calculated were negative show spontaneity of corrosion inhibition process of mild steel in 1 M H_2SO_4 in AEWHL.

BIBLIOGRAPHY

1. Abd El-Rehim S.S, Hassan H.H and Amin M.A., “Corrosion inhibition of aluminium by 1,1 (lauryl amido) propyl ammonium chloride in HCl solution”, *Materials Chemistry and Physics*, 70 (1) (2001), 64-72.
2. Abdel-Fatah H.T.M., Hassan A.A.M., Z.A., Saadi Z.A., Shetify M.M. and El-Sehiety H.E.E., “Corrosion inhibition of mild steel in acidic medium by *Salvadora persica* (Miswak) – Part 1: in sulfamic acid ”, *Chemical Science Transactions* , 3(1) (2014), 221-231.
3. Abdel-Gaber A.M., Abd-El-Nabey B.A., Sidahamed I.M., Ei-Zayady A.M. and Saadawy M., “ Inhibitive action of some plant extracts on the corrosion of steel in acidic media”, *Corrosion science* , 48 (2006), 2765-2779.
4. Abdulrahman A.S., Ganiyu K.A., Ibrahim H.K. and Caroline A.I., “The corrosion inhibition of mild steel in sulphuric acid solution by adsorption of *African perquetina* leaves extract”, *International Journal of Innovative Research in Science, Engineering and Technology*, 4(4) (2015), 1809-1821.
5. Abe F. and Yamauchi T., “Cardenolide triosides of *oleander* leaves”, *Phytochemistry*, 31 (7) (1992), 2459-2463.
6. Abiola O.K. and James A.O., “The effects of *Aloe vera* extract on corrosion and kinetics of corrosion process of zinc in HCl solution”, *Corrosion Science*, 52 (2010), 661–664.
7. Abiola O.K., John M.O., Asekunowo P.O., Okafor P.C. and James O.O., “3[(4-amino-2-methyl-5-pyrimidinyl)]-5-(2-hydroxyethyl)-4-methyl thiazolium chloride hydrochloride as green corrosion inhibitor of copper in HNO₃ solution and its adsorption characteristics”, *Green Chemistry Letters and Reviews*, 3(2011), 273-279.
8. Abiola O.K., Odin E.M., Olowoyo D.N. and Adeloje T.A., “ *Gossipium hirsutum L.* extract as green corrosion inhibitor for aluminum in HCl solution”, *Bulletin of Chemical Society of Ethiopia*, 25(3) (2011), 475-480.
9. Abou-Shanab R. A. I., Angle J.S., and Van Berkum P., “Chromate-tolerant bacteria for enhanced metal uptake by *Eichhornia crassipes*

- (MART.)”, *International Journal of Phytoremediation*, 9 (2) (2007), 91–105.
10. Abubakar G., Ibrahim H., Apugo-Nwosu T. U., Mustafa M., Akuso S. A., Agboun D.T., Nwobi B.E. and Ayilara S. I., “Corrosion inhibition studies of *Ficus abutilifolia* on N-80 oil well tubular steel in 15% hydrochloric acid solution”, *International Journal of Engineering and Computer Science*, 2 (8) (2013), 2364-2370.
 11. Aejiatha S., Kasthuri P.K. and Geethamani P., “Comparison of the corrosion inhibition efficiencies of mild steel in different acidic mediums using *Commiphora caudata* plant extract”, *International Journal of Advanced Technology in Engineering and Science*, 3(5) (2015), 75-85.
 12. Afia L., Salghi R., Bammou L., Bazzi El., Hammouti B., Bazzi L. and Bouyanzer A., “Anti-corrosive properties of Argan oil on C38 steel in molar HCl solution”, *Journal of Saudi Chemical Society*, 18 (2014), 19–25.
 13. Agarwal K., “*Fenugreek* leaves and lemon peel as green corrosion inhibitor for mild steel in 1M HCl Medium”, *Journal of Materials Science & Surface Engineering*, 1 (2) (2014), 44-48.
 14. Ahmed K.K.M., Rana A.C. and Dixit V.K., “*Calotropis* species (Asclepiaceae): A comprehensive review”, *Pharmacognosy Magazine*, 1(2) (2005), 48-52.
 15. Ahmed R., “Allelopathic effects of *Lantana camara* on germination and growth behavior of some agricultural crops in Bangladesh”, *Journal of Forestry Research*, 18(2007), 301-304.
 16. Ahmed U.A.M., Zuhua S., Bashier N.H.H., Muafi K., Zhongping H. and Yuling G., “Evaluation of insecticidal potentialities of aqueous extracts from *Calotropis procera* ait. against *henosepilachna elaterii rossi*”, *Journal of Applied Sciences*, 6(1) (2006), 2466-2470.
 17. Akalezi C.O., Enenebaku C. K. and Oguzie E. E.’ “Inhibition of acid corrosion of mild steel by biomass extract from the *Petersianthus macrocarpus* plant”, *Journal of Materials and Environmental Science*, 4 (2) (2013), 217-226.

18. Alaneme K.K, Daramola Y.S., Olusegun S.J. and Afolabi A.S., “Corrosion inhibition and adsorption characteristics of rice husk extracts on mild steel immersed in 1M H₂SO₄ and HCl solutions”, *International Journal of Electrochemical Science*, 10 (2015), 3553 – 3567.
19. Al-Fakih A.M., Aziz M. and Sirat H.M., “Turmeric and ginger as green inhibitors of mild steel corrosion in acidic medium”, *Journal of Material and Environmental Science*, 6 (5) (2015), 1480-1487.
20. Alinnor I. J. and Ejikeme P. M., “Corrosion inhibition of aluminium in acidic medium by different extracts of *Ocimum gratissimum*”, *American Chemical Science Journal*, 2(4) (2012), 122-135.
21. Al-Mhyawi S.R., “Inhibition of mild steel corrosion using *Juniperus* plants as green inhibitor”, *African Journal of Pure and Applied Chemistry*, 8(1) (2014), 9-22.
22. Al-Sahlane H.H. and Abdul-Wahab A. Sultan and Al-Faize M.M., “Corrosion inhibition of carbon steel in 1M HCl solution using *Sesbania sesban* extract”, *Aquatic Science and Technology*, 1(2) (2013), 135-151.
23. Ambrish S., Yuanhua L., Ebenso. E.E, Liu W. and Huang B., “Determination of corrosion inhibition efficiency using HPHT autoclave by *Gingko biloba* on carbon steels in 3.5% NaCl solution Saturated with CO₂”, *International journal of Electrochemical Science*, 9 (2014), 5993 – 6005.
24. Ambrish S., Yuanhua Li., Eno E.E., Kunhai D., Pan J. and Huang B., “Relevance of electrochemical and surface studies to probe *Zanthoxylum schinifolium* (sichuan pepper) as an effective corrosion inhibitor for N80 steel in CO₂ saturated 3.5% NaCl solution”, *International journal of Electrochemical Science*, 9 (2014), 5585 – 5595.
25. Ambrish Singh A., Singh V. K. and Quraishi M. A., “Inhibition effect of environmentally benign Kuchla (*Strychnos nuxvomica*) seed extract on corrosion of mild steel in hydrochloric acid solution”, *Rasayan Journal of Chemistry* , 3(4) (2010), 811-824.
26. Amin M.A., Abd El-Rehim S.S., El-Sherbini E.E.F. and Bayoumi R.S., “The inhibition of low carbon steel corrosion in hydrochloric acid solution

- by succinic acid : Part1 weight loss, polarization, EIS,PZC,EDX and SEM studies”, *Electrochimica Acta*, 52 (2007), 3588- 3600.
27. Ananth Kumar S., Sankar A. and Ramesh Kumar S., “Vitamin B-12 solution as corrosion inhibitor for mild steel in acid medium”, *International Journal of Computer Engineering & Science*, 3(1) (2013), 57-61.
 28. Ating E.I., Umoren S.A., Udousoro I.I., Ebenso E.E. and Udoh A.P., “Leaves extract of *Ananas sativum* as green corrosion inhibitor for aluminum in hydrochloric acid solutions”, *Green Chemistry Letters and Reviews*, 3(2) (2010), 61-68.
 29. Badiea A.M. and Mohana K.N., “Effect of temperature and fluid velocity on corrosion mechanism of low carbon steel in presence of 2-hydrazino-4,7- dimethylbenzothiazole in industrial water medium,” *Corrosion. Science*, 51 (2009), 2231–2241.
 30. Bai L., Wang L., Zhao M., Toki A., Hasegawa T., Ogura H., Kataoka T., Hirose K., Sakai J., Bai J., and Ando M., “Bioactive pregnanes from *Nerium oleander*”, *Journal of Natural Products*, 70(1) (2007), 14-18.
 31. Bammou L., Chebli B., Salghi R., Bazzi L., Hammouti B., Mihit M. and Idrissi H., “Thermodynamic properties of *Thymus satureioides* essential oils as corrosion inhibitor of tinplate in 0.5M HCl: chemical characterization and electrochemical study”, *Green Chemistry Letters and Reviews*, 3 (3) (2010), 173-178.
 32. Bammou L., Belkhaouda M., Salghi R., Benali O., Zarrouk A., Al-Deyab S. S., Warad I., Zarrok H. and Hammouti B., “Effect of *Harmal* extract on the corrosion of C-steel in hydrochloric solution”, *International journal of Electrochemical Science* , 9 (2014), 1506 – 1521.
 33. Bammou L., Belkhaouda M., Salghi R., Benali O., Zarrouk A., Zarrok H. and Hammouti B., “Corrosion inhibition of steel in sulfuric acid solution by the *Chenopodium ambrosioides* extracts”, *Journal of the Association of Arab Universities for Basic and Applied Sciences*, 16 (2014), 83-90.
 34. Barceloux D.G., “Medical toxicology of natural substances: foods, fungi, medicinal herbs, plants, and venomous animals”, *Wiley*, (2008), 867-868.

35. Barre J.T., Bowden B.F., Coll J.C., De-Jesus J, De-La-Fuente V.E., G Janairo G. and Ragasa C.Y., “A bioactive triterpene from *Lantana camara*”, *Phytochemistry*, 45, (1997), 321-324.
36. Begum S., Siddiqui B.S., Sultana R., Zia A. and Suria A., “Bio-active cardenolides from the leaves of *Nerium oleander*”, *Phytochemistry*, 50 (3) (1999), 435-438.
37. Behpour M., Ghoreishi S.M., Khayatkashani M. and Soltani N., “The effect of two oleo-gum resin exudate from *Ferula assa-foeita* and *Dorema ammoniacum* on mild steel corrosion in acidic media”, *Corrosion Science*, 53(2011), 2489-2501.
38. Beier M. and Schultze J.W., “Kinetic investigations of layer formation by inhibitors with Cu/AHT as example”, *Electrochimica Acta*, 37(12) (1992), 2299-2307.
39. Benabdellah M., Touzani R., Dafali A., Hammouti B. and El Kadiri, S., “Ruthenium–ligand complex an efficient inhibitor of steel corrosion in H₃PO₄ media”, *Materials Letters*, 61 (2007), 1197-1204.
40. Benali O., Benmehdi H., Hasnaoui O., Selles C. and Salghi R., “Green corrosion inhibitor: inhibitive action of tannin extract of *Chamaerops humilis* plant for the corrosion of mild steel in 0.5M H₂SO₄”, *Journal of Material Environmental Science*, 4 (1) (2013), 127-138.
41. Bentiss F., Bouanis M., Mernari B., Traisnel M., Vezin H. and Lagrenee M., “Understanding the adsorption of 4H-1,2,4-triazole derivatives on mild steel surface in molar hydrochloric acid”, *Applied Surface Science*, 253(7) (2007), 3696–3704.
42. Bentiss F., Lebrini M. and Lagrenee M., “Thermodynamic characterization of metal dissolution and inhibitor adsorption processes in mild steel/2,5-bis(*n*-thienyl)-1,3,4-thiadiazoles/hydrochloric acid system”, *Corrosion Science*, 47(2005), 2915-2931.
43. Bharthi K., Lakshmi S. and Geetha S., “*Calotropis procera* as potential corrosion inhibitor for commercial aluminium in HCl medium”, *International Journal of Advanced Scientific and Technical Research*, 3(3) (2013), 248-257.

44. Bhawsar J., Jain P. K., Jain P. and Soni A., “Anticorrosive activity of *Glycine max* (L.) oil against the corrosion of mild steel in acidic medium”, *International Journal of Research in Chemistry and Environment*, 3 (4) (2013), 68-74.
45. Bicudo D., Fonseca B., Bini L., Crossetti L., Bicudo C. and Araujo-Jesus T., “Undesirable side-effects of water hyacinth control in a shallow tropical reservoir”, *Freshwater Biology*, 52 (2007), 1120–1133.
46. Bothi P.R. and Sethuraman M.G., “Atropine sulphate as corrosion inhibitor for mild steel in sulphuric acid medium”, *Materials Letters*, 62 (2008), 1602-1604.
47. Bouammali H., Ousslim A., Bekkouch K., Bouammali B., Aouniti A., Al-Deya S.S., Jama C., Bentiss F. and Hammouti B., “The anti-corrosion behavior of *Lavandula dentata* aqueous extract on mild steel in 1M HCl”, *International journal of Electrochemical Science*, 8 (2013), 6005 – 6013.
48. Boukalah M., Benchat N., Hammouti B., Aouniti A. and Kertit S., “Thermodynamic characterization of steel corrosion and inhibitor adsorption of pyridazine compounds in 0.5M H₂SO₄”, *Materials Letters*, 60 (15) (2006), 1901–1905.
49. Boukalah M., Hammouti B., Lagrenee M. and Bentiss F., “Thermodynamic properties of 2,5-bis(4-methoxyphenyl)-1,3,4-oxadiazole as a corrosion inhibitor for mild steel in normal sulfuric acid medium”, *Corrosion Science*, 48 (9) (2006), 2831–2837.
50. Branzoi V., Branzoi F. and Baibarac M., “The inhibition of the corrosion of Armco iron in HCl solutions in the presence of surfactants of the type of N-alkyl quaternary ammonium salts,” *Materials Chemistry and Physics*, 65 (2000), 288–297.
51. Bright A, Michlin R., Maragatham M.R., Vizhi S.M. and Selvaraj S., “Corrosion behavior of zinc in 1.0 N hydrochloric acid with *Cnidocolus chayamansa* – a green approach”, *International Journal of Recent Scientific Research*, 6(4) (2015), 3594-3601.
52. Buchweishaija J. and Mhinzi G.S., “Natural products as a source of environmentally friendly corrosion inhibitors: the case of gum exudates

- from *Acacia seyal* var. *seyal*”, Portugaliae Electrochimica Acta, 26(3) (2008), 257-265.
53. Chauhan L.R. and Gunasekaran G., “Corrosion inhibition of mild steel by plant extract in dilute HCl medium”, Corrosion Science, 49(3) (2007), 1143-1161.
54. Chetouani A., Hammouti B. and Benkaddour M., “Corrosion inhibition of iron in hydrochloric acid solution by *jojoba* oil”, Pigment & Resin Technology, 33(1) (2004), 26 – 31.
55. Chowdhary R., Jain T., Rathoria M. K. and Mathur S.P., “Corrosion inhibition of mild steel by acid extracts of *Prosopis juliflora*,” Bulletin of Electrochemistry, 20(2) (2004), 67-75.
56. Cristofari G., Znini M., Majidi L., Bouyanzer A., Al-Deyab S.S., J. Paolini, Hammouti B. and Costa J., “Chemical composition and anti-corrosive activity of *Pulicaria mauritanica* essential oil against the corrosion of mild steel in 0.5 M H₂SO₄”, International Journal of Electrochemical Science, 6 (2011), 6699-6717.
57. Dahmani M., Et-Touham A., Al-Deyab S.S., Hammouti B. and Bouyanzer A., “Corrosion inhibition of C38 Steel in 1 M HCl: A comparative study of black pepper extract and its isolated piperine”, International journal of Electrochemical Science, 5 (2010), 1060 – 1069.
58. Damaskin, B.B., “Adsorption of organic compounds on electrodes”, Plenum Press, New York, (1971), 221.
59. De Souza F.S. and Spinelli A., “Caffeic acid as a green corrosion inhibitor for mild steel”, Corrosion science, 51 (2009), 642–649.
60. Dekmouche M., Saidi M., Hadjadj M., Ghiaba Z. and Yousfi M., “Green Approach to corrosion inhibition by ethyl acetate extract from *Pistacia atlantica* gals in hydrochloric acid solution”, International journal of Electrochemical Science, 9 (2014), 3969 – 3978.
61. Desai P.S., “*Hibiscus rosa-sinensis* (Jasud) leaves extracts used as corrosion inhibitors for mild steel in hydrochloric acid”, European Journal of Pharmaceutical and Medical Research, 2(1) (2015), 470-485.

62. Desai P.S., “Inhibitory action of extract of Ankado (*Calotropis gigantea*) leaves on mild steel corrosion in hydrochloric acid solution”, International Journal of Current Microbiology Applied Science, 4(1) (2015), 437-447.
63. Dewan S., Sangraula H., and Kumar V.L., “Preliminary studies on the analgesic activity of latex of *Calotropis procera*”, Journal of Ethnopharmacology, 73 (1-2) (2000), 307-311.
64. Dinodi N. and Shetty A.N., “Alkyl carboxylates as efficient and green inhibitors of magnesium alloy ZE41 corrosion in aqueous salt solution”, Corrosion Science, 85 (2014), 411–427.
65. Durnie W., Marco R.D., Jefferson A., and Kinsella B., “Development of a structure–activity relationship for oil field corrosion inhibitors”, Journal of Electrochemical Society, 146 (1999), 1751–1756.
66. Ebel, Mathias, Evangelou M.W., and Schaeffer A., “Cyanide phytoremediation by water hyacinths (*Eichhornia crassipes*)”, Chemosphere (Elsevier), 66 (5) (2007) 816–823.
67. Ebenso E.E., Alemu H., Umoren S.A. and Obot I.B., “Inhibition of mild steel corrosion in sulphuric acid using alizarin yellow GG dye and synergistic iodide additive”, International Journal of Electrochemical Science, 3 (2008), 1325-1339.
68. Eddy N.O. and Mamza P.A.P., “Inhibitive and adsorption properties of ethanol extract of seeds and leaves of *Azadirachta indica* on the corrosion of mild steel in H₂SO₄”, Portugaliae Electrochimica Acta, 27(4) (2009), 443-456.
69. Eddy N.O., “Adsorption and inhibitive properties of ethanol extract of *Garcinia kola* and *Cola nitida* for the corrosion of mild steel in H₂SO₄”, Pigment and Resin Technology, 39 (2010), 348–354.
70. Ejikeme P.M., Umana S.G., Menkiti M. C. and Onukwuli O. D., “Inhibition of mild steel and aluminium corrosion in 1M H₂SO₄ by leaves extract of African breadfruit”, International Journal of Materials and Chemistry ,5(1) (2015), 14-23.

71. Ekanem U.F., Umoren S.A., Udousoro I.I. and Udoh A.P., “Inhibition of mild steel corrosion in HCl using pineapple leaves (*Ananas comosus L.*) extract”, *Journal of Materials Science*, 45 (20) (2010), 5558–5566.
72. El-Awady A.A., Abd-El-Nabey B.A. and Aziz S.G., “Kinetic - thermodynamic and adsorption isotherms analyses for the inhibition of acid corrosion of steel by cyclic and open chain amines”, *Journal of Electrochemical Society*, 139 (8) (1992), 2149-2154.
73. El-Etre A.Y., Abdallah M. and El-Tantany Z.E., “Corrosion inhibition of some metals using *Lawsonia* extract”, *Corrosion Science*, 47 (2) (2005), 385-395.
74. El-Etre A.Y and El-Tantawy Z., “Inhibition of metallic corrosion using *Ficus* extract”, *Portugaliae Electrochimica Acta*, 24 (2006), 347-356.
75. El-Etre A.Y., “Natural honey as corrosion inhibitor for metals and alloys. I. copper in neutral aqueous solution”, *Corrosion Science*, 40 (11) (1998), 1845-1850.
76. El-Sabbah M.M.B., Khalil H.F.Y., Mahross M.H., Mahran B.N.A. and Gomaa A.Z., “ Aqueous extract of ginger as green corrosion inhibitor for mild steel in hydrochloric acid solution”, *International Journal of Scientific & Engineering Research*, 6(6) (2015), 1500-1508.
77. Emran K.M., Al-Ahmadi A.O., Torjoman B. A., Ahmed N.M. and Sheekh S.N., “Corrosion and corrosion inhibition of cast iron in hydrochloric acid (HCl) solution by cantaloupe (*Cucumis melo*) as green inhibitor”, *African Journal of Pure and Applied Chemistry*, 9(3) (2015), 39-49.
78. Emranuzzaman, Kumar T., Vishwanatham S. and Udayabhanu G., “Synergistic effects of formaldehyde and alcoholic extract of plant leaves for protection of N80 steel in 15% HCl”, *Corrosion Engineering Science Technology*, 39 (2004), 327–332.
79. Faustin M., Maciuk A., Salvin P., Roos C. and Lebrini M. “Corrosion inhibition of C38 steel by alkaloids extract of *Geissospermum laeve* in 1M hydrochloric acid: Electrochemical and phytochemical studies”, *Corrosion science*, 92 (2015), 287–300.

80. Fiori-Bimbi M.V., Alvarez P.E., Vaca H. and Gervasi C.A., “Corrosion inhibition of mild steel in HCl solution by pectin”, *Corrosion Science*, 92 (2015), 192–199.
81. Fouda A.S., Elewady G.Y., Mostafa H.A. and Habbouba S., “Quinazolin derivatives as eco-friendly corrosion inhibitors for low carbon steel in 2 M HCl solutions”, *African Journal of Pure and Applied Chemistry*, 7(5) (2013), 198-207.
82. Fouda A.S., EL-Khateeb A.Y. and Fakih M., “Methanolic extract of *curcum* plant as a green corrosion inhibitor for steel in NaCl polluted solutions”, *Indian Journal of Scientific Research*, 4(2) (2013), 219-227.
83. Fragoza-Mar L., Olivares-Xometl O., Domínguez-Aguilar M.A., Flores E.A., Arellanes-Lozada P. and Jiménez-Cruz F., “Corrosion inhibitor activity of 1,3-diketone malonates for mild steel in aqueous hydrochloric acid solution”, *Corrosion Science*, 61 (2012), 171–184.
84. Geetha S., Lakshmi S. and Bharathi K., “*Solanum trilobatum* as a green inhibitor for aluminium corrosion in alkaline medium”, *Journal of Chemical and Pharmaceutical Research*, 5(5) (2013), 195-204.
85. Gomma G.K. and Wahdan M.H., “Schiff bases as corrosion inhibitors for aluminium in hydrochloric acid solution”, *Materials Chemistry and Physics*, 39 (3) (1995), 209-213.
86. Gopal ji, Shukla S.K., Dwivedi P., Sundaram S., Ebenso E.E. and Prakash R., “*Parthenium hysterophorus* plant extract as an efficient green corrosion inhibitor for mild steel in acidic environment”, *International journal of Electrochemical Sciences*, 7 (2012), 9933 – 9945.
87. Gopal ji, Shukla S.K., Dwivedi P, Sundaram S, Ebenso E., and Prakash R., “ Green *Capsicum annuum* fruit extract for inhibition of mild steel corrosion in hydrochloric acid solution”, *International journal of Electrochemical Science*, 7 (2012), 12146 – 12158.
88. Gopal ji, Shukla S.K., Dwivedi P., Sundaram S. and Prakash R., “Inhibitive effect of *Chlorophytum boriviliannum* root extract on mild steel corrosion in HCl and H₂SO₄ solutions”, *Industrial and Engineering Chemistry Research*, 52 (2013), 10673-10681.

89. Gopal ji, Shukla S.K., Dwivedi P., Sundaram S. and Prakash R., “Inhibitive effect of *Argemone mexicana* plant extract on acid corrosion of mild steel”, *Industrial and Engineering Chemistry Research*, 50 (2011), 11954-11959.
90. Gulsen Avci, “Corrosion inhibition of indole-3-acetic acid on mild steel in 0.5 M HCl”, *Colloids and Surfaces A: Physicochemical and Engineering Aspects*, 317(1–3) (2008), 730–736.
91. Halambek J., Berkovic K. and Vorkapic´-Furac J., “The Influence Of *Lavandula angustifolia L.* oil on corrosion of Al-3Mg alloy”, *Corrosion science*, 52 (2010), 3978–3983.
92. Hart K. and James A.O., “The inhibitive effect of *Aloe vera barbadensis* gel on copper in hydrochloric acid medium”, *Journal of Emerging Trends in Engineering and Applied Sciences*, 5(1) (2014), 24-29.
93. Hebar N., Praveen B.M., Prasanna B.M., and Venkatesha T.V., “Corrosion inhibition behavior of ketosulfone for zinc in acidic medium”, *Journal of Fundamental and Applied Sciences*, 7(2) (2015), 271-289.
94. Hegazy M.A., Ahmed H.M. and El-Tabei A.S., “Investigation of the inhibitive effect of p-substituted 4-(N,N,N-dimethyldodecylammonium bromide)benzylidene-benzene-2-yl-amine on corrosion of carbon steel pipelines in acidic medium”, *Corrosion Science*, 53 (2) (2011), 671–678.
95. Helen L. Y. S. , Rahim A. A., Saad B., Saleh M. I. and Raja P.B., “*Aquilaria crassna* leaves extracts – A green corrosion inhibitor for mild steel in 1M HCl medium”, *International Journal of Electrochemical Science*, 9 (2014), 830 – 846.
96. Huang J, Cang H, Liu Q. and Shao J., “Environment friendly inhibitor for mild steel by *Artemisia halodendron*”, *International journal of Electrochemical Science*, 8 (2013), 8592 – 8602.
97. Hui C., Zhenghao F., Jinling S., Wenyan S. and Qi X., “Corrosion inhibition of mild steel by *Aloes* extract in HCl solution medium”, *International journal of Electrochemical Science*, 8 (2013), 720 – 734.
98. Hussain M.A. and Gorski M.S., “Antimicrobial activity of *Nerium oleander Linn*”, *Asian Journal of plant sciences*, 3(2) (2004), 177-180.

99. Ibrahim T. Alayan H. and Al Mowaquet Y., "Effect of Thyme leaves extract on corrosion of mild steel in HCl", *Progress in Organic Coatings*, 75(2012), 456-462.
100. Ibrahim T.H., Chehade Y. and Mohamed A.Z., "Corrosion inhibition of mild steel using potato peel extract in 2M HCl solution", *International journal of Electrochemical Science*, 6 (2011), 6542 – 6556.
101. Iroha N.B., Akaranta O and James A.O., "Red onion skin extract-furfural resin as corrosion inhibitor for aluminium in acid medium", *Pelagia Research Library Der Chemica Sinica*, 3 (4) (2012), 995-1001.
102. Ismail M., "Solid waste as environmental benign corrosion inhibitors in acid medium", *International Journal of Engineering Science and Technology*, 3 (2) (2011), 1742-1748.
103. Ita B.I. and Offiong O.E., "Corrosion inhibitory properties of 4-phenylsemicarbazide and semicarbazide on mild steel in hydrochloric acid", *Materials Chemistry and Physics*, 5(2) (1999), 179–184.
104. Jia-Jun Fu., Su-ning Li., Ying Wang., Lin-Hua Cao and Lu-de Lu, "Computational and electrochemical studies of some amino acid compounds as corrosion inhibitors for mild steel in hydrochloric acid solution", *Journal of Materials science*, 45(22) (2010), 6255-6265.
105. Jyothi M Joy, Vamsi S, Satish C. and Nagaveni K., "*Lantana camara* Linn: A review", *International Journal of Phytotherapy*, 2 (2) (2012), 66-73.
106. Kamal C. and Sethuraman M.G., "*Spirulina platensis* a novel green corrosion inhibitor for acid corrosion of mild steel", *Arabian Journal of Chemistry*, 5(2012), 155-161.
107. Kamath J.V. and Rana A.C., "Preliminary study on antifertility activity of *Calotropis procera* root in female rats", *Fitoterapia*, 73 (2) (2002), 111-115.
108. Karthik R., Muthukrishnan P., Elangovan A., Jeyaprabha B. and Prakash P., "Extract of *Cassia senna* as green inhibitor for the corrosion of mild steel in 1M hydrochloric acid", *Advances in Civil Engineering Materials*, 3(1) (2014), 413-433.

109. Kavitha N. and Manjula P. and Jeevanantham K., “ Synergistic effect of water hyacinth leaves –Zn⁺² system in corrosion inhibition of mild steel in aqueous medium”, Research Desk, 3(1) (2014), 400-409.
110. Kavitha N. and Manjula P., “Corrosion inhibition of water hyacinth leaves, Zn²⁺ and TSC on mild steel in neutral aqueous medium”, International Journal of Nano Corrosion Science and Engineering, 1(1) (2014), 31-38.
111. Kavitha V. and Dr. Gunavathy N., “Evaluation of *Daucus carota* aerial extract as corrosion inhibitor for mild steel in hydrochloric acid medium”, International Journal of Research in Advent Technology, 2(7) (2014), 146-154.
112. Ketsetzi A., Stathoulopoulou A. and Demadis K.D., “Being “green” in chemical water treatment technologies: issues, challenges and developments”, Desalination, 223 (2008), 487-493.
113. Khadraoui A., Khelifa A., Hamitouche H. and Mehdaoui R., “Inhibitive effect by extract of *Mentha rotundifolia* leaves on the corrosion of steel in 1M HCl solution”, Research on Chemical Intermediates, 40 (2014), 961–972.
114. Khamis E., Ameer M.A., Al-Andis N.M. and Al-Senani G., “Effect of thiosemicarbazones on corrosion of steel in phosphoric acid produced by wet process”, Corrosion, 56 (2) (2000), 127-138.
115. Khamis E., “The effect of temperature on the acidic dissolution of steel in the presence of inhibitors”, Corrosion (NACE), 46(6) (1990), 476-484.
116. Khanna S., Santos M., Ustin S. and Haverkamp P., “An integrated approach to a biophysiological based classification of floating aquatic macrophytes”, International Journal of Remote Sensing, 32(2011), 1067–1094.
117. Kliskic M., Radosevic J., Gudic S. and Katalinic S., “Aqueous extract of *Rosmarinus officinalis L.* as inhibitor of Al-Mg alloy in chloride solution”, Journal of Applied Electrochemistry, 30 (2000), 823-830.
118. Krishnaveni K., Ravichandran J. and Selvaraj A., “Effect of *Morinda tinctoria* leaves extract on the corrosion inhibition of mild steel in acid medium”, Acta Metallurgica Sinca , 26(3) (2013), 321-327.

119. Kulandai Therese S. and Vasudha V. G., "Thermodynamic and adsorption studies for corrosion inhibition of mild Steel using *Millingtonia hortensis*", International Journal of Information Research and Review, 2 (1) (2015), 261-266.
120. Kumar K.P.V., Pillai M.S.N. and Thusnavis G.R., "Seed extract of *Psidium guajava* as ecofriendly corrosion inhibitor for carbon steel in hydrochloric acid medium", Journal of Materials Science & Technology ,27(12) (2011), 1143-1149.
121. Kumar S. and Mathur S.P., "Corrosion inhibition and adsorption properties of ethanolic extract of *Calotropis* for corrosion of aluminium in acidic media", Hindwai Publishing Corporation, ISRN Corrosion, 2013 (2013) 1-9, Article ID 476170.
122. Kumar S., Arora S., Sharma M., Arora P. and Mathur S.P., "Synergistic effect of *Calotropis* plant in controlling corrosion of mild steel in basic solution", Journal of the Chilean Chemical Society, 54(1) (2009), 83-88.
123. Kumar S.A, Sankar A., Vijayan M., and Ramesh Kumar S., "*Magnolia champaca*- flower extracts as corrosion inhibitor for mild steel in acid medium", IOSR Journal of Engineering, 3(8)(2013), 10-14.
124. Kumar S.A., Sankar A. and Ramesh kumar S., "*Magnolia champaca*- Stem extracts as corrosion inhibitor for mild steel in acid medium", International Journal of Engineering Research & Technology, 2(9) (2013), 306-315.
125. Kumar S.A., Sankar A. and Rameshkumar S., "*Oxystelma esculentum* leaves extracts as corrosion inhibitor for mild steel in acid medium", International Journal of Scientific & Technology Research, 2(9) (2013), 55-58.
126. Kumar S.A., Sankar A. and Ramesh Kumar S., "Corrosion inhibition of mild steel in acid media by *Alpina galinga* extract", IOSR Journal of Applied Chemistry, 4(1) (2013), 61-64.
127. Kumpawat N., Chaturvedi A. and Upadhyay R.K., "Comparative study of corrosion inhibition efficiency of naturally occurring ecofriendly varieties

- of *Holy basil* (tulsi) for tin in HNO₃ solution”, *Open Journal of Metal*, 2(2012), 68-73.
128. Ladha D.G., Wadhvani P.M., Kumar S. and Shah N.K., “Evaluation of corrosion inhibitive properties of *Trigonella foenum-graecum* for pure aluminium in hydrochloric acid”, *Journal of Materials and Environmental Science*, 6 (5) (2015), 1200-1207.
 129. Lebrini M., Robert F., Blandinieres P.A. and Roos C., “Corrosion inhibition by *Isertia coccinea* plant extract in hydrochloric acid solution”, *International journal of Electrochemical Science*, 6 (2011), 2443 – 2460.
 130. Lebrini M., Robert F., Lecante A. and Roos C., “Corrosion inhibition of C38 steel in 1 M hydrochloric acid medium by alkaloids extract from *Oxandra asbeckii* plant”, *Corrosion science*, 53 (2011), 687–695.
 131. Leelavathi S. and Rajalakshmi., “*Dodonaea viscosa* (L.) leaves extract as acid corrosion inhibitor for mild steel – A Green Approach”, *Journal of Materials and Environmental Science*, 4 (5) (2013), 625-638.
 132. Li X., Deng S. and Fu H., “Adsorption and inhibition effect of vanillin on cold rolled steel in 3.0 M H₃PO₄”, *Progress in Organic Coatings*, 67 (4) (2010), 420–426.
 133. Li X., Deng S. and Fu H., “Inhibition of the corrosion of steel in HCl, H₂SO₄ solutions by bamboo leaf extract”, *Corrosion Science*, 62(2012), 163–175.
 134. Li X., Deng S., Xie X. and Fu H., “Inhibition effect of bamboo leaves extract on steel and zinc in citric acid solution”, *Corrosion Science*, 87 (2014), 15–26.
 135. Li L., Zhang X., Lei J., He J., Zhang S. and Pan F., “Adsorption and corrosion inhibition of *Osmanthus fragran* leaves extract on carbon steel”, *Corrosion science*, 63 (2012), 82-90.
 136. Li X. and Mu G., “Tween-40 as corrosion inhibitor for cold rolled steel in sulphuric acid: weight loss study, electrochemical characterization, and AFM”, *Applied Surface Science*, 252(5) (2005), 1254–1265.

137. Li X., Deng S., Fu H. and Mu G., “Inhibition effect of 6-benzylaminopurine on the corrosion of cold rolled steel in H₂SO₄ solution”, *Corrosion Science*, 51(2009), 620–634.
138. Loto C. A., Loto R.T. and Popoola A.P.I., “Inhibition effect of extracts of *Carica papaya* and *Camellia sinensis* leaves on the corrosion of duplex (α β) Brass in 1M nitric acid”, *International journal of Electrochemical Science*, 6 (2011), 4900 – 4914.
139. M.A. Quraishi M.A., Yadav D.K. and Ahamad I., “Green approach to corrosion inhibition by black pepper extract in hydrochloric acid solution”, *The Open Corrosion Journal*, 2 (2009), 56-60.
140. Mahdi A.S. and Rahem S.K., “Corrosion inhibition of reinforced steel by *Thymus vulgarize* (thyme) extract in simulated chloride contaminated concrete pore solution”, *International Journal of Civil Engineering and Technology*, 5(7) (2014), 89-99.
141. Mahdi S.M., “Study on the pomegranate's peel powder as a natural inhibitor for mild steel corrosion”, *International Journal of Materials chemistry and physics*, 1(1) (2015), 74-81.
142. Maine M.A., Sune N., Hadad H., Sanchez G. and Bonetto C., “Nutrient and metal removal in a constructed wetland for wastewater treatment from a metallurgic industry”, *Ecological Engineering (Elsevier)*, 26 (4) (2006), 341–347.
143. Malik A., “Environmental challenge vis a vis opportunity: The case of water hyacinth”, *Environment International*, 33(2007), 122-138
144. Mallet J.F., Cerrati C., Ucciani E., Gamsans J. and Gruber M., “Antioxidant activity of plant leaves in relation to their alpha-tocopherol content”, *Food chemistry*, 49(1) (1994), 61-65.
145. Manssouri M., Znini M., Ansari A., Bouyenger A., Faska Z. and Majidi L., “Odorized and deodorized aqueous extracts of *Ammodaucus leucotrichus* fruits as green inhibitor for C38 steel in hydrochloric acid solution” , *Der Pharma Chemica*, 6(6) (2014), 331-345.

146. Markouk M., Bekkouche K., Larhsini M., Bousaid M., Lazrek H.B. and Jana M., "Evaluation of some Moroccan medicinal plant extracts for larvicidal activity", *Journal of Ethnopharmacology*, 73 (1-2) (2000), 293-297.
147. Martinez S. and Ivica Stern, "Thermodynamic characterization of metal dissolution and inhibitor adsorption processes in the low carbon steel/mimosa tannin/sulfuric acid system", *Applied Surface Science*, 199 (1-4) (2002), 83-89.
148. Martinez S., "Inhibitory mechanism of *mimosa* tannin using molecular modeling and substitutional adsorption isotherms," *Materials Chemistry and Physics*, 77(1) (2003), 97-102.
149. Mironga J., Mathooko J. and Onywere S., "The effect of water hyacinth (*Eichhornia crassipes*) infestation on phytoplankton productivity in lake naivasha and the status of control", *Journal of Environmental Science and Engineering* ,5(10) (2011),1252-1261.
150. Moretti G., Guidi F. and Grion G., "Tryptamine as green iron corrosion inhibitor in 0.5M deaerated sulphuric acid", *Corrosion science*, 46 (2007), 387-403.
151. Mourya P., Banerjee S. and Singh M.M., "Corrosion inhibition of mild steel in acidic medium by *Tagetes erecta* (marigold flower) extract as a green inhibitor", *Corrosion science*, 85 (2014), 352-363.
152. Mu G., Li X. and Liu G., "Synergistic inhibition between tween 60 and NaCl on the corrosion of cold rolled steel in 0.5M sulfuric acid", *Corrosion. Science*, 47(2005), 1932-1952.
153. Mu G.N., Li X. and Li F., "Synergistic inhibition between o-phenanthroline and chloride ion on cold rolled steel corrosion in phosphoric acid", *Materials Chemistry and Physics*, 86(1) (2004), 59-68.
154. Nawafleh E.M., Bataineh T.T., Irshedat M.K., Al-Qudah M.A. and Abu Qrabi S.T., "Inhibition of aluminum corrosion by *Salvia judica* extract", *Research Journal of Chemical Sciences*, 3(8) (2013), 68-72.
155. Ndimele P., Kumolu-Johnson C. and Anetekhai M., "The invasive aquatic macrophyte, water hyacinth {*Eichhornia crassipes* (Mart.) Solm-Laubach:

- Pontedericeae}: problems and prospects”, Research Journal of Environmental Sciences, 5(2011), 509–520.
156. Ndubuisi J.A., Emeka E.O. and Ukiwe L.N., “ Physicochemical properties of chloroform extract of water hyacinth (*Eichhornia crassipes*)”, African Journal of Plant Science and Biotechnology, 1(2007), 40-42.
 157. Nkiko M.O., Oguntoyinbo E.S., Bamgbose J.T., and Bamigbade A.A., “Protection of zinc alloy in H₃PO₄ using extract of *Lantana camara*”, Life Science Journal, 11(11) (2014), 899-904.
 158. Noor E.A., “Comparative study on the corrosion inhibition of mild steel by aqueous extract of fenugreek seeds and leaves in acidic solutions”, Journal of Engineering and Applied Sciences, 3 (1) (2008), 23-30.
 159. Noor E.A., “Temperature effects on the corrosion inhibition of mild steel in acidic solutions by aqueous extract of fenugreek leaves”, International Journal of Electrochemical Science, 2 (2007), 996 – 1017.
 160. Noor E.A., “The inhibition of mild steel corrosion in phosphoric acid solutions by some N-heterocyclic compounds in the salt form”, Corrosion Science, 47 (1) (2005), 33-55.
 161. Noor E.A. and Al-Moubaraki A.H., “Thermodynamic study of metal corrosion and inhibitor adsorption processes in mild steel/1- methyl-4[4(-X)-styryl pyridinium iodides/hydrochloric acid systems”, Materials Chemistry and Physics, 110 (2008), 145–154.
 162. Obi-Egbedi N.O., Obot I.B. and Umoren S.A., “*Spondias mombin L.* as a green corrosion inhibitor for aluminium in sulphuric acid: correlation between inhibitive effect and electronic properties of extracts major constituents using density functional theory”, Arabian Journal of Chemistry, 5(2012), 361-373.
 163. Obot I.B. and Obi-Egbedi N.O., “2, 3-Diphenylbenzoquinoxaline: A new corrosion inhibitor for mild steel in sulphuric acid”, Corrosion Science, 52 (1) (2010), 282–285.
 164. Obot I. B. and Obi-Egbedi N. O., “ Ginseng Root: A new efficient and effective eco- friendly corrosion inhibitor for aluminium alloy of type AA

- 1060 in hydrochloric acid solution,” *International Journal of Electrochemical Science*, 4(9) (2009), 1277-1288.
165. Obot I.B. and Obi-Egbedi N.O., “Adsorption properties and inhibition of mild steel corrosion in sulphuric acid solution by ketoconazole: Experimental and theoretical investigation”, *Corrosion Science*, 52 (1) (2010), 198–204.
 166. Obot I.B., Ebenso E.E., Zuhair and Gasem M., “Eco-friendly corrosion inhibitors: Adsorption and inhibitive action of ethanol extracts of *Chalomolaena odorata L.* for the corrosion of mild steel in H₂SO₄ solutions”, *International Journal of Electrochemical Science*, 7 (2012), 1997–2008.
 167. Oguzie E. E. and Ebenso E. E., “Studies on the corrosion inhibiting effect of congo red dye –halide mixtures”, *Pigment & Resin Technology*, 35 (1) (2006), 30-35.
 168. Oguzie E.E., “Corrosion inhibition of aluminium in acidic and alkaline media by *Sansevieria trifasciata* extract”, *Corrosion science*, 49 (2007), 1527–1539.
 169. Oguzie E.E., “Studies on the inhibitive effect of *Ocimum viridis* extract on the acid corrosion of mild steel”, *Materials Chemistry and Physics*, 99 (2006), 441-446.
 170. Oguzie E.E., Onuchukwu A.I., Okafor P.C. and Ebenso E.E., “Corrosion inhibition and adsorption behavior of *Ocimum basilicum* extract on aluminium”, *Pigment & Resin Technology*, 35 (2) (2006), 63-70.
 171. Okafor P.C, Ebenso E.E. and Ekpe U.J. “*Azadirachta indica* extracts as corrosion inhibitor for mild steel in acid medium”, *International journal of Electrochemical Science*, 5 (2010), 978 – 993.
 172. Okafor P.C., Ikpi M.E., Uwaha I.E., Ebenso E.E., Ekpe U.J. and Umoren S.A., “Inhibitory action of *Phyllanthus amarus* extracts on the corrosion of mild steel in acidic media” *Corrosion science* ,50 (2008), 2310–2317.
 173. Okafor P.C., Uwaha I.E., Ekerenam O.O. and Ekpe U.J., “ *Combretum bracteosum* extracts as eco-friendly corrosion inhibitor for mild steel in acidic medium”, *Pigment & Resin Technology*, 38(4) (2009), 236-241.

174. Olasehinde E.F., Adesina A.S., Fehintola E.O. and Badmus B.M., “Corrosion inhibition behaviour for mild steel by extracts of *Musa sapientum* peels in HCl solution: Kinetics and thermodynamic study”, *IOSR Journal of Applied Chemistry*, 2(6) (2012), 15-23.
175. Oloruntoba D.T., “Corrosion inhibition of water hyacinth on 1014 steel in a chloride environment”, *Caspian Journal of Applied Sciences Research*, 2(2) (2013), 6-16.
176. Pasupathy A., Nirmala S., Sakthivel P., Abirami G. and Raja M., “Inhibitive action of *Solanum nigrum* extract on the corrosion of zinc in 0.5 N HCl medium”, *International Journal of Scientific and Research Publications*, 4(1) (2014), 1-4.
177. Patel S., “Threats, management and envisaged utilizations of aquatic weed *Eichhornia crassipes*: an overview”, *Reviews in Environmental Science and Bio/Technology*, 11(2012), 249–259.
178. Patela N., Rawat A., Jauhari S. and Mehta G., “Inhibitive action of *Bridelia retusa* leaves extract on corrosion of mild steel in acidic media”, *European Journal of Chemistry*, 1(2010), 129–133.
179. Petchiammal A. and Selvaraj S., “Anti-corrosive effect of *Lantana camara* fruit peel on mild steel in acid medium”, *Indian Journal of Applied Research*, 4 (12) (2014), 77-79.
180. Popoola A.P.I and Fayomi O.S.I., “Electrochemical study of zinc plate in acid medium: inhibitory effect of bitter leaf (*Vernonia amygdalina*)”, *International journal of Electrochemical Science*, 6 (2011), 4581 – 4592.
181. Popova A., Sokolova E., Raicheva S. and Christov M., “AC and DC study of the temperature effect on mild steel corrosion in acid media in the presence of benzimidazole derivatives”, *Corrosion Science*, 45 (1) (2003), 33–58.
182. Prabhu D. and Rao P., “Adsorption and inhibitor action of a novel green inhibitor on aluminium and 6063 aluminium alloy in 1M H₃PO₄ solution”, *Procedia Materials Science*, 5 (2014), 222 – 231.
183. Putilova I.N., Balezin S.A. and Barannik V.P., “Metallic Corrosion Inhibitors”, Pergamon Press, New York (1960), 31.

184. Qian B., Hou B. and Zheng M., “The inhibition effect of tannic acid on mild steel corrosion in seawater wet/dry cyclic conditions”, *Corrosion Science*, 72 (2013), 1–9.
185. Quartarone G., Ronchin L., Vavasori A., Tortato C. and Bonaldo L., “Inhibitive action of gramine towards corrosion of mild steel in deaerated 1.0 M hydrochloric acid solutions”, *Corrosion science*, 64 (2012), 82–89.
186. Quraishi M.A., Singh A., Singh V.K., Yadav D.K. and Singh, A.K., “Green approach to corrosion inhibition of mild steel in hydrochloric acid and sulphuric acid solutions by the extract of *Murraya koenigii* leaves”, *Materials Chemistry Physics*, 122 (2010), 114–122.
187. Quraishi M.A., Yadav D.K. and Ahamad I., “Green approach to corrosion inhibition by black pepper extract in hydrochloric acid solution”, *The Open Corrosion Journal*, 2(2009), 56-60.
188. Rahim A.A, Rocca E., Steinmetz J. and Kassim M.J., “Inhibitive action of mangrove tannins and phosphoric acid on pre-rusted steel via electrochemical methods”, *Corrosion Science*, 50 (2008), 1546–1550.
189. Raja P. B. and Sethuraman M. G., “Inhibition of corrosion of mild steel in sulphuric acid medium by *Calotropis procera*,” *Pigment and Resin Technology*, 38 (1) (2009), 33–37.
190. Raja P.B. and Sethuraman M.G., “Natural products as corrosion inhibitors for metals in corrosive media- A review”, *Materials Letters*, 62(1) (2008), 113-116.
191. Raja P.B., Qureshi A. K. , Rahim A. A., Osman H. and Awang K., “*Neolamarckia cadamba* alkaloids as eco-friendly corrosion inhibitors for mild steel in 1 M HCl media”, *Corrosion Science*, 69 (2013), 292–301.
192. Rajendran A. and Karthikeyan C., “The inhibitive effect of extract of flowers of *Cassia auriculata* in 2M HCl on the corrosion of aluminum and mild steel”, *International Journal of Plant Research*, 2(1) (2012), 9-14.
193. Rajendran A., “Isolation, characterization, pharmacological and corrosion inhibition studies of flavonoids obtained from *Nerium oleander* and *tecoma stans*”, *International Journal of Pharm Tech Research*, 3(2) (2011), 1005-1013.

194. Rani P.D., Petchiammal A, Selvaraj T.S., Nanthini and Mariammal S., “The effect of *Eugenia jambolana* on zinc in 1.0N hydrochloric acid environment”, *International Journal of Green and Herbal Chemistry*, 2(3) (2013), 510-521.
195. Sangeetha M., Rajendran S., Sathiyabama J. and Prabhakar P., “*Asafoetida* extract (ASF) as green corrosion inhibitor for mild steel in sea water”, *International Research Journal of Environment Sciences*, 1(5) (2012), 14-21.
196. Sangeetha M., Rajendran S., Sathiyabama J. and Prabhakar P., “Eco friendly extract of banana peel as corrosion inhibitor for carbon steel in sea water”, *Journal of Natural Production and Plant Resources*, 2(5) (2012), 601-610.
197. Saratha R. and Vasudha V.G., “Inhibition of mild steel corrosion in 1N H₂SO₄ medium by acid extract of *Nyctanthes arbortristis* leaves”, *E-Journal of Chemistry*, 6(4) (2009), 1003-1008.
198. Saratha, R. and Vasudha, V.G., “*Emblica officinalis* (Indian Gooseberry) leaves extract as corrosion inhibitor for mild steel in 1 N HCl medium”, *European Journal of Chemistry*, 7 (2010), 677–684.
199. Satapathy A.K, Gunasekaran G., Sahoo S.C., Amit K. and Rodrigues P.V., “Corrosion inhibition by *Justicia gendarussa* plant extract in hydrochloric acid solution,” *Corrosion Science*, 51 (2009), 2848–2856.
200. Sathish R., Vyawahare B. and Natarajan K., “Antiulcerogenic activity of *Lantana camara* leaves on gastric and duodenal ulcers in experimental rats”, *Journal of Ethnopharmacology*, 134 (2011), 195–197.
201. Sathiya S., Bharathi K. and Geetha S., “*Datura metel* as a potential corrosion inhibitor for aluminum in 1M HCl solution”, *Journal of Environment and Nanotechnology*”, 3(1) (2014), 1-8.
202. Sathiyathan R.A.L., Maruthamuthu S., Selvanayagam M., Mohanan S. and Palaniswamy N., “Corrosion inhibition of mild steel by ethanolic extracts *Ricinus communis* leaves”, *Indian Journal of Chemical Technology*, 12 (2005), 356-360.

203. Sehgal R., Arya S and Kumar V.L., "Inhibitory effect of extracts of latex of *Calotropis procera* against *Candida albicans*, a preliminary study", *Indian Journal of Pharmacology*, 37(5)(2005),334-335.
204. Seiber J.N., Nelson C.J. and Lee S.M., "Cardenolides in the latex and leaves of seven *Asclepias* species and *Calotropis procera*", *Phytochemistry*, 21(1) (1982), 2343-2348.
205. Selvi J.A., Rajendran S., Ganga Sri V., Amalraj A.J. and Narayanasamy B., "Corrosion Inhibition by beet root extract", *Portugaliae Electrochimica Acta* , 27(1)(2009), 1-11.
206. Setty S.R., Quereshi A.A., Swamy A.H., Patil T and Prakash T., "Hepatoprotective activity of *Calotropis procera* flowers against paracetamol-induced hepatic injury in rats", *Fitoterapia*, 78 (7-8) (2007), 451-454.
207. Shanab S.M.M., Ameer M.A., Fekry A.M., Ghoneim A.A. and Shalaby E.A., "Corrosion resistance of magnesium alloy (AZ31E) as orthopaedic biomaterials in sodium chloride containing antioxidantly active compounds from *Eichhornia crassipes*", *International journal of Electrochemical Science*, 6(2011), 3017-3035.
208. Sharma S.C., Kumar S., Singh V., Sharma J. and Mathur S.P., "Green corrosion inhibitor by ethanolic extract of *Lantana camara* for corrosion of aluminium in acidic media", *International Journal of Pharmaceutics and Drug Analysis*, 2(3) (2014), 341-346.
209. Sharma R.K., Mudhoo A., Jain G. and Sharma J., "Corrosion inhibition and adsorption properties of *Azadirachta indica* mature leaves extract as green inhibitor for mild steel in HNO₃", *Green Chemistry Letters and Reviews*, 3(2010), 7–15.
210. Shivakumar S.S. and Mohana K.N., "*Centella asiatica* extracts as green corrosion inhibitor for mild steel in 0.5 M sulphuric acid medium", *Palegia Research Library*, 3 (5) (2012), 3097-3106.
211. Shukla S.K., Singh A.K., Ahamad I. and Quraishi M.A., "Streptomycin: A commercially available drug as corrosion inhibitor for mild steel in hydrochloric acid solution", *Material Letters*, 63 (9-10) (2009), 819-822.

212. Shukla S.K. and Quraishi M. A., “Ceftriaxone: a novel corrosion inhibitor for mild steel in hydrochloric acid”, *Journal of Applied Electrochemistry*, 39(9) (2009), 1517-1523.
213. Sibel ZOR, Dogan P. and Yazıcı B., “Inhibition of acidic corrosion of iron and aluminium by SDBS at different temperatures”, *Corrosion Reviews*, 23(2-3) (2005), 217-232.
214. Sílvio de Souza F., Giacomelli C., Gonçalves R.S. and Spinelli A., “Adsorption behavior of *caffeine* as a green corrosion inhibitor for copper”, *Materials Science and Engineering*, 32 (2012), 2436–2444.
215. Singh A. and Kalpana S., “Corrosion inhibition studies at iron surface in acetic acid solutions by aqueous extract of *Fenugreek* leaves”, *International Journal of Chemical Sciences*, 10 (2) (2012), 817-823.
216. Singh A. and Kalpana S., “Inhibition of the Corrosion of iron in citric acid solutions by aqueous extract of *Fenugreek* seeds”, *Ultra Chemistry*, 8(2) (2012), 175-179.
217. Singh A., Ahamad I., Yadav D.K., Singh V.K. and Quraishi M.A., “The effect of environmentally benign fruit extract of Shahjan (*Moringa oleifera*) on the corrosion of mild steel in hydrochloric acid solution”, *Chemical Engineering Communications*, 199(1) (2012), 63-67.
218. Singh M.R., and Singh G., “*Hibiscus cannabinus* extract as a potential green inhibitor for corrosion of mild steel in 0.5 M H₂SO₄ solution”, *Journal of Materials Environmental Science*, 3 (4) (2012), 698-705.
219. Sinko, J., “Challenges of chromatic inhibitor pigments replacement in organic coating”, *Progress in Organic Coatings*, 42(3,4) (2001), 267-282.
220. Skinner K., Wright N., Porter-Goff E., "Mercury uptake and accumulation by four species of aquatic plants". *Environmental Pollution (Elsevier)*, 145 (1) (2007), 234–237.
221. Solmaz R., Kardas G., Culha M., Yazıcı B and Erbil M., “Investigation of adsorption and inhibitive effect of 2-mercaptothiazoline on corrosion of mild steel in hydrochloric acid media”, *Electrochimica Acta*, 53 (20) (2008), 5941–5952.

222. Soltani N. and Khayatkashani M., “*Gundelia tournefortii* as a green corrosion inhibitor for mild steel in HCl and H₂SO₄ solutions”, International journal of Electrochemical Science, 10 (2015), 46 – 62.
223. Soltani N., Behpour M. and Ghoreishi S.M. and Naeimi H., “Corrosion inhibition of mild steel in hydrochloric acid solution by some double schiff bases”, Corrosion Science, 52 (4) (2010), 1351–1361.
224. Soltani N., Tavakkoli N., Khayatkashani M., Jalali M.R. and Mosavizade A., “Green approach to corrosion inhibition of 304 stainless steel in hydrochloric acid solution by the extract of *Salvia officinalis* leaves”, Corrosion Science, 62 (2012), 122–135.
225. Tang L. , Mu G. and Liu G., “The effect of neutral red on the corrosion inhibition of cold rolled steel in 1.0 M hydrochloric acid”, Corrosion Science, 45(10) (2003), 2251–2262.
226. Tang L., Li X., Si Y., Mu G. and Liu G., “The synergistic inhibition between 8-hydroxyquinoline and chloride ion for the corrosion of cold rolled steel in 0.5 M sulfuric acid”, Materials Chemistry and Physics, 95 (1) (2006), 29–38.
227. Tebbji K., Faska N., Tounsi A., Oudda H. and Benkaddour M., “The effect of some lactones as inhibitors for the corrosion of mild steel in 1 M hydrochloric acid”, Materials Chemistry and Physics, 106 (2–3) (2007), 260–267.
228. Thomas J.M. and Thomas W.J., “Introduction to the principles of heterogeneous catalysis”, 5th Ed, Academic Press, London (1981), 14.
229. Thusnavis G.R, Kumar K.P.V. and Pillai M.S.N., “Green seed extract of *Tectona grandis* as corrosion inhibitor for mild steel in acid medium”, Advances in Materials and Corrosion , 3 (2014), 5- 8.
230. Ulaeto S.B., Ekpe U.J., Chidiebere M.A. and Oguzie E.E., “Corrosion inhibition of mild steel in hydrochloric acid by acid extracts of *Eichhornia crassipes*”, International Journal of Materials and Chemistry, 2(4) (2012), 158-164.

231. Umoren S.A., Obot I.B. and Obi-Egbedi N.O., “*Raphia hookeri* gum as a potential eco-friendly inhibitor for mild steel in sulfuric acid”, *Journal of Materials Science*, 44(1) (2009), 274–279.
232. Umoren S.A., Eduok U.M., Solomon M.M. and Udoh A.P., “Corrosion inhibition by leaves and stem extracts of *Sida acuta* for mild steel in 1 M H₂SO₄ solutions investigated by chemical and spectroscopic techniques”, *Arabian Journal of Chemistry*, 9 (2016), S209-S224.
233. Umoren S.A., Obot I.B., Ebenso E.E. and Obi-Egbedi N.O., “The Inhibition of aluminium corrosion in hydrochloric acid solution by exudate gum from *Raphia hookeri*”, *Desalination*, 247 (2009), 561-572.
234. Umoren S.A., Obot I.B., Ebenso E.E. and Obi-egbedi N.O., “Synergistic inhibition between naturally occurring exudates gum and halide ions on the corrosion of mild steel in acidic medium”, *International journal of Electrochemical Science*, 3(2008), 1029-1043.
235. Upadhyay Alka R. and Tripathi B. D., "Principle and process of biofiltration of Cd, Cr, Co, Ni & Pb from tropical opencast coalmine effluent", *Water, Air & Soil Pollution (Springer)*, 180 (2007), 213–223.
236. Vasudha V.G. and Priya K.S., “Corrosion inhibition of mild steel in H₂SO₄ media using *Polyalthia longifolia* leaves”, *Chemical Science Review and Letters*, 2(6) (2014), 435-443.
237. Vasudha V.G. and Shanmuga Priya K., “*Polyalthia longifolia* as a corrosion inhibitor for mild steel in HCl solution”, *Research Journal of Chemical Sciences*, 3(1) (2013), 21-26.
238. Verma D.K. and Khan F., “Corrosion inhibition of mild steel by extract of *Bryophyllum pinnatum* leaves in acidic solution”, *Chemistry and Materials Research*, 7(5) (2015), 69-76.
239. Verma Rajesh K. and Verma Suman K., “Phytochemical and termiticidal study of *Lantana camara* var. *aculeata* leaves”, *Fitoterapia*, 77(2006), 466–468.
240. Vijayalakshmi P. R., Rajalakshmi R. and Subhashini S., “Inhibitory action of *Borassus flabellifer* Linn.(Palmyra Palm) shell extract on corrosion of

- mild steel in acidic media”, E-Journal of Chemistry, 7(3) (2010), 1055-1065.
241. Vijayalakshmi P.R. ,Rajalakshmi R. and Subhashini S., “Corrosion inhibition of aqueous extract of *Cocos nucifera* - coconut palm - petiole extract from destructive distillation for the corrosion of mild steel in acidic medium”, Portugaliae Electrochimica Acta, 29(1) (2011), 9-21.
242. Villamagna A. and Murphy B., “Ecological and socio-economic impacts of invasive water hyacinth (*Eichhornia crassipes*): a review”, Freshwater Biology, 55 (2010), 282–298.
243. Uwah I.E., Okafor P.C. and Ebiekpe V.E., “ Inhibitive action of ethanol extracts from *Nauclea latifolia* on corrosion of mild steel in H₂SO₄ solutions and their adsorption characteristics”, Arabian Journal of Chemistry, 6(2013), 285-293.
244. Wang X.M., Plomley J B., Newman R.A., Cisneros A., “LC/MS/MS analyses of an oleander extract for cancer treatment”, Analytical Chemistry, 72 (15) (2000), 3547 – 3552.
245. Xia Z., Chou C. and Smialowska Z.S., “Pitting corrosion of carbon steel in CO₂- containing NaCl brine”, Corrosion, 45 (8) (1989), 636-642.
246. Yadav M., Kumar S., Bahadur I. and Ramjugernath D., “Corrosion inhibitive effect of synthesized thiourea derivatives on mild steel in 15% HCl solution”, International Journal of Electrochemical Science, 9 (2014), 6529-6550.
247. Yadav S.B. and Tripathi V., “A new triterpenoid from *Lantana camara*”, Fitoterapia, 74 (2003), 320–321.
248. Yaro A.S. and Ibraheem H.F., “The inhibition effect of peach juice on corrosion of low carbon steel in hydrochloric acid at different temperatures”, Iraqi Journal of Chemical and Petroleum Engineering, 11 (1) (2010), 65-76.
249. Yaro A.S., Khadom A.A. and Wael R.K., “*Apricot* juice as green corrosion inhibitor of mild steel in phosphoric acid”, Alexandria Engineering Journal ,52(1)(2013), 129–135.

250. Zakvi S. J. and Mehta G. N., "Acid corrosion of mild steel and its inhibition by *Swertia anngustifolia* – study by electrochemical techniques", Transaction of The SAEST, 23(4) (1988), 407-410.
251. Zarrouk A., Dafali A., Hammouti B., Zarrok H., Boukhris S. and Zertoubi M., "Synthesis, characterization and comparative study of functionalized quinoxaline derivatives towards corrosion of copper in nitric acid medium", International Journal of Electrochemical Science, 5(2010),46-55.
252. Zia A., Siddiqui B.S., Begum S., Siddiqui S. and Saira A., "Studies on the constituents of the leaves of *Nerium oleander* on behavior pattern in mice", Journal of Ethnopharmacology, 49 (1) (1995), 33-39.
253. Zibbu G. and Batra A., "A review on chemistry and pharmacological activity of *Nerium oleander L.*", Journal of Chemical and Pharmaceutical Research, 2(6) (2010), 351-358.
254. Znini M., Majidi L., Bouyanzer A., Paolini J., Desjobert J-M., Costa J. and Hammouti B., "Essential oil of *Salvia aucheri mesatlantica* as a green inhibitor for the corrosion of steel in 0.5 M H₂SO₄", Arabian Journal of Chemistry, 5 (4) (2012), 467–474.
255. Znini M., Bouklah M., Majidi L., Kharchouf S., Aouniti A., Bouyanzer A., B.Hammouti B., Costa J. and Al-Dyab S.S., "Chemical composition and inhibitory effect of *Mentha spicata* essential oil on the corrosion of steel in molar hydrochloric acid", International Journal of Electrochemical Science, 6 (2011), 691-704.
256. Znini M., Paolini J., Majidi L., Desjobert J.-M., Costa J., Lahhit N. and Bouyanzer A., "Evaluation of the inhibitive effect of essential oil of *Lavandula multifida L.* on the corrosion behavior of C38 steel in 0.5 M H₂SO₄ medium", Research on Chemical Intermediates, 38 (2) (2012), 669–683.
257. Zucchi F. and Omar I.H., "Plant extracts as corrosion inhibitors of mild steel in HCl solutions", Surface Technology, 24(4) (1985), 391-399.

ABBREVIATIONS

1. **AAS** : Atomic Absorption Spectroscopy
2. **AECPL** : Aqueous extract of Calotropis procera leaves
3. **AELCL** : Aqueous extract of Lantana camara leaves
4. **AENOL** : Aqueous extract of Nerium oleander leaves
5. **AEWHL** : Aqueous extract of Water hyacinth leaves
6. **AFM** : Atomic force microscopy
7. **AO** : Argan oil
8. **CC** : Commiphora caudata
9. **EDX** : Energy-Dispersive X-ray Analysis
10. **EFM** : Electron Frequency Modulation
11. **EIS** : Electron Impedance Spectroscopy
12. **FITR** : Fourier Transform Infrared Spectroscopy
13. **GA** : Gum Arabic
14. **GIE** : Garcina indica extract
15. **HE** : Hydrogen Evolution
16. **LD** : Lavandula dentata
17. **ML** : Mass Loss
18. **OCP** : Open Circuit Potential
19. **PDP** : Potentiodynamic Polarization
20. **SEM** : Scanning Electron Microscopy
21. **TA** : Tryptamine
22. **TSC** : Tri Sodium Citrate
23. **XRD** : X-Ray Diffraction
24. **BLE** : Breadfruit leaves extract

RESEARCH PAPERS PUBLISHED/ COMMUNICATED

1. Paper entitled “GREEN APPROACH TO CORROSION INHIBITION OF MILD STEEL IN 1 M HCl SOLUTION BY AQUEOUS EXTRACT OF *LANTANA CAMARA L.* LEAVES” has been published in International Journal of Chemical Sciences, 13(3), (2015), 1157-1162.
2. Paper entitled “CORROSION INHIBITION OF MILD STEEL WITH AQUEOUS EXTRACT OF *CALOTROPIS PROCERA L.* LEAVES IN 1M HCl SOLUTION” has been published in International Journal of Current Research, 8(2) (2016), 26064-26070.
3. Paper entitled “ ADSORPTION BEHAVIOUR AND CORROSION INHIBITION PROPERTIES OF AQUEOUS EXTRACT OF LEAVES OF *NERIUM OLEANDER L.* IN HYDROCHLORIC ACID SOLUTION” has been published in World Journal of Pharmacy and Pharmaceutical Sciences, 6(5) (2017), 40-49.
4. Paper entitled “CORROSION INHIBITION AND ADSORPTION BEHAVIOUR OF AQUEOUS EXTRACT OF LEAVES OF WATER HYACINTH IN 1M HYDROCHLORIC ACID SOLUTION” has been communicated to Corrosion Science.

**PARTICIPATION IN SEMINARS/ SYMPOSIA/CONFERENCES/
ANNUAL CONVENTIONS**

1. Presented a poster in the International Conference on “Frontiers at the Chemistry- Allied Sciences Interface (FCASI-2016)” organized by Centre of Advanced Study, Department of Chemistry, University of Rajasthan, Jaipur (Raj.) during 25-26 April 2016. (Title: Mitigation of Mild Steel Corrosion by *Calotropis procera* L. Leaves in 1M H₂SO₄ Solution).
2. Presented a poster in the International Conference on “Nascent Developments in Chemical Sciences: Opportunities for Academia-Industry Collaboration” organized by Department of Chemistry, Birla Institute of Technology & Science, Pilani (Raj.), Pilani Campus during 16-18 October 2015. (Title: Green Approach to Protect Mild Steel Corrosion in Acidic Media).
3. Presented a poster in the National Conference on “Recent Advancements in Chemical Sciences” organized by Department of Chemistry, MNIT Jaipur during 21-23 August 2015. (Title: Corrosion Inhibition of Mild Steel in 1M H₂SO₄ Solution by Aqueous Extract of *Lantana camara* L. Leaves).
4. Presented a paper in 4th International Conference on “Advance Trends in Engineering, Technology and Research” (ICATETR-2015), organized by Bal Krishna Institute of Technology, Kota (Raj.) during 19-20 June 2015. (Title: Thermodynamic and Adsorption Parameters of Aqueous Extract of *Lantana camara* L. Leaves on Corrosion of Mild Steel Surface in Acidic Medium).
5. Presented a paper in 3rd International Conference on “Advance Trends in Engineering, Technology and Research” (ICATETR-2014), organized by Bal Krishna Institute of Technology, Kota (Raj.) during 22nd-24th December 2014.(Title: Inhibitory Action of *Carum Copticum* Seeds Extract on Corrosion of Iron in 1M Acetic Acid).

6. Actively participate in 5th National Academic Workshop on “Organic Reaction Mechanisms & Analytical Techniques used in Chemical Sciences” organized by Department of Pure and Applied Chemistry, University of Kota, Kota (Rajasthan) held at University of Kota and sponsored by UGC New Delhi during 21-25 October 2013.
7. Presented a paper in “National Conference on Global Environmental Changes and Disaster Management for Sustainable life on Earth – A burning issue” held at Maharishi Arvind College of Engineering & Technology, Ranpur, Kota on 21st October 2013.
(Title: Inhibition of the corrosion of mild steel in phosphoric acid solutions by aqueous extract of fenugreek seeds).

PUBLISHED PAPERS



ISSN: 0975-833X

RESEARCH ARTICLE

CORROSION INHIBITION OF MILD STEEL WITH AQUEOUS EXTRACT OF *CALOTROPIS PROCERA L.* LEAVES IN 1M HCl SOLUTION

*Priya Bhardwaj, Seema Agarwal and S. Kalpana

Electrochemistry and Environmental Chemistry Lab, Department of Chemistry, Government College,
Kota -324001 (Raj.) India

ARTICLE INFO

Article History:

Received 28th November, 2015
Received in revised form
15th December, 2015
Accepted 15th January, 2016
Published online 14th February, 2016

Key words:

Calotropis Procera L., Corrosion,
Langmuir adsorption isotherm,
Mild steel, Weight loss method.

Copyright © 2016 Priya Bhardwaj et al. This is an open access article distributed under the Creative Commons Attribution License, which permits unrestricted use, distribution, and reproduction in any medium, provided the original work is properly cited.

Citation: Priya Bhardwaj, Seema Agarwal and S. Kalpana, 2016. "Corrosion inhibition of mild steel with aqueous extract of *Calotropis procera L.* leaves in 1m HCl solution", *International Journal of Current Research*, 8, (02), 26064-26070.

ABSTRACT

The inhibition of mild steel (MS) in 1 M HCl solution with aqueous extract of *Calotropis procera L.* leaves (AECPL) was studied by weight loss method at 303-333K temperatures. It was found that inhibition efficiency increased with increase in concentration of extract and decreased with increase in temperature. Maximum 60.86% inhibition efficiency was observed at 303 K and at 8% (v/v) concentration of extract. Adsorption of extract at mild steel surface follows Langmuir adsorption isotherm. Physiosorption is proposed by the values of Gibbs free energy, variation in inhibition energy with temperature and with activation energy values trend. Negative Gibbs energy reveals the spontaneity of inhibition process in extract at studied temperatures.

INTRODUCTION

Steel corrosion inhibition phenomenon have become an industrial and academic topic especially in acidic media (Bentiss et al., 2000). This is because of the increasing industrial applications of acid solutions in acid pickling, industrial cleaning, acid descaling, oil-well acidizing in oil recovery and the petrochemical processes. Besides this corrosion rates are very high in aqueous acidic media especially when soluble corrosion products are formed (Raja et al., 2013). Therefore exploring better green corrosion inhibitors are important for its practical applications and environmental friendly point of view. Synthetic organic corrosion inhibitors are effective but costly, environmental polluting and harmful to living beings during their manufacture and applications. So currently researches on corrosion are focused on "green corrosion inhibitors" that show good inhibition efficiency with low risk of environmental pollution (Amin et al., 2007) All plant extracts, which have been shown effective corrosion inhibitors are comparatively cheap, easily available, biodegradable and called as green corrosion inhibitors.

Different plant parts have been studied as corrosion inhibitors in acidic and alkaline media (Ostovari et al., 2009; Alaneme et al., 2015; Kamal et al., 2012; James et al., 2009; Ambrish et al., 2010; Ibrahim et al., 2011; Bhardwaj et al., 2015). In the present study aqueous extract of leaves of *Calotropis Procera L.* has been chosen as corrosion inhibitor for mild steel in 1M HCl solution and findings are discussed in the light of inhibitor concentration, temperature, adsorption properties, kinetic properties, thermodynamic properties. Weight loss (gravimetric analysis) method is applied to obtain inhibition efficiencies.

MATERIALS AND METHODS

Preparation of extract

The leaves of *Calotropis procera L.* plant were taken, washed and air dried for 6-7 days, crushed and grind mechanically. 20 g of ground leaves were heated in 250 ml distill water for one hour using air condenser at 70°C - 80°C. This extract was left overnight and then filtered and make up to 250 ml with distill water for the experiment.

Preparation of steel specimens

Cylindrical mild steel specimens of 4.9 cm length and 0.70 cm diameter were taken and abraded with a series of emery papers,

*Corresponding author: Priya Bhardwaj,

Electrochemistry and Environmental Chemistry Lab, Department of Chemistry,
Government College, Kota -324001 (Raj.) India.

degreased with acetone, washed with distill water, dried and constant weight was recorded by electronic balance.

Solution Preparation

1M HCl solution was prepared by 37% HCl (Merk Ltd.) using distill water. The employed concentration range of aqueous extract of *Calotropis procera* L. leaves (AECL) was 1% to 8% (v/v).

Gravimetric Measurements

Gravimetric method is widely used method because of its reliability and simplicity in corrosion inhibition experiments. For each experiment 100 ml test solutions were taken in 250 ml beaker and cylindrical specimen was immersed in it with plastic thread for one hour. The experiments were carried out at different temperatures ranges from 303 K to 333K in thermostatic water bath. After one hour specimens were removed, washed with distill water, acetone dried and abraded with series of emery papers and then weighted accurately with electronic balance. It was noted that the surfaces of specimens became more rough in test solutions without the inhibitor than the surfaces of specimens which were immersed in test solutions containing different concentrations of inhibitor.

RESULTS AND DISCUSSION

Effect of temperature on corrosion rates

Corrosion rates were calculated by following equation (Mourya et al., 2014; Yadav et al., 2014).

$$C R (\text{g cm}^{-2}\text{min}^{-1}) = \left(\frac{W_1 - W_2}{A t} \right) \quad (1)$$

Where CR is corrosion rate, W_1 is weight loss of mild steel specimen without inhibitor and W_2 is weight loss of mild steel specimen with inhibitor, A is area of MS specimen and t is immersion time.

Table 1 represents that corrosion rates increases with increase in temperatures and decreases with increase in concentration of inhibitor. It is clear that corrosion rates obey Arrhenius type reactions as it increases with increase in solution temperature (31).

Effect of temperature on inhibition efficiency

From the obtained corrosion rates, inhibition efficiencies were calculated by using following equation (Mourya et al., 2014; Behpour et al., 2011).

$$IE \% = \left(\frac{CR - CR_{inh}}{CR} \right) \times 100 \quad (2)$$

Where CR is the corrosion rate in absence of inhibitor and CR_{inh} is corrosion rate in presence of inhibitor. AECL are given in Table 1.

Data in Table 1 reveal that inhibition efficiency increased with an increase in inhibitor concentration. This suggests that the

inhibitor species adsorbed on steel /solution interface where the adsorbed species mechanically screen the coated part of steel surface from the action of corrosion medium (31). The variation in inhibition efficiency was detected with increasing temperatures in Table 1.

It is clear from the data that inhibition efficiency decreases with rise in temperatures, suggests possible desorption of adsorbed species. It further suggests physisorption of inhibitor molecules on steel surfaces (39). The surface coverage θ is calculated by in the given equation (Yadav et al., 2014).

$$\theta = \left(\frac{CR - CR_{inh}}{CR} \right) \quad (3)$$

θ is the surface coverage, CR is the corrosion rate in absence of inhibitor and CR_{inh} is corrosion rate in presence of inhibitor.

Kinetic parameters

Assuming that corrosion rates of steel specimens against concentration of inhibitor obeys kinetic relationship as equation (Khamis et al., 2000; Noor 2005).

$$\log CR = \log K + B \log C_{inh} \quad (4)$$

Where K is rate constant and equal to CR when inhibitor concentration is unity. B is reaction constant which is measure of inhibitor effectiveness and C_{inh} is the concentration v/v % (ml/100ml) of AECL.

Fig. 2 represents plot between $\log CR$ and $\log C_{inh}$ values at various studied temperatures. B and K were calculated by slope and intercept of straight lines of the graph.

The obtained results in Table 2 can be discussed as follows (Noor 2007).

- Negative values of B indicates that corrosion rate is inversely proportional to concentration of inhibitor. In other words the corrosion rates decrease with increase in concentration of inhibitor species.
- The high negative values of B reflects good inhibitive property of inhibitor. High negative value of B can be observed as steep slope in graph (Fig.1).
- Value of B is high at lower temperatures, indicates that inhibitive species is more effective at comparatively lower temperatures.
- The increase in K values with increase in temperature, indicating the increase in corrosion rates with temperatures.

Thermodynamic and activation parameters

The thermodynamic and activation parameters like apparent activation energy E_{act} , enthalpy of activation ΔH^* , entropy of activation ΔS^* were calculated for steel dissolution process. Activation energy E_{act} were calculated by following Arrhenius equation (Yadav et al., 2014).

$$\log CR = \log A - \left(\frac{E_{act}}{2.303RT} \right) \quad (5)$$

Table 1. Inhibition efficiencies and corrosion rates of mild steel corrosion in 1MHCl in different concentration of AECL at different temperatures

Conc (v/v)%	CR x 10 ⁻³ (g/cm ² /min)				IE %			
	303 K	313 K	323 K	333 K	303 K	313 K	323 K	333 K
0	0.69	1.37	2.33	3.07	--	--	---	---
1	0.59	1.21	2.17	2.88	14.49	11.67	06.86	06.18
2	0.41	1.08	1.94	2.81	40.57	20.16	16.73	08.46
3	0.38	0.99	1.93	2.74	44.92	27.73	17.16	10.74
5	0.33	0.86	1.86	2.64	52.17	37.22	20.17	14.10
8	0.27	0.72	1.57	2.56	60.86	47.44	32.61	16.43

Table 2. Kinetic parameters and regression coefficients for the corrosion of mild steel in 1M HCl containing AECL at different temperatures

Temp (° K)	Kinetic parameters		
	R ² values	B	K(x10 ⁻³)(g/cm ² /min)
303	0.974	-0.3584	-0.5736
313	0.968	-0.2514	-1.2755
323	0.898	-0.1363	-2.1923
333	0.956	-0.0538	-2.9080

Table 3. Thermodynamic Activation parameters for the corrosion process of mild steel in solution containing different concentrations of AECL in 1 mol HCl solutions

CONC (v/v %)	E _{act} (KJ/mol)	Δ H ⁺ (KJ/mol)	Δ S ⁺ (J/mol/K)
0	41.26	38.83	-177.64
1	43.20	41.39	-170.56
2	52.93	50.41	-143.63
3	54.91	52.48	-137.55
5	57.86	54.99	--130.48
8	60.93	58.49	-120.69

Table 4. Adsorption parameters obtained from Langmuir adsorption isotherm (A) and Gibbs free energy, entropy and enthalpy for adsorption process of inhibitor at mild steel in 1 M HCl solution in AECL at different studied temperatures

TEMP (K)	R ²	K _{ads}	Δ G (KJ/mol)	Δ H (KJ/mol)	Δ S (J/mol/K)
303	0.887	0.2358	-13.76		-73.23
313	0.998	0.1389	-12.84	-35.95	-73.83
323	0.912	0.0869	-11.99		-74.17
333	0.994	0.0659	-11.59		-73.15

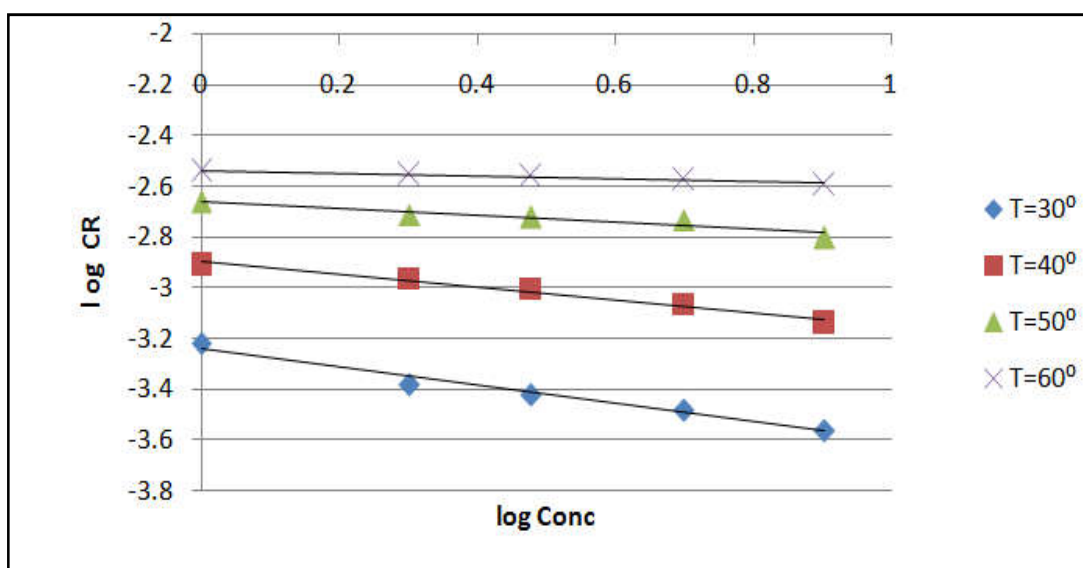


Figure 1. Variation of Log CR vs Log C of corrosion inhibition process by AECL at studied temperatures

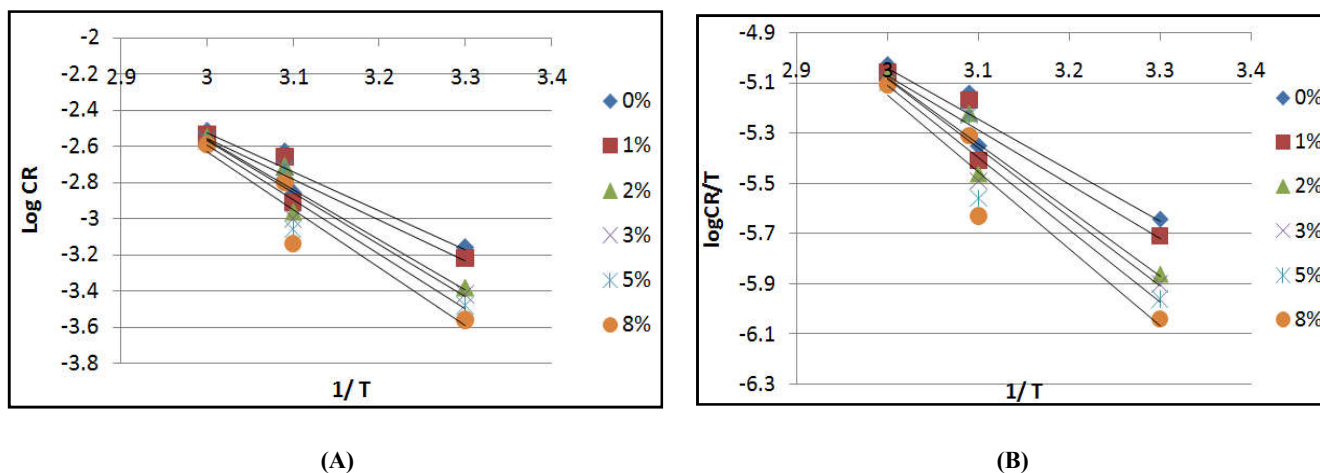


Figure 2. (A) Arrhenius plot and (B) Transition state plot for corrosion of mild steel in 1M HCl in the absence and presence of various concentrations of AECL

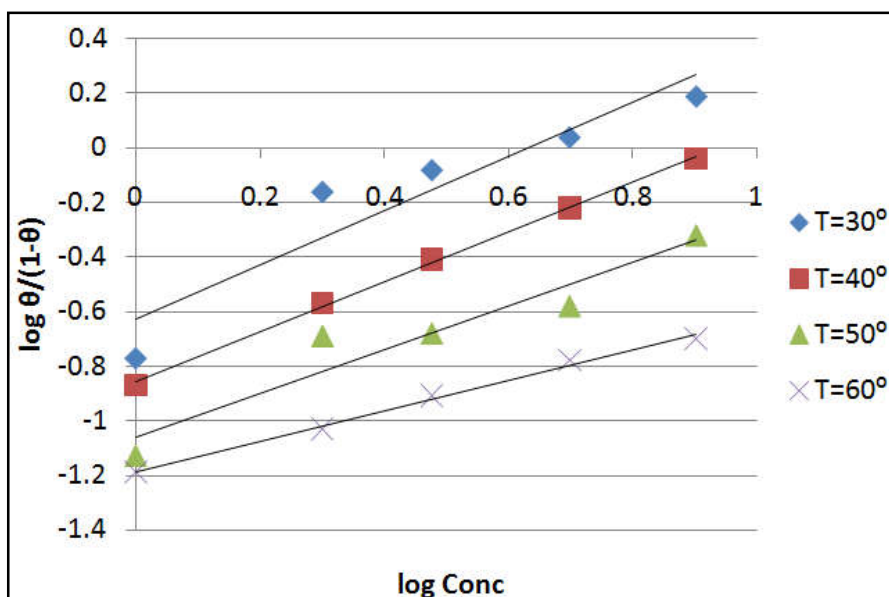


Figure 3. Langmuir adsorption isotherm for corrosion of mild steel in 1M HCl in the absence and presence of various concentrations of AECL at different temperatures

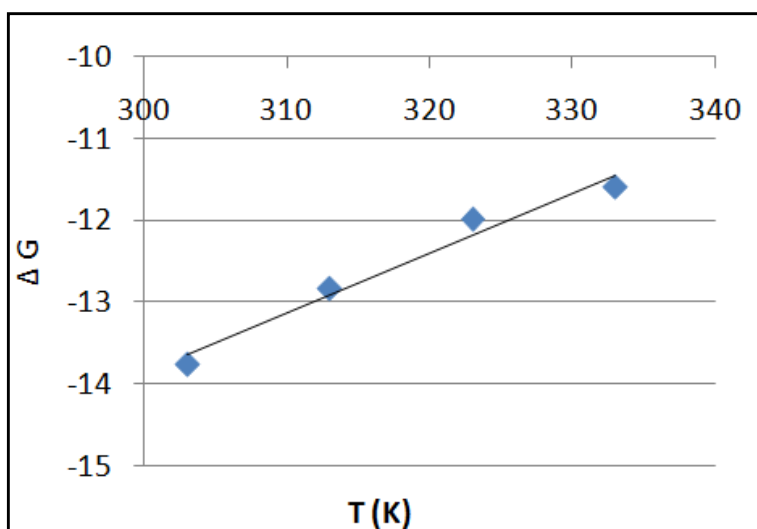


Figure 4. Variation of Gibbs energy change with different studied temperatures

Where A is Arrhenius pre exponential factor, E_{act} is activation energy, R is universal gas constant, T is absolute temperature. The slope of $\log CR$ vs $1/T$ gives the values of activation energies at studied concentrations. Table 3 contains the calculated data of activation energies. The values of activation energies in presence of inhibitor species were found higher than uninhibited solutions. The higher the concentration of inhibitor, the higher the activation energy is observed. It is observed that inhibitive causes a rise in activation energy value when compared to the blank solutions (Manssour *et al.*, 2014). The change in values of activation energies is due to the modification of the mechanism of corrosion process in presence of adsorbed inhibitor molecules (Riggs *et al.*, 1967) and could be often interpreted as an indication for the formation of an adsorbed film on metal surface (Schorr *et al.*, 1972; Clark *et al.*, 1979). The rise in activation energy indicates the formation of energy barrier in corrosion process in presence of the inhibitor and the increase in activation energy with rise in temperature could be interpreted as physical adsorption (40). The values of enthalpy of activation ΔH^* and entropy of activation ΔS^* were calculated by following transition state equation (Yadav *et al.*, 2014).

$$\log\left(\frac{CR}{T}\right) = \left(\log\left(\frac{R}{Nh}\right)\right) + \left[\left(\frac{\Delta S^*}{2.303R}\right) - \left(\frac{\Delta H^*}{2.303RT}\right)\right] \quad (6)$$

Where h is planck's constant, N is Avogadro number R is the gas constant A plot of $\log (CR/T)$ vs $1/T$ gave a straight line with slope of $(-\Delta H^*/2.303R)$ and intercept of $[(\log R/Nh) + (\Delta S^*/2.303R)]$ from which the values of ΔH^* and ΔS^* were calculated. These values are tabulated in Table 3. The values of ΔH^* and ΔS^* in presence of inhibitor were higher than uninhibited solutions. The positive values of ΔH^* reflects endothermic nature of steel dissolution process (Guan *et al.*, 2004) and negative values of ΔS^* indicate the formation of activated complex in rate determining step, represents an association rather than dissociation, means decrease in disorder of system due to adsorption of inhibitor molecules on to the metal surface (Abd-Ei-Nabey *et al.*, 1996). This reveals the formation of an ordered stable layer of inhibitor on steel surface (Yurt *et al.*, 2004).

Adsorption isotherm and gibbs energy

The mechanism of adsorption can also be predicted by metal/electrolyte interface interaction. To understand the nature of adsorption, obtained surface coverage θ were fitted in different adsorption isotherms. The mathematical expressions for Langmuir (Noor and Al-Moubaraki, 2008).

$$\frac{C}{\theta} = \frac{1}{K_{ads}} + C_{inh} \text{ (Langmuir isotherm)} \quad (7)$$

Rearranging the above equation

$$(\theta / 1-\theta) = K_{ads} \cdot C_{inh} \quad (8)$$

$$\text{Or } \log(\theta / 1-\theta) = \log K_{ads} + \log C_{inh} \quad (9)$$

Where K_{ads} is the equilibrium constant of adsorption, a is the molecular interaction factor in adsorbed layer, θ is the surface

coverage, $(1-\theta)$ is the uncovered surface, C_{inh} is the concentration of inhibitor

The value of K_{ads} obtained from Langmuir adsorption isotherm (A) of Fig.3 is related by gibbs energy by the following equation (Khamis 1990).

$$K_{ads} = \frac{1}{C_{H_2O}} \exp(-\Delta G/RT) \quad (10)$$

$$\text{It can be written as: } \Delta G = -2.303 RT \log(K_{ads} \cdot C_{H_2O}) \quad (11)$$

Where C_{H_2O} is the concentration of water in (ml / L) at metal/solution interface, R is universal gas constant and T is absolute temperature. Values of K_{ads} were calculated by the intercept of Langmuir isotherm $\log(\theta / 1-\theta)$ vs $\log C_{inh}$. The values of ΔG_{ads} were tabulated in Table 4. Obtained values of Gibbs energy were plotted against temperature in accordance with the following basic equation (El-Awady *et al.*, 1992).

$$\Delta G_{ads} = \Delta H_{ads} - T \Delta S_{ads} \quad (12)$$

Intercept of graph between ΔG_{ads} vs T give value of ΔH_{ads} and by putting the value of intercept in equation 12 values of ΔS_{ads} were obtained. These values are listed in Table 4.

The negative values of ΔG_{ads} indicated spontaneous corrosion inhibition process (Abd-El-Rahim *et al.*, 2001; Tang *et al.*, 2006; Tang *et al.*, 2003). Table 4 shows increase (values becomes less negative) in Gibbs energy with temperature, indicating the exothermic process, at which adsorption was unfavourable with increase in reaction temperature as a result of inhibitor desorption from the steel surface (Noor 2007). The values of ΔH_{ads} and ΔS_{ads} also predict the mechanism of inhibitor adsorption. The negative values of ΔG_{ads} are between -11.55 KJ/mol to -13.76 KJ/mol indicating physisorption of inhibitor species on steel surface. Generally values of ΔG_{ads} up to -20 KJ/mol are consistent with electrostatic interaction (physisorption) while more negative values than -40 KJ/mol are due to charge sharing from inhibitor species to metal surface to form a co-ordinate type of bond (Umoren *et al.*, 2009). The values of ΔH_{ads} are come out to be negative, shows exothermic adsorption process of adsorption of inhibitor on steel surfaces (Obi-Egbedi *et al.*, 2012), and this is further proved by lower inhibition efficiencies in Table 1 at higher temperatures.

The exothermic process is attributed to either physical or chemical adsorption or mixture of both (Bentiss *et al.*, 2005), whereas an endothermic process corresponds to chemisorptions (Lebrini *et al.*, 2011). In exothermic process values of ΔH_{ads} predicts physisorption or chemisorption process. For physisorption values of ΔH_{ads} is lower than 40 KJ/mol while for chemisorption it approaches to 100 KJ/mol (Zarrouk *et al.*, 2010). The value of ΔH_{ads} in table 4 indicates physisorption process. The negative value of ΔS_{ads} in Table 4 shows decrease in entropy. This agrees with what expected, when the adsorption is an exothermic process, it must be accompanied by a decrease in the entropy energy change and vice versa (Thomas and Thomas, 1981)

Conclusion

1. Result showed that AECPL is good corrosion inhibitor for mild steel in 1M HCl solution.
2. Corrosion rates increases with increase in temperature and decreases with increase in inhibitor concentration.
3. Inhibition efficiencies increases at lower temperature suggest the physisorption process of inhibitor on mild steel surface.
4. Apparent activation energy increases with increase in inhibitor concentrations also suggests physisorption.
5. Enthalpy of activation comes out to be negative which show endothermic process.
6. The values of Gibbs free energies calculated were negative shows spontaneity of corrosion inhibition process of mild steel in 1 M HCl in AECPL.

Acknowledgement

The authors are thankful to the Head of Chemistry Department and Principal, Government College, Kota for providing necessary laboratory facilities.

REFERENCES

- Abd El Rehim, S.S, Hassan, H.H and Amin, M.A. 2001. Corrosion inhibition of aluminium by 1,1(lauryl amido) propyl ammonium chloride in HCl solution. *Mater. Chem. Phys.*, 70(1):64-72.
- Abd-El-Nabey, B.A., Khamis, E., Ramadan, M. and El-Gindy, A. 1996. Application of the Kinetic-Thermodynamic Model for Inhibition of Acid Corrosion of Steel by Inhibitors Containing Sulfur and Nitrogen. *Corrosion*, 52(9):671-679.
- Alaneme, K. K., Daramola, Y. S., Olusegun, S. J. and Afolabi, A. S. 2015. Corrosion Inhibition and Adsorption Characteristics of Rice Husk Extracts on Mild Steel Immersed in 1M H₂SO₄ and HCl Solutions. *Int. J. Electrochem. Sci.*, 10(4): 3553-3567.
- Amin, M.A., Abd El-Rehim, S.S., El-Sherbini, E.E.F. and Bayoumi, R.S. 2007. The inhibition of low carbon steel corrosion in hydrochloric acid solutions by succinic acid: Part I. Weight loss, polarization, EIS, PZC, EDX and SEM studies. *Electrochimica Acta*, 52(11):3588–3600
- Behpour, M., Ghoreishi, S.M., Khayatkashani, M. and Soltani, N. 2011. The effect of two oleo-gum resin exudate from *Ferula assa-foetida* and *Dorema ammoniacum* on mild steel corrosion in acidic media. *Corros. Sci.*, 53(8) :2489–2501.
- Bentiss F., Lebrini, M. and Lagrenée, M. 2005. Thermodynamic characterization of metal dissolution and inhibitor adsorption processes in mild steel/2,5-bis(n-thienyl)-1,3,4-thiadiazoles/hydrochloric acid system. *Corros. Sci.*, 47(12):2915-2931.
- Bentiss, F., Lagrenée, M, Traisnel., M. 2000. 2,5-Bis(n-Pyridyl)-1,3,4-Oxadiazoles as Corrosion Inhibitors for Mild Steel in Acidic Media. *Corros Sci.*, 56 (7):733-742
- Bhardwaj, P., Singh, A., Agarwal, S. and Kalpana, S. 2015. Green Approach to Corrosion Inhibition of Mild Steel in 1M HCl Solution by Aqueous Extract of *Lantana Camara* L. Leaves, *Int. J. Chem. Sci.*, 13(3): 1157-1162.
- Clark, P.N., E. Jackson, E. and Robinson, M. 1979. Effect of Thiourea and Some of its Derivatives on the Corrosion Behaviour of Nickel in 50% v/v (5·6M) Hydrochloric Acid. *Br. Corros. J.*, 14(1): 33–39.
- El-Awady, A.A., Abd-El-Nabey, B.A. and Aziz, S.G. 1992. Kinetic-Thermodynamic and Adsorption Isotherms Analysis for the Inhibition of Acid Corrosion of steel by Cyclic and Open Chain Amines. *J. Electrochem. Soc.*, 139(8): 2149-2154.
- Fouda, A.S., Tawfik, H. and Badr, A.H. 2013. Corrosion inhibition of mild steel by *Camellia Sinensis* extract as green inhibitor. *Adv. Mater. Corros.*, 2:1-7.
- Guan, N. M., Xueming Li, Fei Li. 2004. Synergistic inhibition between o-phenanthroline and chloride ion on cold rolled steel corrosion in phosphoric acid. *Mater. Chem. Phys.*, 86(1):59-68.
- Ibrahim, T. H., Chehade, Y. and Mohamed Zour, A. 2011. Corrosion Inhibition of Mild Steel using Potato Peel Extract in 2M HCl Solution. *Int. J. Electrochem. Sci.*, 6(12): 6542-6556.
- James, A. O. and Akaranta, O. 2009. Corrosion inhibition of aluminum in 2.0 M hydrochloric acid solution by the acetone extract of red onion skin. 3(12), pp. 262-268.
- Kamal, C. and Sethuraman, M.G. 2012. *Spirulina platensis* – A novel green inhibitor for acid corrosion of mild steel. *Arab. J. Chem.*, 5(2):155-161.
- Khamis, E. 1990. The Effect of Temperature on the Acidic Dissolution of Steel in the Presence of Inhibitors. *Corrosion (NACE)*.46(6):476-484.
- Khamis, E., Ameer, M.A., AlAndis, N.M., Al-Senani, G. 2000. Effect of Thiosemicarbazones on Corrosion of Steel in Phosphoric Acid Produced by Wet Process. *Corros. Sci.*, 56(2):127-138.
- Lebrini, M., Robert, F., Blandinières P.A. and Roos, C. 2011. Corrosion Inhibition by *Isertia coccinea* Plant Extract in Hydrochloric Acid Solution. *Int. J. Electrochem. Sci.*, 6(7):2443-2460.
- Mourya, P., Banerjee, S. and Singh, M.M. 2014. Corrosion inhibition of mild steel in acidic solution by *Tagetes erecta* (Marigold flower) extract as a green inhibitor. *Corros. Sci.*, 85:352-363
- Naderi, E., Jafari, A.H., Ehteshamzadeh and Hossein, M.G. 2009. Effect of carbon steel microstructures and molecular structure of two new Schiff base compounds on inhibition performance in 1 M HCl solution by EIS. *Mater. Chem. Phys.*, 115(2–3): 852-858.
- Noor, E.A. 2005. The inhibition of mild steel corrosion in phosphoric acid solutions by some N-heterocyclic compounds in the salt form. *Corros. Sci.*, Volume 47(1): 33-55.
- Noor, E.A. 2007. Temperature Effects on the Corrosion Inhibition of Mild Steel in Acidic Solutions by Aqueous Extract of Fenugreek Leaves. *Int. J. Electrochem. Sci.*, 2:996 – 1017.
- Noor, E.A. and Al-Moubaraki, A.H. 2008. Thermodynamic study of metal corrosion and inhibitor adsorption processes in mild steel/1-methyl-4[4'(-X)-styryl] pyridinium iodides/hydrochloric acid systems *Mater. Chem. Phys.*, 110(1):145-154
- Obi-Egbedi, N.O., Obot, I.B., Umoren, S.A. 2012. *Spondias mombin* L. as a green corrosion inhibitor for aluminium in sulphuric acid: Correlation between inhibitive effect and

- electronic properties of extracts major constituents using density functional theory. *Arab. J. Chem.*, 5(3): 361-373.
- Ostovari, A., Hoseinie, S.M., Peikari, M., Shadizadeh, S.R. and Hashemi, S.J., 2009. Corrosion inhibition of mild steel in 1 M HCl solution by henna extract: A comparative study of the inhibition by henna and its constituents (Lawsone, Gallic acid, α -D-Glucose and Tannic acid). *Corros. Sci.*, 51(9):1935-1949.
- Popova, A., Sokolova, E., Raicheva, S. and Christov, M. 2003. AC and DC study of the temperature effect on mild steel corrosion in acid media in the presence of benzimidazole derivatives. *Corros. Sci.*, 45(1):33-58.
- Raja, P.B., Qureshi, A.K., Rahim, A.A., Osman, H. and Awang, K. 2013. Neolamarckia cadamba alkaloids as eco-friendly corrosion inhibitors for mild steel in 1 M HCl media. *Corros. Sci.*, 69:292-301.
- Riggs, O., Hurd, I.R. and Ray, M. 1967. Temperature Coefficient of Corrosion Inhibition. *Corrosion.*, 23(8): 252-260.
- Schorr, M. and Yahalm, J. 1972. The significance of the energy of activation for the dissolution reaction of metal in acids. *Corros. Sci.*, 12 (11):867-868.
- Shivakumar, S.S. and Mohana, K.N. 2012. Centella asiatica extracts as green corrosion inhibitor for mild steel in 0.5 M sulphuric acid medium. *Adv. App. Sci. Res.*, 3 (5):3097-3106.
- Singh, A., Singh, V. K. and Quraishi, M. A. 2010. Inhibition Effect of Environmentally Benign Kuchla (Strychnos Nuxvomica) Seed Extract on corrosion of Mild Steel in Hydrochloric Acid Solution. *Rasayan. J. Chem.*, 3 (4):811-824.
- Tang, L., Lie, X., Si, Y., Mu, G., and G. Liu, 2006. The synergistic inhibition between 8-hydroxyquinoline and chloride ion for the corrosion of cold rolled steel in 0.5 M sulfuric acid. *Mater. Chem. Phys.*, 95(1)29-38.
- Tang, L., Mu, G. and Liu, G. 2003. The effect of neutral red on the corrosion inhibition of cold rolled steel in 1.0 M hydrochloric acid. *Corros. Sci.*, 45(10): 2251-2262
- Thomas, J. M. and Thomas, W. J. 1981. Introduction to the Principles of Heterogeneous Catalysis, Academic Press, London, 5th Ed., 14.
- Umoren, S.A., Obot, I.B., Ebenso, E.E. and Obi-Egbedi, N.O. 2009. The Inhibition of aluminium corrosion in hydrochloric acid solution by exudate gum from Raphia hookeri. *Desalination* 247 (1): 561-572.
- Yadav, M., Kumar, S., Bahadur, I. and Ramjugernath, D. 2014. Corrosion Inhibitive Effect of Synthesized Thiourea Derivatives on Mild Steel in a 15% HCl Solution. *Int. J. Electrochem. Sci.*, 9:6529 -6550.
- Yadav, M., Kumar, S., Bahadur, I. and Ramjugernath, D. 2014. Corrosion Inhibitive Effect of Synthesized Thiourea Derivatives on Mild Steel in a 15% HCl Solution. *Int. J. Electrochem. Sci.*, 9:6529 -6550.
- Yurt, A., Balaban, A., Kandemir, S.U., Bereket, G. and Erk, B. 2004. Investigation on some Schiff bases as HCl corrosion inhibitors for carbon steel. *Mater. Chem. Phys.*, 85(2-3): 420-426
- Zarrouk, A., Dafali, A., Hammouti, B., Zarrok, H., Boukhris, S. and Zertoubi, M. 2010. Synthesis, Characterization and Comparative Study of Functionalized Quinoxaline Derivatives towards Corrosion of Copper in Nitric Acid Medium. *Int. J. Electrochem. Sci.*, 5(1):46-55.



ADSORPTION BEHAVIOUR AND CORROSION INHIBITION PROPERTIES OF AQUEOUS EXTRACT OF LEAVES OF NERIUN OLENDER L. IN HYDROCHLORIC ACID SOLUTION

Priya Bhardwaj^{1*}, Seema Agarwal² and S. Kalpana³

Electrochemistry & Environmental Chemistry Lab, Department of Chemistry,
Government College KOTA –324001 (Rajasthan) INDIA.

Article Received on
10 April 2017,

Revised on 30 April 2017,
Accepted on 20 May 2017,

DOI: 10.20959/wjpps20176-9365

*Corresponding Author

Priya Bhardwaj

Electrochemistry &
Environmental Chemistry
Lab, Department of
Chemistry, Government
College KOTA –324001
(Rajasthan) INDIA.

ABSTRACT

The inhibition of mild steel (MS) in 1 M HCl solution with aqueous extract of *Nerium oleander L.* leaves (AENOL) was studied by weight loss method at 303-333K temperatures. It was found that inhibition efficiency increased with increase in concentration of extract and decreased with increase in temperature. Maximum 83.76% inhibition efficiency was observed at 303 K and at 10% (v/v) concentration of extract. Adsorption of extract at mild steel surface follows Langmuir adsorption isotherm. Physorption is proposed by the values of Gibbs free energy, variation in inhibition energy with temperature and with activation energy values trend. Negative values of Gibbs energy reveals the spontaneity of inhibition process in extract at studied temperatures.

KEYWORDS: Nerium oleander L., Corrosion, Langmuir adsorption isotherm, Mild steel, Weight loss method.

1. INTRODUCTION

Steel is widely used alloy in transportation, mechanical and petrochemical industries. However it is suffered from a major problem known as corrosion. Corrosion is the degradation of metals and their alloys by an electrochemical reaction and environment. The introduction of corrosion inhibitors is the best way to prevent metallic corrosion and can save the great economic loss of a country.

This has been provoked the researchers to search new eco-friendly, low cost, easy available effective corrosion inhibitors to foster green environment and for the sustainability of living beings. These compounds are natural products like leaves, roots, barks and stem extracts which effectively absorbs on metal surface and protect metals and their alloys from corrosion in acidic, basic and neutral media.

Literature survey reveals various plant extracts that have been used as corrosion inhibitors for protection of different metals and their alloys. Extract of fenugreek seeds and leaves^[18], essential oils of *Mentha spicata*, *Lavandula multifida*, *Pulicaria mauritanica*^[6,37,38] *Azadirachta indica*^[24,27], extract of *Ananas comosus L.*^[9], *Embilica officinalis*^[26], *Garcinia cola* and *Cola nitida*^[8] etc. have been studied. In the continuity of above corrosion inhibition studies, the present work reveals the adsorption behavior and corrosion prevention properties of aqueous extract of leaves of *Nerium oleander L.* for mild steel in 1 M HCl solution.

2. MATERIALS AND METHODS

Preparation of extract

The leaves of *Nerium oleander L.* plant were taken, washed and air dried for 6-7 days, crushed and grind mechanically. 20 g of ground leaves were heated in 200 ml distill water for one hour using air condenser at 70°C - 80°C. This extract was left overnight and then filtered and make up to 200 ml with distill water for the experiment.

Preparation of steel specimens

Cylindrical mild steel specimens of 4.9 cm length and 0.70 cm diameter were taken and abraded with a series of emery papers, degreased with acetone, washed with distill water, dried and constant weight was recorded by electronic balance.

Solution Preparation

1M HCl solution was prepared by 37% HCl (Merk Ltd.) using distill water. The employed concentration range of aqueous extract of *Nerium oleander L.* leaves (AENOL) was 1% to 10% (v/v).

Gravimetric Measurement

Gravimetric method is widely used method because of its reliability and simplicity in corrosion inhibition experiments. For each experiment 100 ml test solutions were taken in 250 ml beaker and cylindrical specimen was immersed in it with plastic thread for one hour.

The experiments were carried out at different temperatures ranges from 303 K to 333K in thermostatic water bath. After one hour specimens were removed, washed with distill water, acetone dried and abraded with series of emery papers and then weighted accurately with electronic balance. It was noted that the surfaces of specimens became more rough in test solutions without the inhibitor than the surfaces of specimens which were immersed in test solutions containing different concentrations of inhibitor.

3. RESULT AND DISCUSSION

3.1 Corrosion rates

Corrosion rates were calculated by following equation (1).^[1, 34]

$$C R (g \text{ cm}^{-2} \text{ min}^{-1}) = \frac{(W_1 - W_2)}{A t} \quad (1)$$

Where CR is corrosion rate, W_1 is weight loss of mild steel specimen without inhibitor and W_2 is weight loss of mild steel specimen with inhibitor, A is area of MS specimen and t is immersion time. **Table1** shows that corrosion rates of mild steel decrease with increase in concentration of AENOL inhibitor at all studied temperatures. This could be subjected to the adsorption of the phyto-constituents of inhibitor molecules with increase in concentration of inhibitor. The corrosion rate obeys Arrhenius type reaction, as it increases with rise in temperature.^[19]

3.2 Inhibition efficiency

From the obtained corrosion rates, inhibition efficiencies were calculated by using following equation (2).^[1, 34]

$$IE \% = \left(\frac{CR_{\text{blank}} - CR_{\text{inh}}}{CR} \right) \times 100 \quad (2)$$

Where CR_{blank} is the corrosion rate in absence of inhibitor and CR_{inh} is corrosion rate in presence of inhibitor. AENOL are given in **Table 1**. Data in **Table1** show that %IE increase with increase in extract concentration, which is an indication of an increase in number of components of extract adsorbed on mild steel surface, which block the active sites of metal from acid attack and protect the metallic corrosion.^[20] Further the decrease in % I.E. with rise in temperature suggests electrostatic interaction (physical adsorption) of the extract molecules on mild steel surface. This further indicates desorption of adsorbed inhibitor species at higher

temperatures and metal dissolution takes place.^[35] 83.76% inhibition efficiency is observed at 10% (v/v) concentration of inhibitor.

Table 1. Mild steel corrosion rates and inhibition efficiencies in 1 M HCl solution in absence and presence of different concentrations of AENOL at different temperatures

Conc (v/v)%	CR x 10 ⁻³ (g/cm ² /min)				IE %			
	303K	313K	323K	333K	303K	313K	323K	333K
0	1.17	1.75	3.72	3.85	-	-	-	-
1	0.83	1.41	3.08	3.19	29.05	19.42	17.20	17.14
2	0.79	1.32	2.84	3.14	32.47	24.57	23.65	18.44
3	0.44	0.89	2.27	2.97	62.39	49.14	38.97	22.85
5	0.34	0.79	1.73	2.74	70.94	54.85	53.49	28.83
10	0.19	0.45	1.00	1.77	83.76	74.28	73.11	54.02

3.3 KINETIC PARAMETERS

Assuming that corrosion rates of steel specimens against concentration of inhibitor obeys kinetic relationship as equation (3).^[19,38]

$$\log CR = \log K + B \log C_{inh} \quad (3)$$

Where K is rate constant and equal to CR when inhibitor concentration is unity. B is reaction constant which is measure of inhibitor effectiveness and C_{inh} is the concentration v/v % (ml/100ml) of AENOL. Figure 2 represents plot between log CR and log C_{inh} values at various studied temperatures. B and K were calculated by slope and intercept of straight lines obtained in Figure 1. The obtained results are summarized in **Table 2** which can be discussed as follows^[19]

- Negative values of B indicate that corrosion rate is inversely proportional to concentration of inhibitor. In other words the corrosion rates decrease with increase in concentration of inhibitor species.
- The high negative values of B reflects good inhibitive property of inhibitor High negative value of B can be observed as steep slope in graph (Fig.1).
- Value of B is high at lower temperatures, indicates that inhibitive species is more effective at comparatively lower temperatures.
- The increase in K values with increase in temperature, indicating the increase in corrosion rates with temperatures.

Table2. Kinetic parameters for mild steel corrosion in 1 M HCl solution in AENOL

Temp (K)	Kinetic Parameters	
	B	K x 10 ⁻³ (g cm ² min ⁻¹)
303 K	-0.6753	0.9831
313 K	-0.5013	1.6084
323 K	-0.5002	3.6132
333 K	-0.2466	3.6157

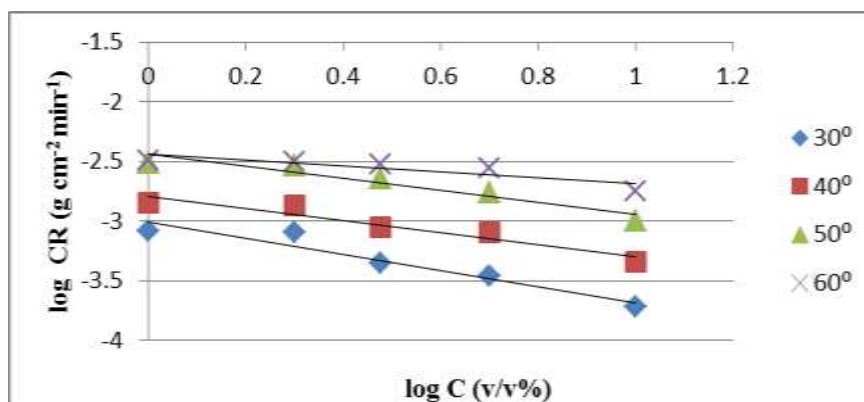


Figure 1. Variation of log CR with logC_{inh.} for mild steel corrosion in 1M HCl in presence of different concentrations of AENOL at various temperatures

3.4 THERMODYNAMIC AND ACTIVATION PARAMETERS

Thermodynamic and activation parameters like apparent activation energy E_{act} , enthalpy of activation ΔH^* entropy of activation ΔS^* were calculated for steel dissolution process. Activation energy E_{act} were calculated by following Arrhenius equation (4).^[34,35]

$$\log CR = \log A - \left(\frac{E_{act}}{2.303 RT} \right) \quad (4)$$

Where A is Arrhenius pre-exponential factor, E_{act} is activation energy, R is universal gas constant, T is absolute temperature. The slope of log CR vs 1/T in Figure 2 gives the values of activation energies at studied concentrations. **Table 3** represents the calculated data of activation energies. The values of activation energies in presence of inhibitor were found higher than in uninhibited solution. This indicates the formation of higher energy barrier in corrosion reaction by inhibitor molecules. The increase in E_{act} for corrosion process in inhibitor solution further interpreted as physical adsorption of inhibitor species on mild steel surface.^[16, 23, 25] Besides this According to Damaskin^[47], the value of activation energy lesser than 80kJ/ mol and even smaller than 5kJ /mol represents physical adsorption. This assertion supports the experimental results obtained in the present study. The values of enthalpy of activation ΔH^* and entropy of activation ΔS^* were calculated by following transition state equation (5).^[34, 35]

$$\log \left(\frac{CR}{T} \right) = \left[\log \left(\frac{R}{Nh} \right) + \left[\frac{\Delta S^*}{2.303 R} \right] - \left[\frac{\Delta H^*}{2.303 RT} \right] \right] \quad (5)$$

Where h is planck's constant, N is Avogadro number R is the gas constant A plot of $\log (CR/T)$ vs $1/T$ gave a straight line with slope of $(-\Delta H^*/2.303R)$ and intercept of $[(\log R/Nh) + (\Delta S^*/2.303 R)]$ from which the values of ΔH^* and ΔS^* were calculated (see Figure 3). These values are tabulated in **Table 3**. Values of ΔH^* were found positive. Positive values indicate endothermic nature of steel dissolution process.^[1, 17, 35] Endothermic process further indicates that mild steel dissolution reduces at lower temperatures and increases with increase in temperatures. Negative values of ΔS^* are indicative of formation of activated complex in rate determining step, which represents association rather than dissociation step, meaning the decrease in disorder takes place on going from reactants to activated complex.^[1, 11, 30]

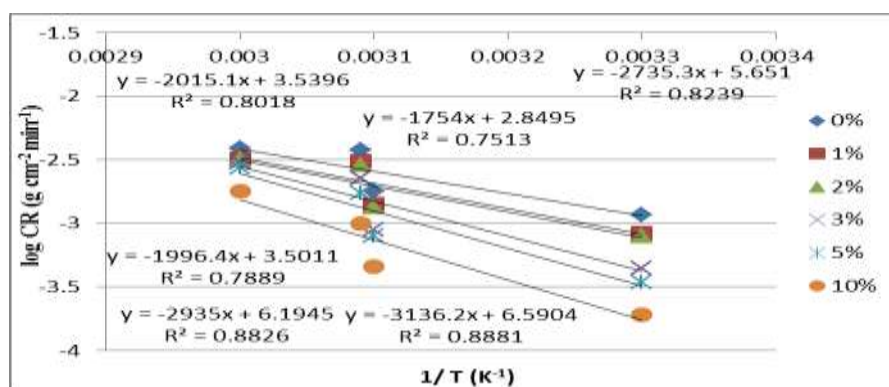


Figure 2. Arrhenius plots for mild steel corrosion rates in 1 M HCl in absence and presence of various concentrations of AENOL

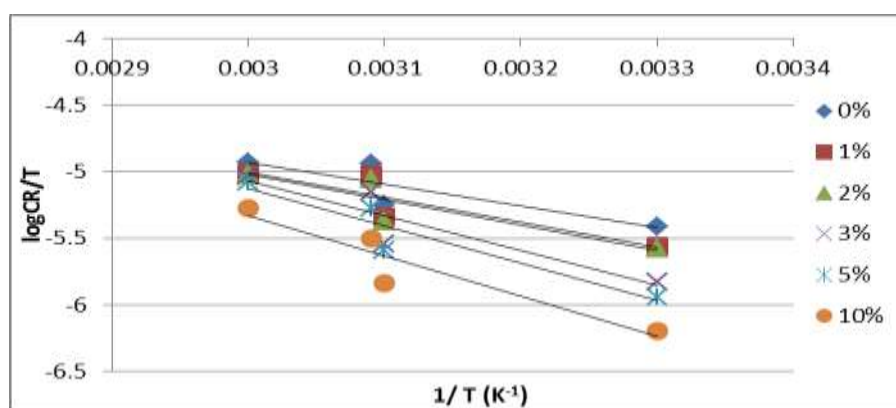


Figure 3. Transition state plots for mild steel corrosion in 1 M HCl in absence and presence of various concentrations of AENOL

It is also observed from data in **Table 3** that E_{act} and ΔH^* vary in the same manner. Values of both E_{act} and ΔH^* increase with increase in concentration of inhibitor, suggesting that energy

barrier is increases with increase in inhibitor concentration. This means that corrosion reaction will further be pushed to surface sites that are characterized by progressively higher values of E_{act} as the concentration of inhibitor becomes greater.^[1, 29, 31]

Table 3. Activation and thermodynamic parameters for mild steel corrosion in 1M HCl solution with AENOL

Conc. (v/v)%	E_{act} (KJ/mol)	ΔH^* (KJ/mol)	ΔS^* (J/mol/K)
0	33.58	30.93	-199.27
1	38.22	35.79	-186.02
2	38.58	36.06	-185.61
3	52.37	49.94	-144.85
5	56.19	53.76	-134.45
10	60.05	57.66	-126.74

The values of activation energy were found larger than corresponding values of enthalpy of activation, indicate the involvement of a gaseous reaction, simply hydrogen evolution in corrosion process, associated with a decrease in total reaction volume.^[19]

3.5. ADSORPTION ISOTHERM AND GIBBS ENERGY

The nature of adsorption can be explained by understanding the process at metal/electrolyte interface. Further to understand the nature of adsorption, obtained surface coverage θ were fitted in different adsorption isotherms. Langmuir adsorption isotherm was the best fit. The mathematical expressions for Langmuir adsorption isotherm can be expressed by the following equation.^[10,40,42- 44]

$$\frac{c}{\theta} = \frac{1}{K_{ads}} + C_{inh} \quad (6)$$

Rearranging the above equation (6) we get

$$\left[\frac{\theta}{(1-\theta)} \right] = K_{ads} C_{inh} \quad (7)$$

$$\text{Or } \log \left[\frac{\theta}{(1-\theta)} \right] = \log K_{ads} + \log C_{inh} \quad (8)$$

Where K_{ads} is the equilibrium constant of adsorption, θ is the surface coverage, $(1-\theta)$ is the uncovered surface, C_{inh} is the concentration of inhibitor. Values of K_{ads} were calculated from the intercept of Langmuir adsorption isotherm drawn according to the equation (8) between

$\log(\theta / 1 - \theta)$ and $\log C_{inh}$ (see Figure 4). The value of K_{ads} obtained from Langmuir adsorption isotherm is related to Gibbs energy according to the following equation (9).^[19, 38]

$$K_{ads} = \frac{1}{C_{H_2O}} \exp(-\Delta G/RT) \quad (9)$$

It can be written as: $\Delta G_{ads} = -2.303 RT \log(K_{ads} \cdot C_{H_2O})$ (10)

Where C_{H_2O} is the concentration of water in (ml / L) at metal/ solution interface, R is universal gas constant and T is absolute temperature. The values of ΔG_{ads} were tabulated in **Table 4**. Obtained values of Gibbs energy were plotted against temperature in accordance with the following basic equation.^[19,39]

$$\Delta G_{ads} = \Delta H_{ads} - T \Delta S_{ads} \quad (11)$$

Intercept of graph between ΔG_{ads} vs T in Figure 5 gives value of ΔH_{ads} and by putting the value of intercept in equation (11) values of ΔS_{ads} were obtained. These obtained adsorption parameters Gibbs free energy of adsorption (ΔG_{ads}), enthalpy of adsorption (ΔH_{ads}) and entropy of adsorption (ΔS_{ads}) are listed in **Table 4**. ΔG_{ads} values has been found negative at all studied temperatures indicating spontaneous adsorption process of inhibitor molecules on metal surface.^[1,4,5,7,19,28] Generally values of ΔG_{ads} upto -20 KJ/mol are consistent with electrostatic interactions (physical adsorption) between charged molecules and charged metal surface and values upto -40 KJ/mol or higher involve charge sharing or transfer from inhibitor molecules to metal surface to form coordinate type of bond (chemical adsorption).^[1, 4, 5, 12, 13, 21, 22, 33] The obtained values of ΔG_{ads} were found less than -20kJ/mol indicated physical adsorption of inhibitor molecules. It has been observed that adsorption of negatively charged species is facilitated due to the positively charged metal. But positively charged species can also be adsorbed and protect the positively charged metal surface acting with a negatively charged intermediate such as acid anions, adsorbed on metal surface.^[1, 25, 33] Values of ΔH_{ads} has been found negative indicating the exothermic adsorption process^[11, 14, 16,20, 34], which further indicates lower %IE at higher temperatures, due to desorption of inhibitor molecules. The exothermic process is attributed to either physical or chemical adsorption or mixture of both.^[3] In exothermic process, values of ΔH_{ads} predict physisorption or chemisorption. For physisorption values of ΔH_{ads} is lower than 40kJ/mol while for chemisorption it approaches to 100kJ/mol.^[36,21] Values of ΔH_{ads} in **Table 4** indicate physisorption. Negative values of ΔS_{ads} indicate decrease in entropy of adsorption process. This behavior can be explained as follows: Before the adsorption of inhibitor molecules onto

mild steel surface, they might freely move in bulk solution (inhibitor molecules were chaotic). But with the process of adsorption, inhibitor molecules were orderly adsorbed onto the steel surface as a result decrease in entropy is observed.^[13] A more interesting behavior is observed in **Table 4** that negative ΔH_{ads} value is accompanied with negative ΔS_{ads} value. This further agrees that when the adsorption is an exothermic process, it must be accompanied by a decrease in the entropy change and vice versa.^[20,35]

The obtained positive values of ΔS_{ads} are the algebraic sum of the adsorption of organic molecules and the desorption of water molecules.^[15, 46] Therefore the positive values of entropy of adsorption is the result of the substitution process, which can be attributed to the increase in the solvent entropy and more positive water desorption entropy.^[45]

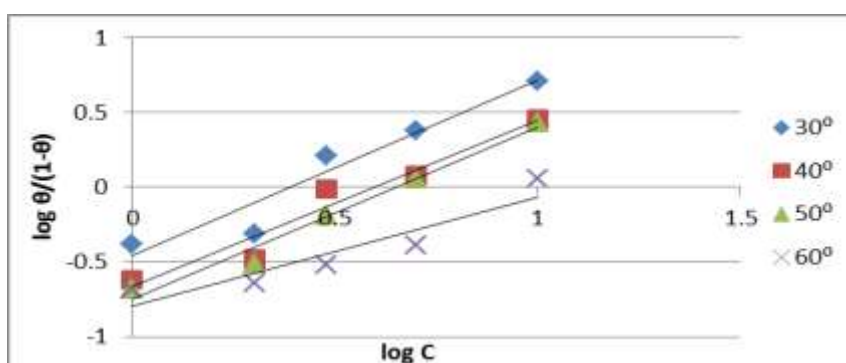


Figure 4. Langmuir adsorption isotherm of AENOL on mild steel surface in 1 M HCl at various studied temperatures

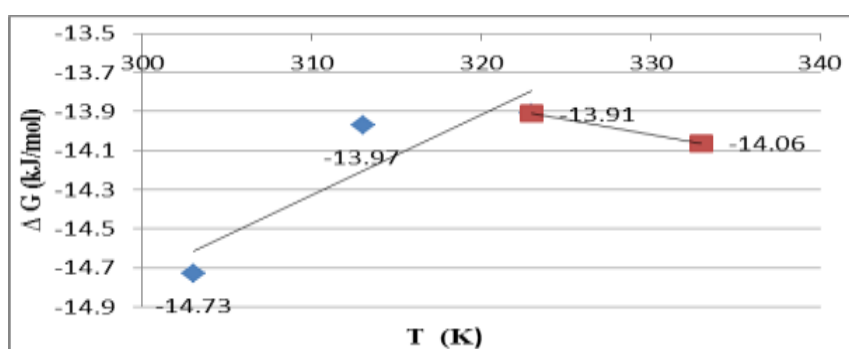


Figure 5. The variation of ΔG_{ads} (kJ/mol) with T (K) for mild steel corrosion in 1M HCl at different studied temperature in AENOL

Table 4. Adsorption parameters for mild steel corrosion in 1 M HCl solution with AENOL

Temp (k)	ΔG_{ads} (kJ/mol)	ΔH_{ads} (kJ/mol)	ΔS_{ads} (J/mol/K)
303	-14.73	-27.04	-40.63

313	-13.97	-27.04	-41.76
323	-13.91	-27.04, -09.07	- 40.65, 14.98
333	-14.06	-09.07	14.98

4. CONCLUSIONS

1. Result showed that AENOL is good corrosion inhibitor for mild steel in 1M HCl solution.
2. Corrosion rates increase with increase in temperature and decrease with increase in inhibitor concentration.
3. Inhibition efficiencies increases at lower temperature suggest the physisorption process of inhibitor on mild steel surface.
4. Apparent activation energy increases with increase in inhibitor concentrations also suggests physisorption.
5. Enthalpy of adsorption comes out to be negative and lower than 40kJ/mol, which shows exothermic and physical adsorption process of inhibitor.
6. The values of Gibbs free energies calculated were negative shows spontaneity of corrosion inhibition process of mild steel in 1 M HCl in AENOL.

5. ACKNOWLEDGEMENT

The authors are thankful to the Head of Chemistry Department and Principal, Government College, Kota for providing necessary laboratory facilities.

REFERENCES

1. Behpour M., Ghoreishi S.M., Khayatkashani M. and Soltani N., The effect of two oleo-gum resin exudate from *Ferula assa-foetida* and *Dorema ammoniacum* on mild steel corrosion in acidic media, *Corrosion Science*, 2011; 53: 2489–2501.
2. Benabdellah, M., Touzani, R., Dafali, A., Hammouti, B. and El Kadiri, S., Ruthenium–ligand complex, an efficient inhibitor of steel corrosion in H_3PO_4 media, *Materials Letters*, 2007; 61: 1197-1204.
3. Bentiss F., Lebrini M. and Lagrenée M., Thermodynamic characterization of metal dissolution and inhibitor adsorption processes in mild steel/2,5-bis(*n*-thienyl)-1,3,4-thiadiazoles/hydrochloric acid system., *Corrosion. Science*, 2005; 47: 2915-2931.
4. Bouklah M., Benchat N., Hammouti B., Aouniti A. and Kertit S., Thermodynamic characterisation of steel corrosion and inhibitor adsorption of pyridazine compounds in 0.5 M H_2SO_4 , *Materials Letters*, 2006; 60(15): 1901–1905.

5. Boukalah M., Hammouti B., Lagrenee M. and Bentiss F., Thermodynamic properties of 2,5-bis(4-methoxyphenyl)-1,3,4-oxadiazole as a corrosion inhibitor for mild steel in normal sulfuric acid medium, *Corrosion Science*, 2006; 48(9): 2831–2842.
6. Cristofari G., Znini M., Majidi L., Bouyanzer A., Al-Deyab S.S., J. Paolini, Hammouti B. and Costa J., Chemical Composition and Anti-Corrosive Activity of *Pulicaria Mauritanica* Essential Oil Against the Corrosion of Mild Steel in 0.5 M H₂SO₄, *International Journal of Electrochemical Science*, 2011; 6: 6699-6717.
7. Ebenso, E.E., Alemu, H., Umoren, S.A. and Obot, I.B., Inhibition of mild steel corrosion in sulphuric acid using alizarin yellow GG dye and synergistic iodide additive, *International Journal of Electrochemical. Science*, 2008; 3: 1325-1339.
8. Eddy N.O., Adsorption and inhibitive properties of ethanol extract of *Garcinia kola* and *Cola nitida* for the corrosion of mild steel in H₂SO₄, *Pigment and Resin Technology*. 2010; 39: 348–354.
9. Ekanem U.F., Umoren, S.A., Udousoro, I.I. and Udoh, A.P., Inhibition of mild steel corrosion in HCl using pineapple leaves (*Ananas comosus* L.) extract. *J. Mater. Sci.* 2010; 45: 5558–5566.
10. Fragoza-Mar L., Olivares-Xometl O., Domínguez-Aguilar M.A., Flores E.A., Arellanes-Lozada P. and Jiménez-Cruz F., Corrosion inhibitor activity of 1,3-diketone malonates for mild steel in aqueous hydrochloric acid solution, *Corrosion Science*, 2012; 61: 171–184.
11. Gomma G.K. and Wahdan M.H. Schiff bases as corrosion inhibitors for aluminium in hydrochloric acid solution, *Materials Chemistry and Physics*, 1995; 39(3): 209-213.
12. Gülşen Avci, Corrosion inhibition of indole-3-acetic acid on mild steel in 0.5 M HCl, *Colloids and Surfaces A: Physicochemical and Engineering Aspects*, 2008; 317;(1–3): 730–736.
13. Li X. , Deng S. and Fu H., Adsorption and inhibition effect of vanillin on cold rolled steel in 3.0 M H₃PO₄, *Progress in Organic Coatings*, 2010; 67(4): 420–426.
14. Li X., Deng S., Xie X. and Fu H., Inhibition effect of bamboo leaves' extract on steel and zinc in citric acid solution, *Corrosion Science*, 2014; 87: 15–26.
15. Li X., Deng S., Fu H. and Mu G., Inhibition effect of 6-benzylaminopurine on the corrosion of cold rolled steel in H₂SO₄ solution, *Corrosion Science*, 2009; 51: 620–634.

16. Li X. and Mu G., Tween-40 as corrosion inhibitor for cold rolled steel in sulphuric acid: Weight loss study, electrochemical characterization and AFM, *Applied Surface Science*, 2005; 252(5): 1254–1265.
17. Mu G.N., Li X. and Li F., Synergistic inhibition between o-phenanthroline and chloride ion on cold rolled steel corrosion in phosphoric acid, *Materials Chemistry and Physics*, 2004; 86(1): 59–68.
18. Noor E.A., Comparative Study on the Corrosion Inhibition of Mild Steel by Aqueous Extract of Fenugreek Seeds and Leaves in Acidic Solutions, *Journal of Engineering and Applied Sciences*, 2008; 3(1): 23-30.
19. Noor E.A., Temperature Effects on the Corrosion Inhibition of Mild Steel in Acidic Solutions by Aqueous Extract of Fenugreek Leaves, *International Journal of Electrochemical Science*, 2007; 2: 996 – 1017.
20. Obi-Egbedi N.O. Obot I.B. and Umoren S.A., Spondias mombin L. as a green corrosion inhibitor for aluminium in sulphuric acid: Correlation between inhibitive effect and electronic properties of extracts major constituents using density functional theory, *Arabian Journal of Chemistry*, 2012; 5: 361–373.
21. Obot I.B. and Obi-Egbedi N.O., 2,3-Diphenylbenzoquinoxaline: A new corrosion inhibitor for mild steel in sulphuric acid, *Corrosion Science*, 2010; 52(1): 282–285.
22. Obot I.B. and Obi-Egbedi N.O., Adsorption properties and inhibition of mild steel corrosion in sulphuric acid solution by ketoconazole: Experimental and theoretical investigation, *Corrosion Science*, 2010; 52(1): 198–204.
23. Obot I.B., Ebenso E.E., Zuhair and Gasem M., Eco-friendly corrosion inhibitors: Adsorption and inhibitive action of ethanol extracts of *Chalomolaena odorata* L. for the corrosion of mild steel in H₂SO₄ solutions, *International Journal of Electrochemical Science*, 2012; 7: 1997–2008.
24. Okafor P.C., Ebenso E.E. and Ekpe U.J., *Azadirachta indica* extracts as corrosion inhibitor for mild steel in acid medium, *International Journal of Electrochemical Science*, 2010; 5: 973–998.
25. Popova A., Sokolova E., Raicheva S. and Christov M., AC and DC study of the temperature effect on mild steel corrosion in acid media in the presence of benzimidazole derivatives, *Corrosion Science*, 2003; 45(1): 33–58.

26. Saratha R. and Vasudha V.G., *Emblca officinalis* (Indian Gooseberry) leaves extract as corrosion inhibitor for mild steel in 1 N HCl medium, *European Journal of Chemistry*, 2010; 7: 677–684.
27. Sharma R.K., Mudhoo A., Jain G. and Sharma J., Corrosion inhibition and adsorption properties of *Azadirachta indica* mature leaves extract as green inhibitor for mild steel in HNO₃, *Green Chemistry Letters and Reviews*, 2010; 3: 7–15.
28. Sibel ZOR, Doğan P. and Yazıcı B., Inhibition of Acidic Corrosion Of Iron And Aluminium By Sdbs at Different Temperatures, *Corrosion Reviews*, 2005; 23(2-3): 217-232.
29. Solmaz R., Kardaş G., Çulha M., Yazıcı B. and Erbil M., Investigation of adsorption and inhibitive effect of 2-mercaptothiazoline on corrosion of mild steel in hydrochloric acid media, *Electrochimica Acta*, 2008; 53(20): 5941–5952.
30. Soltani N., Behpour M. and Ghoreishi S.M., Corrosion inhibition of mild steel in hydrochloric acid solution by some double Schiff bases, *Corrosion Science*, 2010; 52(4): 1351–1361.
31. Tebbji K., Faska N., Tounsi A., Oudda H. and Benkaddour M., The effect of some lactones as inhibitors for the corrosion of mild steel in 1 M hydrochloric acid, *Materials Chemistry and Physics*, 2007; 106(2–3): 260–267.
32. Thomas J. M. and Thomas W. J., *Introduction to the Principles of Heterogeneous Catalysis*, 5th Ed, Academic Press, London, 1981; 14.
33. Umoren S.A., Obot I.B., Ebenso E.E. and Obi-Egbedi N.O., The Inhibition of aluminium corrosion in hydrochloric acid solution by exudate gum from *Raphia hookeri*, *Desalination*, 2009; 247(1–3): 561-572.
34. Umoren S.A., Eduok U.M., Solomon M.M. and Udoh A.P., Corrosion inhibition by leaves and stem extracts of *Sida acuta* for mild steel in 1 M H₂SO₄ solutions investigated by chemical and spectroscopic techniques, *Arabian Journal of Chemistry*, 2016; 9: S209-S224.
35. Yadav M., Sushil Kumar, Bahadur I. and Ramjugernath D., Corrosion Inhibitive Effect of Synthesized Thiourea Derivatives on Mild Steel in a 15% HCl Solution, *International Journal of Electrochemical Science*, 2014; 9: 6529 – 6550.
36. Zarrouk A., Dafali A., Hammouti B., H. Zarrok, S. Boukhris and M. Zertoubi, Synthesis, Characterization and Comparative Study of Functionalized Quinoxaline Derivatives

- towards Corrosion of Copper in Nitric Acid Medium, *International Journal of Electrochemical Science*, 2010; 5: 46-55.
37. Znini M., Paolini J., Majidi L., Desjobert J.M., Costa J., Lahhit N. and Bouyanzer A., Evaluation of the inhibitive effect of essential oil of *Lavandula multifida* L., on the corrosion behavior of C38 steel in 0.5 M H₂SO₄ medium, *Research on Chemical Intermediates*, 2012; 38(2): 669–683.
38. Khamis, E., The Effect of Temperature on the Acidic Dissolution of Steel in the Presence of Inhibitors, *Corrosion (NACE)*, 1990; 46(6): 476-484.
39. El-Awady A.A., Abd-El-Nabey B.A. and Aziz, S.G., Kinetic-Thermodynamic and Adsorption Isotherms Analysis for the Inhibition of Acid Corrosion of steel by Cyclic and Open Chain Amines, *Journal of Electrochemical Society*, 1992; 139(8): 2149-2154.
40. Quartarone G., Ronchin L., Vavasori A., Tortato C., Bonaldo L., Inhibitive action of gramine towards corrosion of mild steel in deaerated 1.0 M hydrochloric acid solutions, *Corrosion Science*, 2012; 64: 82–89.
41. Branzoi V., Branzoi F., Baibarac M., The inhibition of the corrosion of Armco iron in HCl solutions in the presence of surfactants of the type of N-alkyl quaternary ammonium salts, *Materials Chemistry and Physics*, 2000; 65: 288–297.
42. Noor E.A. and Al-Moubaraki A.H., Thermodynamic study of metal corrosion and inhibitor adsorption processes in mild steel/1- methyl-4[4(-X)-styryl pyridinium iodides/hydrochloric acid systems, *Materials Chemistry and Physics*, 2008; 110: 145–154.
43. Quraishi M.A., Yadav D.K. and Ahamad I., Green Approach to Corrosion Inhibition by Black Pepper Extract in Hydrochloric Acid Solution, *The Open Corrosion Journal*, 2009; 2: 56-60.
44. Vasudha V.G. and Shanmuga Priya K, *Polyalthia Longifolia* as a Corrosion Inhibitor for Mild Steel in HCl Solution, *Research Journal of Chemical Sciences*, 2013; 3(1): 21-26.
45. Badiea A.M. and Mohana K.N., Effect of temperature and fluid velocity on corrosion mechanism of low carbon steel in presence of 2-hydrazino-4,7- dimethylbenzothiazole in industrial water medium, *Corrosion. Science*, 2009; 51: 2231–2241.
46. Emranuzzaman Kumar T., Vishwanatham S., Udayabhanu G., Synergistic effects of formaldehyde and alcoholic extract of plant leaves for protection of N80 steel in 15% HCl, *Corrosion Engineering Science Technology*. 2004; 39: 327–332.
47. Damaskin B.B., *Adsorption of Organic Compounds on Electrodes*, Plenum Press, New York, 1971; 221.

SUMMARY

The thesis consists of four different chapters.

Chapter 1: Introduction and Review of Literature:

This chapter contains an introduction about corrosion phenomenon and corrosion of mild steel and its importance. It contains brief idea about natural corrosion inhibitor substances and corrosion inhibition of mild steel using natural plant products. It also contains a concise report of review of literature of subject along with the objective and significance of study.

Chapter 2: Materials, Methods And Methodology :

This chapter consists of description of four selected plants for corrosion inhibition studies viz. *Lantana camara* , *Nerium oleander* , *Calotropis procera* and *Eichhornia crassipes* , two selected acids for preparation of different aggressive media viz. hydrochloric acid and sulphuric acid. It also includes detailed description of standard methods adopted for determination of weight loss, corrosion rates, inhibition efficiency, kinetic parameters, thermodynamic parameters, adsorption parameters and complete adopted methodology. Weight loss is determined gravimetrically , corrosion rates and inhibition efficiencies are calculated by using equation [1] and [2]. Kinetic parameters , different thermodynamic parameters like activation energy (E_{act}), enthalpy of activation (ΔH^*) , entropy of activation (ΔS^*) and adsorption parameters like Gibbs energy of adsorption , enthalpy of adsorption , entropy of adsorption are calculated at four different temperatures with the help of corrosion rates using the equation [3] , [4] , [5] , [6] , [7] , [13], [14] respectively. These all were studied at various concentrations of leaves extract of selected plant materials in different aggressive media.

Selection of plants as corrosion inhibitors;

Four different plants viz. *Lantana camara*, *Nerium oleander*, *Calotropis procera* and *Eichhornia crassipes* were taken as natural green corrosion inhibitors for mild steel in two different aggressive media. Aqueous extract of *Lantana camara*

leaves (AELCL), aqueous extract of *Nerium olender* leaves (AENOL), aqueous extract of *Calotropis procera* leaves (AECPL) and aqueous extract of *Eichhornia crassipes* (water hyacinth) leaves (AEWHL) were prepared for corrosion studies.

Acids selected for different aggressive media;

Hydrochloric acid and sulphuric acid were selected for preparation of aggressive media. 1M solutions of each acid were prepared for experimental studies.

Methods adopted for determination of weight loss , corrosion rates , inhibition efficiency , kinetic parameters , thermodynamic and activation parameters , Gibbs energy and adsorption parameters :

Determination of weight loss ;

Gravimetric technique was used for weight loss determination. Weight loss method described by Mettson was adopted for corrosion studies. For weight loss determination cylindrical mild steel specimens of various dimensions (5.0 cm in length and 0.80 cm in diameter), (4.7 cm in length and 0.50 cm in diameter), (4.9 cm in length and 0.70 cm in diameter), (4.8 cm in length and 0.60 cm in diameter) were taken, abraded with different emery papers, degreased in acetone and washed with distilled water, dried and then the constant weight was recorded by electronic balance Citizen model CY204. Stock solutions of leaves extracts viz. AELCL was prepared by heating 20 g of powdered leaves in 500 ml of distilled water for one hour, of AECPL was prepared by 20 g of powdered leaves in 250 ml of distilled water for one hour, of AENOL was prepared by 20 g of powdered leaves in 200 ml of distilled water for one hour ,of AEWHL was prepared by 20 g of powdered leaves in 500 ml of distilled water for one hour at 70°C-80°C in round bottom flask respectively. These extracts were left overnight filtered and then made up to above-mentioned volume with distilled water. Aggressive media were prepared by 1M HCl and 1M H₂SO₄ in distilled water. The cylindrical mild steel specimens were hanged by plastic thread and glass rod in 250 ml borosil glass beakers, each containing 100 ml of aggressive media for one hour at four different temperatures in presence and absence of different

concentrations of extracts of four selected plants. After completion of immersion time, specimens were taken out washed with distilled water, dried and again abraded mildly with emery paper to remove the adhered material and weighed accurately by electronic balance and weight loss is calculated. The employed concentration range of plant extracts were 2%-6%(v/v) for AELCL, 1%-10%(v/v) for AENOL, 1%-8%(v/v) for AECPL, and 1%-5%(v/v) for AEWHL extract. The observations were taken at four different temperatures (303K, 313K, 323K, 333K).

Determination of Corrosion Rates (CR);

In 1M HCl and 1M H₂SO₄, corrosion rates of mild steel specimens at different temperatures were calculated by equation (1)

$$C R (\text{gm cm}^{-2} \text{min}^{-1}) = \left(\frac{\Delta W}{A t} \right) \quad (1)$$

Where ΔW is the weight loss calculated of mild steel specimen before and after immersion in acidic media. A is the total surface area of different specimen and t is immersion time in minute.

Determination of Inhibition Efficiency (IE%);

By using corrosion rate data, inhibition efficiency was calculated by following equation (2).

$$IE \% = \left(\frac{CR_{\text{blank}} - CR_{\text{inh}}}{CR_{\text{blank}}} \right) \times 100 \quad (2)$$

Where CR_{blank} and CR_{inh} are the corrosion rates of mild steel in the absence and presence of the specific concentration of inhibitor respectively.

Determination of Kinetic Parameters;

Kinetic parameters B (reaction constant) and K (rate constant) were calculated by the equation (3).

$$\log CR = \log K + B \log C_{\text{inh}} \quad (3)$$

where K is equal to CR at the inhibitor concentration of unity. B is the reaction constant which is the measure of inhibitor effectiveness and C_{inh} is the concentration in % (v/v) of inhibitor.

Determination of the thermodynamic and activation parameters;

Thermodynamic and activation parameters like energy of activation (E_{act}), enthalpy of activation (ΔH^*) entropy of activation (ΔS^*) were calculated by equation (4), (5).

$$\log CR = \log A - \left(\frac{E_{act}}{2.303 RT}\right) \quad (4)$$

Where A is Arrhenius pre-exponential factor, CR is corrosion rate and T is temperature in Kelvin. For calculating E_{act} values, the graph was plotted between log CR values and (1/T) values.

$$\log \left(\frac{CR}{T}\right) = \left[\left(\log \left(\frac{R}{N_h}\right)\right) + \left(\frac{\Delta S^*}{2.303 R}\right) \right] - \left[\left(\frac{\Delta H^*}{2.303 RT}\right)\right] \quad (5)$$

Where N is Avogadro's number, h is Planck's constant. For calculating the values of (ΔS^*) and (ΔH^*), graph was plotted between log (CR/T) and (1/T) values.

Adsorption Isotherms;

To study the adsorption process of inhibitor, different adsorption isotherms viz. Langmuir adsorption isotherm, Freundlich adsorption isotherm, Temkin adsorption isotherm were drawn by using the following equations (8), (10), (11)

$$\frac{C}{\theta} = \frac{1}{K_{ads}} + C_{inh} \quad (6)$$

Rearranging the above equation

$$\frac{\theta}{1-\theta} = K_{ads} \cdot C_{inh} \quad (7)$$

$$\text{Or } \log \left(\frac{\theta}{1-\theta}\right) = \log (K_{ads} \cdot C_{inh}) \quad (8)$$

Where θ is the degree of surface coverage and is equal to $IE\%/100$, K_{ads} is the equilibrium constant of adsorption in $(ml^{-1}L)$, (C_{inh}/θ) is the inhibitor bulk concentration in $(ml L^{-1})$.

Freundlich isotherm is given by the following equations.

$$\theta = K_{ads} C_{inh}^n \quad (9)$$

$$\text{or } \log\theta = \log(K_{ads}) + n \log C_{inh} \quad (10)$$

Where $\theta < n < 1$ θ and K_{ads} is the equilibrium adsorption constant and C_{inh} is the inhibitor concentration in ml/L .

Temkin adsorption is given by the following equation.

$$-2a\theta = \ln(K_{ads}) + \ln(C_{inh}) \quad (11)$$

Determination of Adsorption Parameters:

Gibbs Energy ΔG_{ads} :

Different adsorption parameters Gibbs energy of adsorption (ΔG_{ads}), enthalpy of adsorption (ΔH_{ads}), entropy of adsorption (ΔS_{ads}) were calculated by following equations (13), (14), (15) respectively.

$$K_{ads} = \frac{1}{C_{H_2O}} \exp(-\Delta G_{ads}/RT) \quad (12)$$

It can be written as

$$\Delta G_{ads} = -2.303RT \log(K_{ads} \cdot C_{H_2O}) \quad (13)$$

Where K_{ads} is the equilibrium adsorption constant calculated from Langmuir adsorption isotherm C_{H_2O} is the concentration of water in $(1000 ml/L)$. ΔG_{ads} is Gibbs energy change in adsorption process. R is universal gas constant and T is the temperature in Kelvin.

Enthalpy of Adsorption(ΔH_{ads}) and Entropy of Adsorption (ΔS_{ads});

Enthalpy and entropy of adsorption (ΔS_{ads}) are calculated by the following equation (14).

$$\Delta G_{ads} = \Delta H_{ads} - T \Delta S_{ads} \quad (14)$$

Where ΔH_{ads} is enthalpy of adsorption process, ΔS_{ads} is entropy of adsorption process and ΔG_{ads} is Gibbs energy of adsorption.

Chapter 3: Observations and Results:

This chapter contains all observations and results in tabular and graphical forms for corrosion studies of mild steel in selected media. These tables show the data of calculated corrosion rates, inhibition efficiencies, kinetic parameters, thermodynamic activation parameters and adsorption parameters in absence and presence of corrosion inhibitors. The graphs include Arrhenius plots, various adsorption isotherms, transition state plots, plots between logarithm of corrosion rates and logarithm of concentrations of inhibitors etc. for various plant extracts taken for study.

Chapter 4: Discussions on findings and conclusions:

This chapter includes interpretation of findings. Obtained results revealed that corrosion rate generally increases with temperature and decreases with increase in concentration of inhibitor. Moreover inhibition efficiencies also increase with increase in inhibitor concentrations. Mechanisms of inhibition at mild steel surface are explained and discussed by various adsorption isotherms and Arrhenius plots.

Systematic alphabetically arranged bibliography is given at the end of thesis.